UNIVERSITY OF SOUTHAMPTON

ANALYTICAL AND NUMERICAL INVESTIGATIONS OF LINEAR AND NON-LINEAR BEAM-WATER INTERACTION SYSTEMS

By

Shenglin ZHAO

Thesis submitted for the degree of Ph.D.

School of Engineering Sciences,

SHIP SCIENCE

December 2005

UNIVERSITY OF SOUTHAMPTON

ABSTRACT

FACULTY OF ENGINEERING, SCIENCE AND MATHEMATICS
SCHOOL OF ENGINEERING SCIENCES, SHIP SCIENCE

Ph.D. degree Document

ANALYTICAL AND NUMERICAL INVESTIGATIONS OF LINEAR AND NONLINEAR BEAM-WATER INTERACTION SYSTEMS

by Shenglin ZHAO

This thesis describes analytical and numerical studies of linear and nonlinear beam-water interaction problems. The mathematical model and analytical methods investigated, developed and the results derived provide a contribution to the study of the dynamics of beam-water interaction systems and the influence of modelling.

Natural characteristics and dynamic responses of linear beam-water interaction systems are investigated subject to an undisturbed or a Sommerfeld radiation condition imposed at infinity in the water domain. As a simple idealisation of a typical offshore structure, the influence of an attached mass with moment of inertia at the free end of the beam is discussed. The natural frequencies determined for the Sommerfeld condition are complex valued with real component values close to the corresponding natural frequencies for the undisturbed condition and the small imaginary components reflects a damping mechanism. That is, the imposition of this condition demonstrates energy dissipation in the system as indicated by the complex valued form of the natural frequency.

An iterative multi-block approach is developed to simulate the dynamic behaviour of nonlinear beam-water interaction systems using a computational fluid dynamics solver coupled to a structural dynamics solver. The selected combination cases involving linear/nonlinear springs and rigid/elastic beams are studied and compared. The results show that even for small movement, the flexibility of the structure is an important physical quantity in assessing the dynamic behaviour of the system.

KEY WORDS: fluid-structure interaction, iterative technique, radiation condition, wave-maker, beam-water interaction system, tip mass, real and complex valued natural frequency.

Table of contents

List of figures

List of tables

Acknowledgements

Firstly I would like to express my sincere gratitude to my supervisors, Professor W.G. Price and Professor Jing Tang Xing for their academic supervision, support and their kind encouragement to me to accomplish all aspects of this study over the past years.

Secondly I wish to thank my tutor in Peking University, Professor Dajun Wang, for his kind support and helpful discussions of some mechanics problems; Dr. K. Djidjeli, Dr. Zhimin Chen, Dr. Weibo Wang and Dr. Yeping Xiong for their discussions of some problems of mechanics and mathematics; Dr. Mingyi Tan and Professor P. A. Wilson for helping to solve computer problems, as well as to all members of the School of Engineering Sciences, Ship Science, for helping me over the years.

Last, but not least, I want to thank my parents, my elder sister and my friends for their everlasting support.

Nomenclature

c	velocity of sound in water
$\bar{c}$	non-dimensional velocity of sound in water
C_k	twisting stiffness of the spring
E	elastic modulus of the beam
F	depth of beam
F_i	component in the ith direction of the fluid force $\mathbf{F}$ acting on the structure
g	acceleration due to gravity
h	depth of water
H	length of beam
$\mathbf{i}$	square root of -1
$\mathbf{i}_0$	unit coordinate vector in y direction of the fixed coordinate system $O-yz$
$\mathbf{i}_1$	unit coordinate vector in Y direction of the moving coordinate system $O-YZ$
I_0	concentrated moment of inertia of the attached mass at the free end of the beam
$\mathbf{j}_0$	unit coordinate vector in z direction of the fixed coordinate system $O-yz$
$\mathbf{j}_1$	unit coordinate vector in Z direction of the moving coordinate system $O-YZ$
J	second moment of section area of the beam (Chapter 2-5); Jacobian of the transformation (Chapter 6)
L	length of the reservoir
m_0	concentrated mass attached to the free end of the beam
M_i	component in the *i-th* direction of the fluid moment $\mathbf{M}$ acting on the structure

p	dynamic pressure in the water
$P(x,y)$	spatial function
r_i	non-dimensional ratio of moment of inertia I_0 to m_0H^2 $(=1000I_0/m_0H^2)$
r_m	ratio of concentrated mass m_0 to mass of the beam $(=m_0/(\rho_s HF\times 1))$
$\mathbf{R}$	an 8×8 square matrix (Chapter 2-5); position vector relative to coordinate system $O-YZ$ (Chapter 6)
Re	Reynolds number
S_{ij}	strain rate tensor
t	time variable
$T(t)$	time function
u_1,u_2	deflections of wet and dry parts of the beam
$u_i(i=1,2,3)$	velocity components of fluid
U_1,U_2	deflection functions of wet and dry parts of the beam
w	beam deflection in moving coordinate system $O-YZ$
x	horizontal direction coordinate
$x_i=(x,y,z)$	coordinates in fluid domain (Chapter 6)
$X(x)$	spatial x direction function
X_n	*n-th* spatial x direction function
y	vertical direction coordinate (Chapter 2-5); horizontal direction coordinate in fixed coordinate system $O-yz$ (Chapter 6)
Y	horizontal direction coordinate in moving coordinate system $O-YZ$ (Chapter 6)
$Y(y)$	spatial y direction function
Y_n	*n-th* spatial y direction function
z	vertical direction coordinate in fixed coordinate system $O-yz$ (Chapter 6)

Z	vertical direction coordinate in moving coordinate system $O-YZ$ (Chapter 6)
γ	ratio of beam height to beam depth ($=\rho_f H/\rho_s F$)
θ	rotation angle of the beam at the spring supported end
κ	positive real number; when a purely imaginary number, $\hat{\kappa}=\mathbf{i}\kappa$
$\hat{\kappa}$	eigenvalue of $Y(y)$ function
$\hat{\kappa}_n$	*n-th* eigenvalue of $Y(y)$ function
$\overline{\kappa}_n$	*n-th* non-dimensional eigenvalue of Y function ($=\hat{\kappa}_n H$)
λ	positive real number; when a purely imaginary number, $\hat{\lambda}=\mathbf{i}\lambda$
$\hat{\lambda}$	eigenvalue of $X(x)$ function
λ_n	positive real number; when a purely imaginary number, $\hat{\lambda}_n=\mathbf{i}\lambda_n$
$\hat{\lambda}_n$	*n-th* eigenvalue of $X(x)$ function
$\overline{\lambda}_n$	*n-th* non-dimensional eigenvalue of $X(x)$ function ($=\hat{\lambda}_n H$)
ν	ratio of water depth to beam height (Chapter 2-5); turbulent kinetic viscosity (Chapter 6)
ξ	non-dimensional y direction coordinate (Chapter 2-5);
$\xi_i,(\xi,\eta,\zeta)$	body-fitted coordinate system (Chapter 6)
ρ_f	mass density of fluid
ρ_s	mass density of solid
τ_{ij}	fluid stress tensor
$\phi_1,\cdots,\phi_8$	real or complex valued beam functions
ω	non-dimensional frequency of the coupled system
Ω	positive real number, when $\hat{\Omega}$ is a purely imaginary number, $\hat{\Omega}=\mathbf{i}\Omega$
$\hat{\Omega}$	eigenvalue of time function
Ω_b	frequency parameter of dry beam ($=\left[EJ/\rho_s FH^4\right]^{1/2}$)

Chapter 1
Introduction

1.1 Engineering background

Many engineering structural designs, e.g. piles, dams, offshore structures or towers, are subject to various dynamic loads caused by earthquakes, wind, currents and waves. Knowledge of their dynamic response is necessary to achieve safe, economical and competitive designs. In this respect, to describe fluid-structure interaction dynamic problems in engineering, simple models of beams surrounded by water or other medium are used to derive understanding of the fundamental dynamical characteristics of the design.

1.1.1 Dam-water system

Man has from antiquity been obliged to provide storage water for survival. This has driven the construction of barrages and dams to provide water for irrigation or town or city water supply, improving navigation, generating hydroelectric power, creating recreation areas or habitats for fish and wildlife, flood control and containing effluent from industrial sites such as mines or factories.

Reservoirs containing tens of hundreds of millions of cubic metres of water stored at heights of tens of metres above the normal course level of a river are a public safety hazzard. In the case of a failure of a dam, there would result a flood whose depths would be equal to the depth of water stored at the time of rupture, and whose volume would be many times that of a natural flood. The volume of water released by dam failure would travel down the river with a much higher velocity than a natural flood and be capable of causing destruction of a catastrophic character (see Leonards (1987)).

There exists a large quantity of research about dams (see for example, Bourgin (1953), Jansen (1988)) and they are of various types. For example, embankment dams (see Casagrande (1973)), gravity dams, arched dams and gravity-arched dams (see Bourgin (1953) and Jansen (1988)).

Dykes or embankment dams are the most ancient form of dam. They are walls built at the edge of a lake, river or stream to protect adjacent land from flooding. They are

triangular in shape with flat upstream and downstream slopes. A gravity dam is considered to be formed by a triangular profile, the crest of which lies on a straight line, circle or parabola. It is assumed to transmit the applied forces (the pressure of the water acting horizontally, and the weight of the masonry acting vertically) directly to the foundation rock. The gravity dam is very sensitive to an increase in water level and runs the risk of failure by overturning or sliding. The arched dam, unlike the straight gravity dam, distributes the major part of the forces acting on it, by arch action, to the abutments in the rock forming the walls of the gorge in which the dam is built. The arch dam is designed as a series of horizontal arch rings, each supposed independent of neighbouring rings and each submitted to a constant radial hydrostatic pressure. The arched dam is not suitable for very wide sites, as it is uneconomical and arch action is doubtful. Therefore, a mixed type of dam is considered to be adopted, either the arched gravity dam of reduced section, or an arched dam carried to extremes but with a thickened section at the centre and still further thickened at the abutments.

According to height, a large dam is higher than 15 metres and a major dam is over 150 metres in height. Alternatively, a low dam is less than 30 metres high; a medium-height dam is between 30 and 100 metres high, and a high dam is over 100 metres high. For example, the Three Gorge Dam in China will be the largest hydroelectric dam in the world when completed in 2009. Its height will be 181 metres. The expected investment is between 24.65 to 75 billion US dollars with installed power generation capacity of 19.2 Gigawatts. Its function includes flood control, power generation and improved navigation.

Although the interaction between the dam and the foundation should be included in the problem, simple models like beam-water interaction systems are used to derive the basic understanding of the complex dam-water problems. In practice, it is assumed that there exists enough length of dam so that the displacement along its length direction is considered very small and therefore can be neglected and the dam is assumed to undergo a plane strain process (see Novozhilov (1961)) during the motion. As a result, a three-dimensional dam-water system is reduced to a two-dimensional dynamics system, see Figure 1.1. Furthermore, for dams of sufficient height, experience suggests that a beam model accurately describes its motion and provides useful results for engineering

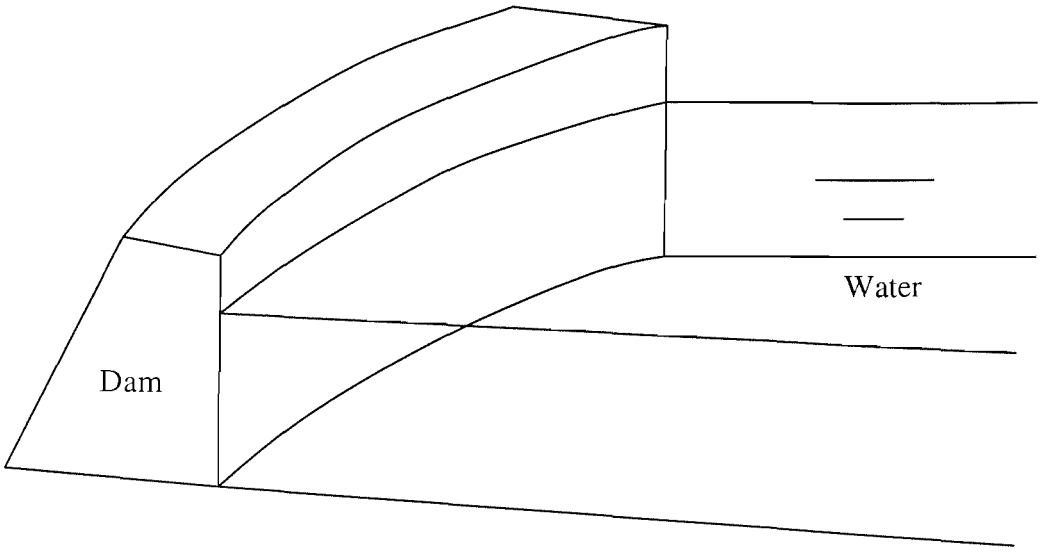

3-D dam-water system

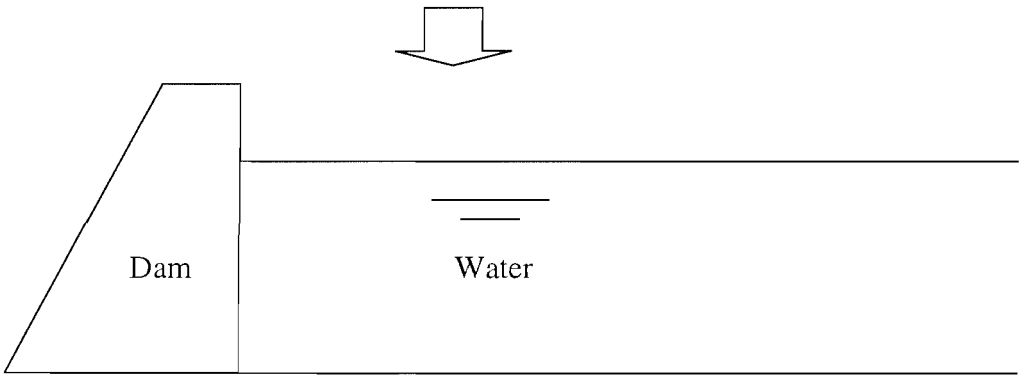

2-D dam-water system

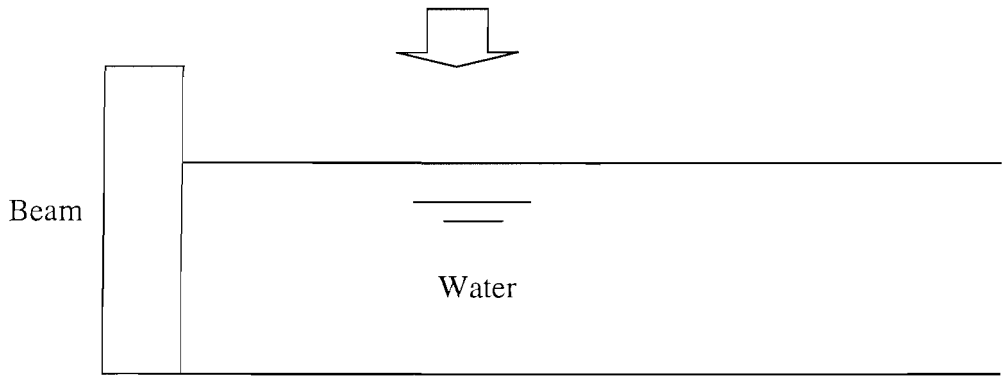

2-D beam-water system

Figure 1.1 Dam-water system to beam-water model.

applications. The beam-water interaction system studied in this thesis provides an essential model to solve dam-water interaction systems.

Observation showed that the displacement in the vertical harmonic motion, caused by earthquake, is only about one-third that of the horizontal motion (see Bourgin (1953)). Therefore, the dynamic response of beam-water system to horizontal foundation vibration is investigated in this research.

1.1.2 Offshore structure

Offshore structures are used worldwide for a variety of functions and in a variety of water depths, and environments. Offshore structures may be used for a variety of reasons: Oil and gas exploration, Navigation aid towers, Bridges and causeways, Ship loading and unloading facilities.

Almost half of the oil and gas resources of the world are beneath the seas. To access these resources, man was forced to develop various types of offshore platforms. The most commonly used structures in the Gulf of Mexico are made of steel, and are used for oil/gas exploration and production.

Offshore structures can be designed for installation in protected waters, such as lakes, rivers, and bays or in the open sea, many kilometers from shorelines. The oil and gas exploration platforms are the best example of offshore structures that can be placed in water depths of 2 kilometers or more. These structures may be made of steel, reinforced concrete or a combination of both. Some environments, where offshore platforms operate, are in hurricane areas with wind loads much larger than experienced in calm or sheltered water regions and these can severely damage the structure. For example, in 2004 Hurricane Ivan damaged seven platforms in the Gulf of Mexico, 100 underwater pipelines and shut down production at some facilities for several months. Also in August 2005, Hurricane Katrina swept towards the heart of the U.S. oil and refinery operations in the Gulf of Mexico, where 20 percent of the United States' energy is produced, shutting down an estimated 1 million barrels of refining capacity. At least two drilling rigs were knocked adrift in the gulf and another in Mobile Bay, Alabama, broke free of its mooring and slammed into a bridge. Therefore, the dynamic response of the structure to exciting forces above the water level such as wind load is of interest in this study.

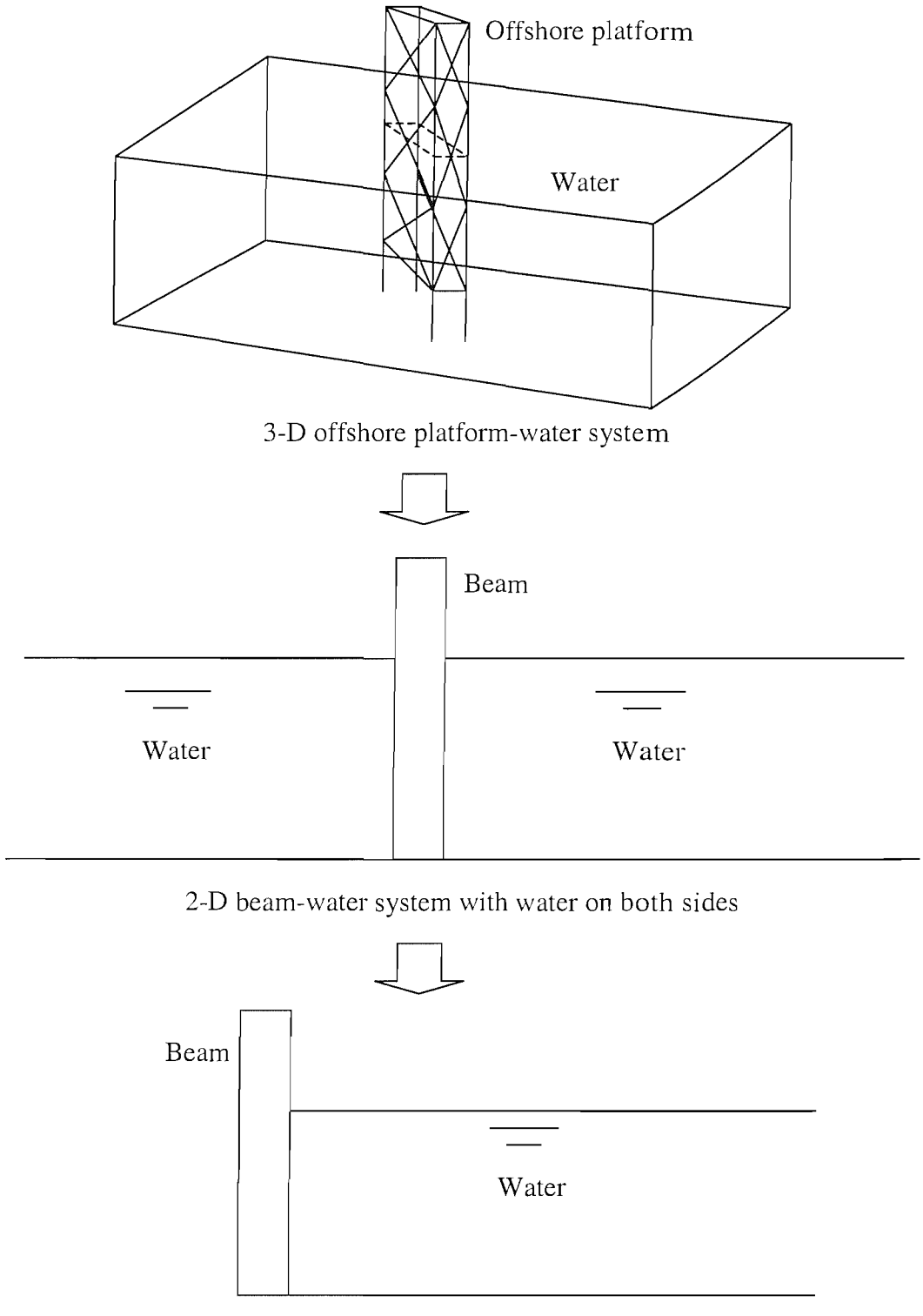

Figure 1.2 3-D offshore platform to 2-D semi-infinite beam-water system.

When external forces act in one plane, a three-dimensional offshore structure-water problem can be reduced to a two-dimensional beam-water system with water on both sides (see Figure 1.2). Furthermore, this two-sided water model can be simplified to a single-sided semi-infinite water model on which the water pressure acting along the beam equals the difference of the water pressures on both sides of the beam, due to the fact that the system is symmetric but the motion of the beam is anti-symmetric. The method to solve the problem is the same, but a one-sided case is simpler and easier to find the solution.

1.1.3 Long thin ship

For some long thin ships, designers sometimes adopt a free-free beam-water system model to derive the basic behavioural knowledge of a ship (see Attwood and Pengelly (1922), Evans (1975), Bishop and Price (1979)). For example, Attwood and Pengelly (1922) used the equivalent beam model to convert an elaborate ship box girder into an I-beam of several flanges. The simple beam idealization of stress distribution is used quite generally for first-order effects from end to end of the ship. But this model can only be used for long thin ships. When the breadth/depth proportions of ships makes the I-beam span/depth ratio too small, the simple beam stress distributions are no longer so predominant as to represent the true total picture.

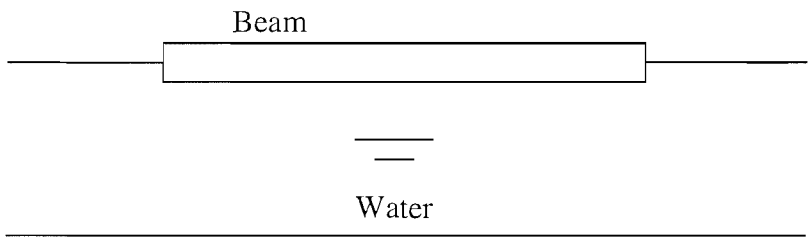

Figure 1.3 Free-free beam-water system to simulate long thin ship-water system.

Simple models like beam-water models can represent various fluid-structure interaction systems including dams, offshore structures and even ships. Therefore, this study focuses on the dynamic behaviour of beam-water interaction systems.

1.2 Beam-water interaction problems

1.2.1 Natural vibration

When a system is displaced from its position of equilibrium and released, it oscillates. In theory, there are as many natural frequencies as degrees of freedom. Natural vibration is the vibration of a mechanical system at the natural frequency in the absence of external influences, as well as assuming no damping.

Resonance occurs when a mechanical system is exposed to a periodic force whose frequency is equal or very close to the natural undamped frequency of the system, which means the increase in amplitude of oscillation of the mechanical system. For many mechanical structures, resonance may cause damage to the structure and the life expectancy and reliability of the structure can be considerably reduced, therefore resonance must be avoided to keep a structure in working condition. In engineering designs, the working frequency of the system must be far away from any natural frequency of the system. Therefore, knowledge of the natural frequency of a mechanical system is of extreme importance.

For linear systems, the mode superposition method is often used to derive the dynamic response of a system (see Popov (1968)). This method requires a preliminary modal analysis to derive the natural characteristic of the system and then to calculate the structure's response.

Due to the above two main reasons, a good understanding of the natural frequencies and natural modes of the mechanical system is very useful in engineering designs.

1.2.2 Dynamic response

Dynamic response is the behaviour of the output of a device as a function of the input, both with respect to time. Many engineering structural designs, e.g. piles, dams, offshore structures or towers, are subject to various dynamic loads caused by earthquakes, wind, currents and waves. The objectives of the dynamic response analysis are to obtain the dynamic displacements, velocities, accelerations, strains and stresses of a system subjected to various external forces. The results of the dynamic response analysis are used to check the dynamic rigidity and strength of the system. Knowledge of the dynamic response is necessary to achieve safe, economical and competitive designs.

1.3 Previous work

Many publications involving theoretical and numerical studies of this kind of fluid-structure dynamical problems are found in the literature and a selection is now discussed.

1.3.1 Natural vibration

Linear natural vibration problems

In solid mechanics, the natural vibration and dynamic responses of a cantilever beam with a tip mass attached to the free end, have been well investigated by many researchers, such as, for example, Takahashi (1980), To (1982), Laura and Gutierrez (1986), etc. Nagaya (1985) and Nagaya and Hai (1985) applied elastodynamic theory and a transfer matrix method to solve problems relating to transient and seismic flexural responses of variable cross section beams with tip inertia immersed in a fluid. Chang and Liu (1989) extended this study to determine the natural frequencies of an immersed restrained column subject to an axial force and compared the results with analytical solutions. Uscilowska and Kolodziej (1998) considered an offshore structure of column shape with an attached tip mass partially immersed in a fluid. They considered the fluid affects as an additional added mass to modify the mass density of the beam and studied the effects of the tip mass and its rotation inertia on the free vibration of the beam. The concept of added mass was defined by Pramila (1986, 1987) as the weight added to a system due to the fact that an accelerating or decelerating body must move some volume of surrounding fluid with it as it moves. The added mass can be incorporated into most physics equations by considering an effective mass as the sum of the mass and added mass. The above four investigations account for fluid effects by including an added mass to the beam governing equation to simplify the fluid effect on the structure, and the main focus of the investigation was the behaviour of the structure, and no results were presented for fluid motion. To overcome this, based on a linear wave equation of the fluid subject to an undisturbed condition at infinity of the fluid domain, Xing, *et al.* (1997) developed an eigenvalue equation to represent the natural vibration of a uniform cantilever beam-water interaction system. They obtained the solutions of the natural frequencies and the corresponding vibration modes for different combinations of boundary conditions. Calculations showed the natural frequencies of the coupled dynamic system are lower

than those of the flexible dry beam, indicating that the influence of water on the beam frequencies has the main effect of an additional mass, i.e., an added mass, due to the water can be treated as an incompressible fluid in lower frequency range. This exact fluid-beam interaction model raveled the pressure modes in fluid domain. However, the study has not considered the effects of tip mass on the beam-water interactions. Furthermore, as it is well known, for infinite fluid domain problems, the Sommerfeld radiation condition was introduced which represents energy transmitting from the system through the fluid to infinity without reflection. The natural vibration of a fluid-structure interaction system subject to the Sommerfeld condition has not been addressed although Xing (2002) presented an initial investigation.

In this research, these unsolved problems are addressed. For both linear and nonlinear problems in the study, fluid forces along the fluid-structure interface are used to represent their interactions and the governing equations describing structure and fluid motions are solved. The effect of tip mass and rotation inertia and Sommerfeld radiation condition on the dynamic behaviour of the system are investigated. Part of this investigation on the natural frequency of a cantilever beam-water interaction system with a concentrated mass attached to its free end has been completed and published (see Zhao, *et al.* (2002)). The natural frequency of a two-dimensional fluid-structure interaction problem with Sommerfeld radiation condition imposed at infinity is investigated and compared with the results for the undisturbed condition. The several chosen fluid-structure interaction systems are analyzed to reveal the physical mechanism caused by Sommerfeld condition.

1.3.2 Dynamic response

Linear dynamic response cases

Eatock Taylor (1981) summarized the analyses available to evaluate hydrodynamic loads acting on submerged structures in the context of a seismic design of dams, intake towers and offshore platforms. The structures were considered to be flexible, and a linear fluid-structure interaction analysis was developed using the modes of vibration of the structure oscillating in the absence of the surrounding fluid. The significance of fluid compressibility and free surface wave effects were discussed in the review and an illustration of their influence was presented through a closed form solution relating to a

simple rectangular reservoir-dam system. He concluded that in practice the interaction between surface waves and compressibility may be safely neglected. Westermo (1981) examined the dynamics of multiple cylindrical elastic beams in a horizontal fluid layer assuming the fluid to be linearly compressible water and each cylindrical beam modelled by Euler-Bernoulli beam theory. He concluded that the multiple cylinder fluid interaction has significant influence on the dynamic response of the system, particularly for frequencies higher than the first natural frequency of a free beam. Kuang and Cao (1993) presented an approximate method to investigate the earthquake response of a fluid-single leg gravity platform-soil interaction system. The dynamic response of the system was analyzed and the influences of various foundation geometric dimensions and water-depths on the hydrodynamic loading were examined. In these previous researches, the effect of tip mass and the Sommerfeld radiation condition have not clearly analyzed and compared. The present study investigates the dynamic responses of the two-dimensional beam-water interaction system with either undisturbed or Sommerfeld radiation conditions imposed at infinity. The calculated results show little difference (error within 1%) between the dynamic behaviour of the beam-water interaction system subject to the two different boundary conditions. It suggests that for simple beam-water interaction problems, we can implement an undisturbed condition at infinity instead of the Sommerfeld radiation condition, and derive a very good approximate solution with reduced analytical and computational effort.

Nonlinear dynamic response cases

Bergan, *et al.* (1985) outlined a method for nonlinear static and dynamic analysis of flexible systems submerged in water. The formulation used allows for very large deformations and material non-linearities. Aspects concerning efficient solution of the nonlinear static and dynamic equations were discussed. Xing and Price (2000) developed some nonlinear mathematical models to provide formulations of the equations of motion describing the dynamical interaction behaviour between an incompressible or compressible ideal fluid and a moving or fixed, elastic or rigid structure. The general theoretical approach is based on the fundamental equations of continuum mechanics, the concept of Hamilton's principle and suitably formulated variational principles. The

resultant mathematical model, expressed in a fixed or a moving frame of reference, allows the theoretical establishment of nonlinear problems associated with ship dynamics and offshore engineering.

In the first MIT conference (see Bathe (2001)) on computational fluid and solid mechanics, Zhang and Bathe (2001), Kroyer (2001), Matthies and Steindorf (2001), Mok, *et al.* (2001) and Drews and Horst (2001) discussed suitable numerical methods to solve a range of nonlinear fluid-structure interaction problems. The solutions of the coupling equations reported were categorized into two approaches. Namely, one is commonly referred to as the partitioned or iterative solution procedure where the dynamics of the fluid and structure are solved separately and data exchanged at every time-step or iteration. The other is a direct or simultaneous solution procedure which establishes the fully coupled governing fluid flow and structural equations and the equations are solved using an iterative method. The mathematical models reported include finite element models for both fluid and solid and a combination model adopting a finite element method in the solid and a finite volume approach to describe the fluid dynamics. In these models, the developed powerful techniques of finite element methods (see, for example, Bathe (1982), Zienkiewitz and Taylor (1989,1991)) are used to describe the dynamics of the solid in the solid domain, but benefits arising from adoption of a finite difference formulation to describe the dynamics of the fluid is reduced, being replaced by a finite volume method.

Price and Xing (2000) proposed a finite element method to model the solid with a finite difference method to describe the fluid in the development of a mixed finite element – finite difference numerical scheme of study to calculate nonlinear fluid-solid dynamical interaction problems. The proposed coupled iterative scheme is a partitioned or iterative procedure as defined later (see, for example, Bathe (2001)), which solves the fluid flow equations for the last calculated structural configuration before the forces along the fluid structure interface are calculated. The application of these forces in the structural model allows evaluation of the incremental structural displacements that are applied to the fluid model and the process of data exchange between structure and fluid continues until convergence of the load/time behaviour is reached. In this preliminary numerical investigation, the structure was treated as a rigid body undergoing large motions so that

ideas and concepts were clarified before considering a fully flexible solid (Xing *et al.* (2002, 2003)). The present thesis continues this study by examining the behaviour of structures through a spring-nonlinear beam-water interaction system. The beam is assumed to undergo a large rigid motion and a small elastic deformation.

Some of the previous researches account for the fluid influence by adding added mass to the dynamic equation of the beam. But there is no added mass in a standard structure solver program. By using fluid forces as the external forces to include all effects from the fluid in the motion, we can use the standard structure solver and fluid solver and combine them without much modification. Therefore, we use this approach in both linear and nonlinear cases in this study.

1.4 Scope and outline of the present work

A general motivation of the present study is to investigate beam water interaction problems theoretically and numerically, with particular reference to the natural vibration and the dynamic response of a beam-water system considering the effects of the tip mass and the different boundary conditions at infinity of the fluid.

There are two parts in this study. Namely the first part discusses linear problems in Chapter 2 to Chapter 5. The second part deals with nonlinear problems in Chapter 6. Chapter 7 discusses conclusions derived and deduced from this research.

The natural frequencies and dynamic response of a beam water interaction system with an attached tip mass are studied in Chapters 2-5. Chapter 2 discusses the governing equations of the natural vibration of a beam water system with an imposed undisturbed or Sommerfeld radiation condition at infinity in the water domain. Chapter 3 discusses how to solve the equations in Chapter 2 and derive solutions for natural frequency and dynamic response of the system. Chapter 4 studies the natural vibration and dynamic response of the beam-water interaction system with undisturbed condition imposed at infinity. Chapter 5 discusses the natural frequency of a one-dimensional spring-mass-water system and a two-dimensional rigid beam-water system with Sommerfeld radiation condition imposed at infinity. The investigation is extended to the natural frequency and dynamic response of the same two-dimensional beam water system as discussed in previous Chapters with a Sommerfeld radiation condition imposed at infinity. Chapter 6

investigates the nonlinear beam water interaction problem using numerical analysis through developed numerical iterative procedures. These solve the fluid flow equations for the last calculated structural configuration and then calculate the forces acting along the fluid structure interface before applying these forces to the structure. This allows evaluation of incremental structural displacements, which then are applied to the fluid model. The interactive process continues until solution convergence is reached satisfying suitably selected error criteria.

Chapter 2

Governing equations describing two-dimensional beam water dynamic interaction systems

In Chapters 2 - 5, linear problems of the natural vibrations and dynamic responses of two-dimensional beam-water interaction systems are investigated. We assume that all disturbances are of small quantity in these four Chapters such that all products of the disturbances are negligibly small. For the general case, the governing equations describing the dynamics of a fixed-free, flexible beam-water interaction system are formulated and presented in this Chapter. Figure 2.1 illustrates the flexible beam-water interacting system in which a concentrated mass m_0 with moment of inertia I_0 is attached to the free end of the beam with water filling the domain $F/2 \le x \le \infty$, $0 \le y \le h$. The beam width F is assumed finite but very small compared to the infinite fluid domain and length of beam. For this reason and to simplify analysis, we use $x = 0$ to approximate for position $x = F/2$ on the fluid structure interface. That is, Figure 2.1 represents an idealised two-dimensional dam or reservoir.

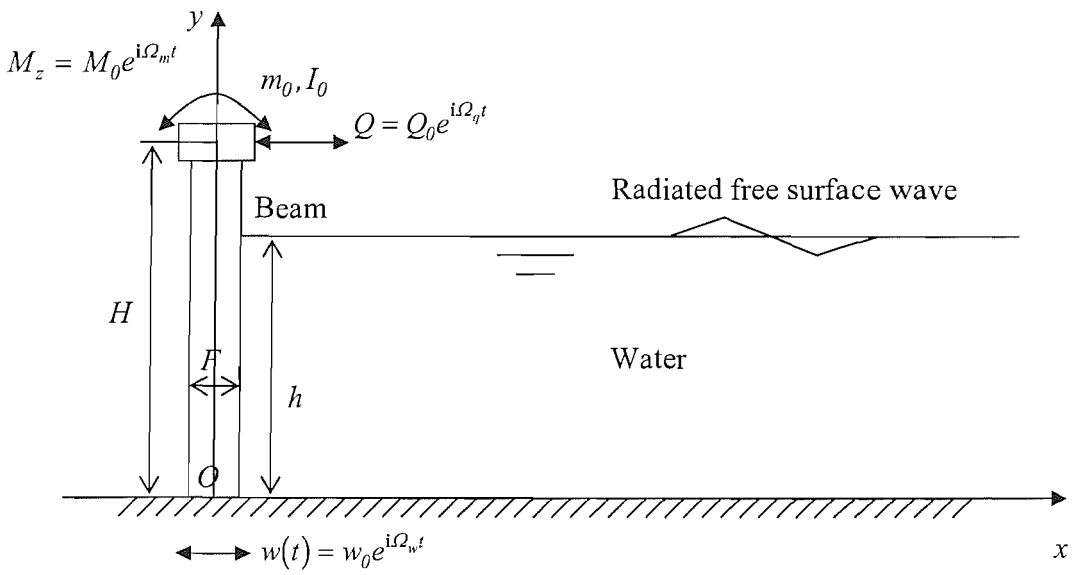

Figure 2.1 Coupled beam-water interaction system

Here, x and y represent a two dimensional Cartesian coordinate system with its origin O located at the intersection of the central line of the beam and the horizontal floor of the reservoir. It is assumed that the water is compressible, inviscid, its motion irrotational and the reservoir is of mean depth h; the flexible uniform beam is of height $H(>h)$, immersed height h, of depth F and of unit thickness $B=1$ perpendicular to the $o-xy$ plane. The bending stiffness of the beam, mass density with a unit thickness of the beam material and mass density of the water are denoted by EJ, ρ_s and ρ_f respectively. Under the assumption of small disturbances, the linearised equations describing the dynamic pressure $p(x,y,t)$ in the water, the horizontal deflections $u_1(y,t)$, $(0<y<h)$ and $u_2(y,t)$, $(h<y<H)$ of the beam are described in section 2.1. The loads applied to the beam-water interaction system are illustrated in Figure 2.1 and defined in the nomenclature. At the free end of the beam at $y=H$, a concentrated exciting force $Q=Q_0e^{\mathrm{i}\Omega_q t}$ and a bending moment $M_z=M_0e^{\mathrm{i}\Omega_m t}$ act on the concentrated mass. At the foundation of the beam at $y=0$, there exists a horizontal displacement $w(t)=w_0e^{\mathrm{i}\Omega_w t}$ simulating a seismic displacement, in which Ω_q, Ω_m and Ω_w are the corresponding exciting frequencies.

2.1 Governing equations

2.1.1 Fluid domain

Dynamic equation

$$\frac{\partial^2 p}{\partial x^2}+\frac{\partial^2 p}{\partial y^2}=\frac{1}{c^2}\frac{\partial^2 p}{\partial t^2}, \qquad 0<x<\infty,\ 0<y<h. \tag{2.1}$$

where c denotes the velocity of sound in water. Because we use the pressure variable p in the structure equations, it is more convenient to use a wave equation to describe the fluid movement.

Boundary conditions

On the free surface, this condition takes one of the two following forms:

(1) Zero free surface wave disturbance

$$p=0, \qquad y=h, \tag{2.2}$$

or

(2) a free surface wave disturbance governed by the equation

$$\frac{\partial p}{\partial y} = -\frac{1}{g}\frac{\partial^2 p}{\partial t^2}, \qquad y = h. \tag{2.3}$$

On the bottom of the reservoir, assumed impermeable and rigid,

$$\frac{\partial p}{\partial y} = 0, \qquad y = 0. \tag{2.4}$$

At infinity in the water domain, it is assumed that either an undisturbed condition or a radiation condition applies.

For an undisturbed condition, it is assumed that the pressure disturbance in the water caused by the beam motion does not transmit to infinity. This implies that the undisturbed condition is governed by the equation

$$p = 0, \qquad x \to \infty. \tag{2.5}$$

To solve wave radiation problems in an infinite domain, Sommerfeld (1949) proposed a radiation condition to be imposed at infinity in the medium. Physically, this represents a disturbance in the water transmitting along the positive x direction with no wave reflected. Arens (1999) listed the following Sommerfeld radiation condition,

$$\lim_{r\to\infty} r^{\frac{m-1}{2}}\left(\frac{\partial u^s(x)}{\partial r} - \mathbf{i}ku^s(x)\right) = 0, \qquad r = |x|, \tag{2.6}$$

uniformly in all direction x/r, where u^s denotes a suitable variable defining dynamic behaviour in the scattered field, k the wave number and $m = 1,2,3$ the spatial dimension of the problem. Only in equation (2.6) does x represent a vector, and r its length.

For the two-dimensional cases studied in this chapter, the Sommerfeld radiation condition can be written as follows, see Xing *et al* (1997),

$$p(x,y,t) = P(x,y)e^{-\mathbf{i}\hat{\Omega}t}, \quad \frac{\partial P}{\partial x} - \mathbf{i}\hat{\lambda}P = P_{,x} - \mathbf{i}\hat{\lambda}P = 0, \quad x \to \infty. \tag{2.7}$$

2.1.2 Solid domain

Dynamic equation

The equation of motion governing the submerged part of the beam, treated for simplicity as a Bernoulli-Euler beam (see Popov (1968)), is given by

$$EJB\frac{\partial^4 u_1}{\partial y^4}+\rho_s FB\frac{\partial^2 u_1}{\partial t^2}=-p(0,y,t)B,\qquad 0<y<h, \tag{2.8.1}$$

and for the dry portion in air

$$EJB\frac{\partial^4 u_2}{\partial y^4}+\rho_s FB\frac{\partial^2 u_2}{\partial t^2}=0,\qquad h<y<H. \tag{2.8.2}$$

Deleting the parameter B, we have

$$EJ\frac{\partial^4 u_1}{\partial y^4}+\rho_s F\frac{\partial^2 u_1}{\partial t^2}=-p(0,y,t),\qquad 0<y<h, \tag{2.9.1}$$

and for the dry portion in air

$$EJ\frac{\partial^4 u_2}{\partial y^4}+\rho_s F\frac{\partial^2 u_2}{\partial t^2}=0,\qquad h<y<H. \tag{2.9.2}$$

For an undisturbed condition at infinity, the dynamical pressure $p(x,y,t)$, the horizontal deflections $u_1(y,t)$ and $u_2(y,t)$ are all real value variables whereas, for the radiation condition at infinity, these variables may have complex values.

Boundary conditions

At its base the beam is assumed fixed to the foundation such that,

$$u_1(0,t)=w(t), \tag{2.10}$$

$$\frac{\partial u_1(0,t)}{\partial y}=0. \tag{2.11}$$

At the free end, the concentrated mass m_0 with moment of inertia I_0, the concentrated exciting force $Q=Q_0e^{i\Omega_q t}$ and bending moment $M_z=M_0e^{i\Omega_m t}$ are taken into account. By accounting for bending moment and shearing force at the free end of the beam, we derive the following boundary conditions,

$$EJ\frac{\partial^2 u_2(H,t)}{\partial y^2}=-I_0\frac{\partial^2}{\partial t^2}\left(\frac{\partial u_2(H,t)}{\partial y}\right)+M_0e^{i\Omega_m t}, \tag{2.12}$$

$$EJ\frac{\partial^3 u_2(H,t)}{\partial y^3}=m_0\frac{\partial^2 u_2(H,t)}{\partial t^2}+Q_0e^{i\Omega_q t}. \tag{2.13}$$

To develop a natural vibration analysis for the fixed-free beam-water system in the absence of external force acting, it follows that $Q=0$, $M_z=0$.

On the interface between the wet and the dry portions of the beam, the horizontal deflection, the rotation angle, the bending moment and internal shear force of the beam must be continuous. These conditions are expressed as follows:

$$u_1(h,t) = u_2(h,t), \tag{2.14}$$

$$\frac{\partial u_1(h,t)}{\partial y} = \frac{\partial u_2(h,t)}{\partial y}, \tag{2.15}$$

$$\frac{\partial^2 u_1(h,t)}{\partial y^2} = \frac{\partial^2 u_2(h,t)}{\partial y^2}, \tag{2.16}$$

$$\frac{\partial^3 u_1(h,t)}{\partial y^3} = \frac{\partial^3 u_2(h,t)}{\partial y^3}. \tag{2.17}$$

2.1.3 Fluid-structure interaction interface

On the fluid-structure interaction interface, we assume an impermeable and motion consistent boundary condition which implies that the fluid cannot flow into the structure and has the same displacement, velocity and acceleration as the beam on the interface, therefore the pressure p in the water and the horizontal displacement u_1 of the wet beam section satisfy equation (2.9.1) and the relation (see Xing *et al* (1997))

$$\frac{\partial p}{\partial x} = -\rho_f \frac{\partial^2 u_1}{\partial t^2}, \qquad x = 0,\ 0 < y < h. \tag{2.18}$$

2.2 Variable separable forms of governing equations

By using the separation of variables method (see, for example, Courant & Hilbert 1962), solutions of the pressure p, displacements u_1 and u_2 are sought in the forms

$$p(x,y,t) = P(x,y)T(t) = X(x)Y(y)T(t), \tag{2.19}$$

$$u_1(y,t) = U_1(y)T(t), \tag{2.20}$$

$$u_2(y,t) = U_2(y)T(t). \tag{2.21}$$

The substitution of these expressions into the governing equations (2.1)-(2.18) allows separation of variables and it can be shown that each of the variables $X(x)$, $Y(y)$, $T(t)$,

$U_1(y)$ and $U_2(y)$ satisfy the following sets of equations in which an overdot implies a time derivative and a dash or upper (n) a spatial differentiation. That is,

(1) Time function $T(t)$:

$$\ddot{T} + \hat{\Omega}^2 T = 0, \tag{2.22}$$

(2) Spatial y-function $Y(y)$:

$$Y'' + \hat{\kappa}^2 Y = 0, \tag{2.23}$$

$$Y'(0) = 0, \tag{2.24}$$

subject to the boundary condition derived from equation (2.2). Namely,

$$Y(h) = 0, \quad \text{neglecting free surface waves,} \tag{2.25}$$

or from equation (2.3)

$$Y'(h) - \frac{\hat{\Omega}^2}{g} Y(h) = 0, \text{ including free surface waves.} \tag{2.26}$$

(3) Spatial x-function $X(x)$:

$$X'' + \hat{\lambda}^2 X = 0, \tag{2.27}$$

For undisturbed condition (2.5), the pressure disturbance in the water does not transmit to infinity,

$$X(x) = 0, \qquad x \to \infty, \tag{2.28}$$

For Sommerfeld radiation condition (2.7), the pressure disturbance may not be zero at infinity,

$$X' - \mathbf{i}\hat{\lambda} X = 0, \qquad x \to \infty. \tag{2.29}$$

(4) Displacement functions $U_1(y)$ and $U_2(y)$:

$$EJU_1^{(4)} - \rho_s F \hat{\Omega}^2 U_1 = -X(0)Y(y), \quad 0 < y < h, \tag{2.30}$$

$$EJU_2^{(4)} - \rho_s F \hat{\Omega}^2 U_2 = 0, \qquad h < y < H, \tag{2.31}$$

subject to the boundary conditions from equations (2.10)-(2.13)

$$U_1(0) = w_0 e^{\mathbf{i}(\Omega_w - \hat{\Omega})t}, \tag{2.32}$$

$$U_1'(0) = 0, \tag{2.33}$$

$$EJU_2''(H) = I_0 \hat{\Omega}^2 U_2'(H) + M_0 e^{\mathbf{i}(\Omega_m - \hat{\Omega})t}, \tag{2.34}$$

$$EJU_2'''(H) = -m_0\hat{\Omega}^2 U_2(H) + Q_0 e^{i(\Omega_q - \hat{\Omega})t}, \tag{2.35}$$

and the continuous conditions from equations (2.14)-(2.17)

$$U_1(h) = U_2(h), \tag{2.36}$$

$$U_1'(h) = U_2'(h), \tag{2.37}$$

$$U_1''(h) = U_2''(h), \tag{2.38}$$

$$U_1'''(h) = U_2'''(h). \tag{2.39}$$

(5) On the fluid-solid interaction interface it follows from equation (2.18) that

$$\rho_f \hat{\Omega}^2 U_1(y) = X'(0)Y(y), \qquad 0 < y < h. \tag{2.40}$$

In these equations, $(\ )', (\ )'', (\ )'''$ and $(\ )^{(4)}$ indicate the differential order of the function $(\ )$. $\hat{\Omega}^2$, $\hat{\kappa}^2$ and $\hat{\lambda}^2$ represent three complex parameters to be determined. They satisfy the relation

$$\hat{\lambda}^2 = \frac{\hat{\Omega}^2}{c^2} - \hat{\kappa}^2. \tag{2.41}$$

2.3 Dimensionless equations

For a more general discussion of the proposed solutions, the following non-dimensional parameters are defined by Xing *et al* (1997),

$$\xi = \frac{y}{H},$$

$$\nu = \frac{h}{H},$$

$$\gamma = \frac{\rho_f H}{\rho_s F},$$

$$\omega^2 = \frac{\hat{\Omega}}{\Omega_b},$$

$$\overline{\kappa} = \hat{\kappa} H,$$

$$\overline{\lambda}^2 = \frac{\omega^4}{\overline{c}^2} - \overline{\kappa}^2,$$

$$\bar{c} = \frac{c}{\Omega_b H}. \tag{2.42}$$

Here $\Omega_b = \left[EJ/\left(\rho_s F H^4\right)\right]^{1/2}$ represents the frequency parameter of the dry beam. The variable ξ denotes a non-dimensional coordinate and ν defines the ratio of water depth to beam length; γ represents the mass ratio of water to beam and ω^2 denotes the frequency parameter. We see from equation (2.41) and (2.42) that $\bar{\lambda} = \hat{\lambda} H$ and we introduce the following parameters

$$r_m = \frac{m_0}{\rho_s F H},$$

$$r_i = \frac{1000 I_0}{m_0 H^2}, \tag{2.43}$$

to study the effect of attached top mass and concentrated moment of inertia.

In order to derive the dimensionless equations, we assume the beam deflection functions have the following forms,

$$U_1(y) = \bar{U}_1(\xi) H,$$

$$U_2(y) = \bar{U}_2(\xi) H, \tag{2.44}$$

where $\bar{U}_1$ and $\bar{U}_2$ are dimensionless variables. Substituting equations (2.42) and (2.44) into equation (2.30), we derive

$$EJ U_1^{(4)} - \rho_s F \hat{\Omega}^2 U_1 = EJ \frac{H d^4 \bar{U}_1(\xi)}{H^4 d\xi^4} - \rho_s F \hat{\Omega}^2 H \bar{U}_1(\xi)$$

$$= -X(0) Y(y), \qquad 0 \le \xi \le \nu. \tag{2.45.1}$$

The multiplication of $\frac{H^3}{EJ}$ to both sides of the above equation allows derivation of the dimensionless equation,

$$\frac{d^4 \bar{U}_1(\xi)}{d\xi^4} - \frac{\rho_s F H^4}{EJ} \hat{\Omega}^2 \bar{U}_1(\xi) = \bar{U}_1^{(4)}(\xi) - \frac{\hat{\Omega}^2}{\Omega_b^2} \bar{U}_1(\xi) =$$

$$\bar{U}_1^{(4)}(\xi) - \omega^4 \bar{U}_1(\xi) = -\frac{H^3}{EJ} X(0) Y(y), \qquad 0 \le \xi \le \nu. \tag{2.45.2}$$

Substituting equations (2.42) and (2.44) into equation (2.31) and (2.40) and using a similar technique, we obtain

$$\overline{U}_2^{(4)}(\xi) - \omega^4 \overline{U}_2(\xi) = 0, \qquad \nu < \xi \le 1, \tag{2.46}$$

$$\overline{U}_1(\xi) = \frac{X'(0)Y(y)}{\rho_f H \hat{\Omega}^2} = \frac{H^4}{EJ}\frac{X'(0)Y(y)}{\gamma\omega^4}, \qquad 0 \le \xi \le \nu. \tag{2.47}$$

Again, substituting equations (2.42) and (2.44) into equations (2.32)-(2.39) and using a similar technique, we derive the dimensionless boundary conditions,

$$\overline{U}_1(0) = \frac{w_0}{H} e^{\mathrm{i}(\Omega_w - \hat{\Omega})t}, \tag{2.48}$$

$$\overline{U}_1'(0) = 0, \tag{2.49}$$

$$\overline{U}_2''(1) = \frac{I_0 \hat{\Omega}^2 H}{EJ}\overline{U}_2'(1) + \frac{H}{EJ} M_0 e^{\mathrm{i}(\Omega_m - \hat{\Omega})t}, \tag{2.50}$$

$$\overline{U}_2'''(1) = -\frac{m_0 \hat{\Omega}^2 H^3}{EJ}\overline{U}_2(1) + \frac{H^2}{EJ} Q_0 e^{\mathrm{i}(\Omega_q - \hat{\Omega})t}, \tag{2.51}$$

$$\overline{U}_1(\nu) = \overline{U}_2(\nu), \tag{2.52}$$

$$\overline{U}_1'(\nu) = \overline{U}_2'(\nu), \tag{2.53}$$

$$\overline{U}_1''(\nu) = \overline{U}_2''(\nu), \tag{2.54}$$

$$\overline{U}_1'''(\nu) = \overline{U}_2'''(\nu). \tag{2.55}$$

We will discuss how to solve these equations in Chapter 3 and illustrate how to derive the natural frequencies and dynamic responses of the system in the following Chapters.

Chapter 3

Solution procedure of beam water interaction systems

In this Chapter, we discuss the solution of the equations describing the natural vibration and dynamic response of beam water interaction system described in Chapter 2. We first need to derive expressions defining functions $X(x)$, $Y(y)$ and $T(t)$.

3.1 Solutions of functions $X(x)$, $Y(y)$ and $T(t)$

The adoption of the parameters $\hat{\Omega}^2$, $\hat{\kappa}^2$ and $\hat{\lambda}^2$ allows the general solution of the previous sets of equations (2.22)-(2.29), subject to the imposed boundary conditions, to be represented as follows (for reference to solve ordinary differential equations, see Hairer *et al* 1987).

(i) For the time function, two solutions are possible depending on the value of $\hat{\Omega}$. That is

$$T(t) = At + B, \qquad \hat{\Omega} = 0, \tag{3.1}$$

$$T(t) = ae^{\mathrm{i}\hat{\Omega}t} + be^{-\mathrm{i}\hat{\Omega}t}, \qquad \hat{\Omega} \neq 0. \tag{3.2}$$

(ii) The function $Y(y)$ satisfying equations (2.23), (2.24) takes the form

$$Y(y) = D\cos(\hat{\kappa}y). \tag{3.3}$$

(iii) The solutions of the function $X(x)$ satisfying equation (2.27) take the form

$$X(x) = S_1 x + S_2, \qquad \hat{\lambda} = 0, \tag{3.4}$$

$$X(x) = qe^{\mathrm{i}\hat{\lambda}x} + se^{-\mathrm{i}\hat{\lambda}x}, \qquad \hat{\lambda} \neq 0. \tag{3.5}$$

Here, $A, B, D, S_1, S_2, a, b, q$ and s represent constants to be determined depending on the boundary conditions. These constants are complex valued in general.

The well known relations

$$e^{\mathrm{i}x} = \cos x + \mathbf{i}\sin x, \tag{3.6}$$

$$\cos \mathbf{i}x = \cosh x, \tag{3.7}$$

$$\sin \mathbf{i}x = \mathbf{i}\sinh x, \tag{3.8}$$

$$\cosh \mathbf{i}x = \cos x, \tag{3.9}$$

$$\sinh \mathbf{i}x = \mathbf{i}\sin x, \tag{3.10}$$

allow the complex forms of the functions $X(x)$, $Y(y)$ or $T(t)$ to be transformed into other forms. For example, the function $T(t)$ in equation (3.2) and the function $X(x)$ in equation (3.5) can be expressed alternatively in the forms,

$$T(t) = \tilde{a}\cos(\hat{\Omega}\, t) + \tilde{b}\sin(\hat{\Omega}\, t), \qquad \text{for } \hat{\Omega}^2 \neq 0, \tag{3.11}$$

$$X(x) = \tilde{q}\cos(\hat{\lambda}x) + \tilde{s}\sin(\hat{\lambda}x), \qquad \text{for } \hat{\lambda}^2 \neq 0, \tag{3.12}$$

where $\tilde{a}, \tilde{b}, \tilde{q}$ and $\tilde{s}$ are constants to be determined depending on the boundary conditions (different from a, b, q and s in equations (3.2) and (3.5)).

In Section 3.1.1 to Section 3.1.4, four kinds of boundary conditions in the water domain are examined and the corresponding solutions of functions $X(x)$ and $Y(y)$ are given, respectively. No assumption is introduced concerning fluid compressibility (i.e. $0 < c \leq \infty$). Solutions for $T(t)$ are shown in equations (3.1) and (3.2). The discussed boundary conditions are: undisturbed condition or Sommerfeld radiation condition at infinity, free surface wave disturbance neglected or included. In the following sections or chapters, different solutions to the problem depend on the chosen combinations of the above four kinds of boundary conditions.

3.1.1 Undisturbed condition at infinity

From equation (2.27), (3.4) and (3.5), it is found that

$$X(x) \equiv 0, \qquad \hat{\lambda} = 0, \tag{3.13}$$

$$X(x) = e^{-\lambda x}, \qquad \hat{\lambda} = \mathbf{i}\lambda. \tag{3.14}$$

Therefore, a nontrivial solution of the problem is obtained only if $\hat{\lambda} = \mathbf{i}\lambda$, where $\hat{\lambda}$ is a pure imaginary number, and λ represents a positive real number. Although the solution should be $\hat{\lambda} = \lambda_r + \mathbf{i}\lambda_i$, ($\lambda_i > 0$), where λ_r and λ_i are the real and imaginary parts of $\hat{\lambda}$, only the real form of the solution is discussed in this case. It must be noted that only the real parts of these complex functions p, u_1 and u_2 represent real physical quantities

as discussed by Pippard (1978). For a real value of $\hat{\Omega}$, the function $T(t)$ given in equation (3.2) represents a complex function and the real pressure $p(x,y,t)$, displacements $u_1(y,t)$ and $u_2(y,t)$ defined in equation (2.19)-(2.21) are represented by their corresponding complex functions.

It should be pointed out that in equation (2.42), we define the relation

$$\overline{\lambda}^2 = \frac{\omega^4}{\overline{c}^2} - \overline{\kappa}^2, \tag{3.16}$$

but for the undisturbed condition at infinity, we use the real form of solution $\hat{\lambda} = \mathrm{i}\lambda$. This causes equation (2.41) to become

$$\lambda^2 = \hat{\kappa}^2 - \frac{\hat{\Omega}^2}{c^2}, \tag{3.17}$$

and the dimensionless parameter $\overline{\lambda} = \lambda H$ changes to

$$\overline{\lambda}^2 = \overline{\kappa}^2 - \frac{\omega^4}{\overline{c}^2}. \tag{3.18}$$

3.1.2 Sommerfeld radiation condition at infinity

From equations (2.7) and (2.29), the solution of the spatial x-function $X(x)$ can be expressed as follows (constant coefficients neglected),

$$X(x)T(t) = \begin{cases} 1, & \hat{\Omega} = 0 = \hat{\lambda} \\ e^{\mathrm{i}(\hat{\lambda}x - \hat{\Omega}t)}, & \hat{\Omega} \neq 0 \quad or \quad \hat{\lambda} \neq 0 \end{cases}. \tag{3.19}$$

3.1.3 Free surface wave disturbance neglected

The function $Y(y)$ expressed in equation (3.3) must satisfy the boundary condition of equation (2.25), from which it follows that

$$D\cos(\hat{\kappa}h) = 0. \tag{3.20}$$

Solving this equation, we find that the following results are derived.

$$Y_n(y) = \cos(\hat{\kappa}_n y), \text{ for } \hat{\kappa}_n = (2n-1)\pi/2h, \; n = 1,2,3,\cdots \tag{3.21}$$

$$Y(y) \equiv 0, \qquad \text{for } \hat{\kappa} = \text{ other complex value.} \tag{3.22}$$

3.1.4 Free surface wave disturbance included

The function $Y(y)$ in equation (3.3) satisfies the boundary condition given in equation (2.26), from which it follows that

$$tan(\hat{\kappa}h) = -\frac{\hat{\Omega}^2}{g\hat{\kappa}}. \tag{3.23}$$

Solution to this equation allows $Y(y)$ to be expressed in the forms

$$Y(y) = D, \qquad \hat{\kappa} = 0 = \hat{\Omega}, \tag{3.24}$$

$$Y_0(y) = cos(\hat{\kappa}_0 y) = cosh(\kappa_0 y), \qquad \hat{\kappa}_0 = \mathbf{i}\kappa_0, \quad \hat{\Omega} > 0 \tag{3.25}$$

$$Y_n(y) = cos(\hat{\kappa}_n y), \qquad n = 1,2,3,\cdots \text{ for arbitrary } \hat{\Omega} \tag{3.26}$$

where $\hat{\kappa}_n$ ($n = 1,2,3,\cdots$) is derived by solving equation (3.23), and D represents a constant number. κ_0 satisfies the following equation

$$tanh(\kappa_0 h) = \frac{\hat{\Omega}^2}{g\kappa_0}. \tag{3.27}$$

The solutions of $\hat{\kappa}_n$ and κ_0 given in equations (3.23) and (3.27), respectively, can be derived numerically or in graphical form (for example in real form solution, see Xing, *et al* (1997)).

For the case $\hat{\Omega} = 0 = \hat{\lambda}$, it follows from equation (2.41) that $\hat{\kappa} \equiv 0$ and the only possible solutions of $Y(y)$, $X(x)$ and $T(t)$ is the constant pressure solution as defined by

$$\begin{aligned} &X(x)T(t) = 1, \\ &Y(y) = D, \\ &\hat{\Omega} = 0 = \hat{\lambda}, \\ &\hat{\kappa} = 0. \end{aligned} \tag{3.28}$$

The above solutions represent a static constant fluid pressure.

The main purpose of this study is not the static case solution but an investigation of the natural vibration characteristics and dynamic responses of the fluid-structure interaction system. For each given value of $\hat{\Omega}$ ($\hat{\Omega} \neq 0$), there exist infinite pairs of

parameters $\hat{\lambda}_n$ and $\hat{\kappa}_n$, which satisfy equation (2.41). Therefore, there exists a series of functions $X_n(x)$ and $Y_n(y)$. By adopting the superposition principle, it can be shown that for the undisturbed condition case,

$$P(x,y) = \sum_n X_n(x)Y_n(y) = \sum_n G_n \cos(\hat{\kappa}_n y)e^{-\lambda_n x}, \tag{3.29}$$

or for Sommerfeld radiation condition case,

$$P(x,y) = \sum_n X_n(x)Y_n(y) = \sum_n G_n \cos(\hat{\kappa}_n y)e^{i\hat{\lambda}_n x}, \tag{3.30}$$

where each unknown G_n represents a real constant in equation (3.29) and a complex constant in equation (3.30). Here $\sum_n$ represents $\sum_{n=1}^{\infty}$ in exact solution forms or $\sum_{n=1}^{n_m}$ in approximate forms for numerical analysis, and n_m denotes the number of solutions $\hat{\kappa}_n$ adopted in equations (3.29) and (3.30).

3.2 General solutions to displacements u_1, u_2

In order to use the dimensionless forms of equations (2.45.2)-(2.47) in Chapter 2, we first write the spatial functions in the following dimensionless forms,

$$X_n(x) = e^{i\hat{\lambda}_n x} = e^{i\hat{\lambda}_n H\frac{x}{H}} = e^{i\bar{\lambda}_n \bar{x}} = X_n(\bar{x}), \tag{3.31}$$

$$Y_n(y) = \cos(\hat{\kappa}_n y) = \cos\left(\hat{\kappa}_n H\frac{y}{H}\right) = \cos(\bar{\kappa}_n \xi) = Y_n(\xi), \tag{3.32}$$

where $\bar{x} = x/H$ and $\xi = y/H$ represent the two non-dimensional coordinates, $\bar{\lambda}_n = \hat{\lambda}_n H$ and $\bar{\kappa}_n = \hat{\kappa}_n H$ are defined in equation (2.42), such that

$$X_n'(x) = \frac{de^{i\bar{\lambda}_n \bar{x}}}{dx} = \frac{de^{i\bar{\lambda}_n \bar{x}}}{Hd\bar{x}} = \frac{i\bar{\lambda}_n}{H}e^{i\bar{\lambda}_n \bar{x}} = \frac{i\bar{\lambda}_n}{H}X_n(\bar{x}). \tag{3.33}$$

In the following deduction, we only use solutions for Sommerfeld radiation condition. Similar results can be obtained for the undisturbed condition following the same procedure.

By using the results expressed in equations (3.30)-(3.33), we find that the right hand side of equation (2.45) takes the form

$$-\frac{H^3}{EJ}P(0,y) = -\frac{H^3}{EJ}\sum_n G_n \cos(\hat{\kappa}_n y) = -\frac{H^3}{EJ}\sum_n G_n \cos(\bar{\kappa}_n \xi) = \sum_n A_n \cos(\bar{\kappa}_n \xi), \tag{3.34}$$

where each $A_n = G_n H^3 / EJ$ denotes a dimensionless complex constant. In a similar manner, the right hand side of equation (2.47) changes into

$$\frac{H^4}{EJ}\frac{X'(0)Y(y)}{\gamma\omega^4} = \frac{H^4}{EJ}\sum_n \frac{X_n'(0)Y_n(y)}{\gamma\omega^4} = \frac{H^4}{EJ}\sum_n \frac{\mathbf{i}\bar{\lambda}_n}{H}\frac{X_n(0)Y_n(y)}{\gamma\omega^4}$$

$$= \frac{H^4}{EJ}\sum_n \frac{\mathbf{i}\bar{\lambda}_n}{H}\frac{X_n(0)Y_n(y)}{\gamma\omega^4} = \sum_n \frac{\mathbf{i}\bar{\lambda}_n}{\gamma\omega^4}\frac{H^3}{EJ}G_n \cos(\bar{\kappa}_n \xi) = \sum_n \frac{\mathbf{i}\bar{\lambda}_n A_n}{\gamma\omega^4}\cos(\bar{\kappa}_n \xi). \tag{3.35}$$

Therefore, equations (2.45.2)-(2.47) can be written as

$$\bar{U}_1^{(4)}(\xi) - \omega^4 \bar{U}_1(\xi) = -\sum_n A_n \cos(\bar{\kappa}_n \xi), \qquad 0 \le \xi \le \nu, \tag{3.36}$$

$$\bar{U}_2^{(4)}(\xi) - \omega^4 \bar{U}_2(\xi) = 0, \qquad \nu < \xi \le 1, \tag{3.37}$$

$$\bar{U}_1(\xi) = \sum_n \frac{\mathbf{i}\bar{\lambda}_n A_n}{\gamma\omega^4}\cos(\bar{\kappa}_n \xi), \qquad 0 \le \xi \le \nu. \tag{3.38}$$

The solution $\bar{U}_1(\xi)$ satisfying equation (3.36) and the solution $\bar{U}_2(\xi)$ satisfying equation (3.37) are expressible in the following forms

$$\bar{U}_1(\xi) = \sum_{j=1}^{4} D_j \phi_j(\xi) + \sum_{n=1}^{\infty} B_n \cos(\bar{\kappa}_n \xi),$$

$$\bar{U}_2(\xi) = \sum_{j=5}^{8} D_j \phi_j(\xi), \tag{3.39}$$

where beam functions ϕ_j ($j = 1,2,...,8$) are defined in equation (3.40) in complex forms or in (3.41) in real forms,

$$\phi_1(\xi) = e^{\mathbf{i}\omega\xi},$$

$$\phi_2(\xi) = e^{-\mathbf{i}\omega\xi},$$

$$\phi_3(\xi) = e^{\omega\xi},$$

$$\phi_4(\xi) = e^{-\omega\xi},$$

$$\phi_5(\xi) = e^{\mathrm{i}\omega(\xi-1)},$$

$$\phi_6(\xi) = e^{-\mathrm{i}\omega(\xi-1)},$$

$$\phi_7(\xi) = e^{\omega(\xi-1)},$$

$$\phi_8(\xi) = e^{-\omega(\xi-1)}, \tag{3.40}$$

or in real form,

$$\phi_1(\xi) = cos(\omega\xi),$$

$$\phi_2(\xi) = sin(\omega\xi),$$

$$\phi_3(\xi) = cosh(\omega\xi)$$

$$\phi_4(\xi) = sinh(\omega\xi),$$

$$\phi_5(\xi) = cos\left[\omega(\xi-1)\right],$$

$$\phi_6(\xi) = sin\left[\omega(\xi-1)\right],$$

$$\phi_7(\xi) = cosh\left[\omega(\xi-1)\right],$$

$$\phi_8(\xi) = sinh\left[\omega(\xi-1)\right]. \tag{3.41}$$

3.3 General equations for dynamic problems

3.3.1 General equations

Substituting $\overline{U_1}(\xi)$ of equation (3.39) into equation (3.36), we obtain

$$\sum_n \left(A_n + \left(\overline{\kappa}_n^4 - \omega^4\right)B_n\right)cos(\overline{\kappa}_n\xi) = 0. \tag{3.42}$$

This equation is valid if and only if all the coefficients in brackets of the series equal zero. Therefore, we derive that

$$B_n = \frac{-A_n}{\overline{\kappa}^4 - \omega^4}. \tag{3.43}$$

From equation (3.32), it can be shown that the functions $Y_n(\xi)$ satisfy the orthogonality relation,

$$\int_0^{\nu} Y_n(\xi)Y_m(\xi)d\xi = \begin{cases} 0, & m \neq n \\ \dfrac{\nu}{2} + \dfrac{sin(2\bar{\kappa}_n \nu)}{4\bar{\kappa}_n} = I_n & m = n \end{cases}. \tag{3.44}$$

Substituting $\bar{U}_l(\xi)$ of equation (3.39) into equation (3.36), multiplying both sides of the equation by $Y_n(\xi)$ and integrate the equation from 0 to ν with respect to ξ, we derive the result

$$\sum_{j=1}^{4} D_j \int_0^{\nu} cos(\bar{\kappa}_n \xi)\phi_j(\xi)d\xi + B_n I_n = \frac{\mathbf{i}\bar{\lambda}_n A_n}{\gamma\omega^4} I_n . \tag{3.45}$$

If we assume that

$$I_{n1} = \int_0^{\nu} cos(\bar{\kappa}_n \xi)\phi_1(\xi)d\xi ,$$

$$I_{n2} = \int_0^{\nu} cos(\bar{\kappa}_n \xi)\phi_2(\xi)d\xi ,$$

$$I_{n3} = \int_0^{\nu} cos(\bar{\kappa}_n \xi)\phi_3(\xi)d\xi ,$$

$$I_{n4} = \int_0^{\nu} cos(\bar{\kappa}_n \xi)\phi_4(\xi)d\xi , \tag{3.46}$$

equation (3.45) is simplified to

$$\left(B_n - \frac{\mathbf{i}\bar{\lambda}_n A_n}{\gamma\omega^4} \right) I_n = -\sum_{j=1}^{4} D_j I_{nj} . \tag{3.47}$$

We solve equations (3.43) and (3.47) and derive the following relations,

$$A_n = E_n \sum_{j=1}^{4} D_j I_{nj} ,$$

$$B_n = \tilde{E}_n \sum_{j=1}^{4} D_j I_{nj} , \tag{3.48}$$

where

$$E_n = \frac{1}{I_n \left[\dfrac{1}{\bar{\kappa}_n^4 - \omega^4} + \dfrac{\mathbf{i}\bar{\lambda}_n}{\gamma\omega^4} \right]},$$

$$\widetilde{E}_n = \frac{-1}{I_n\left[1+\dfrac{\mathbf{i}\bar{\lambda}_n\left(\bar{\kappa}_n^4-\omega^4\right)}{\gamma\omega^4}\right]}, \tag{3.49}$$

with each $\bar{\lambda}_n^2 = \dfrac{\omega^4}{\bar{c}^2} - \bar{\kappa}_n^2$ from equation (2.42). All these functions and unknown constants are complex.

The substitution of equations (3.39), (3.44), (3.46) and (3.48)-(3.49) into equations (2.48)-(2.55) produces a linear system of algebraic equations which can be written in the matrix form

$$\mathbf{RD} = \mathbf{f}, \tag{3.50}$$

where $\mathbf{D}$ represents a vector

$$\mathbf{D}^T = [D_1 \quad D_2 \quad \cdots \quad D_8], \tag{3.51}$$

with each D_j $(j = 1,2,\ldots,8)$ is a complex constant. The superscript $(\ )^T$ denotes a transpose matrix, $\mathbf{f}$ represents a 1×8 vector defined by

$$\mathbf{f}^T = \left[\frac{w_0}{H}e^{\mathbf{i}(\Omega_w-\hat{\Omega})t} \quad 0 \quad \frac{H}{EJ}M_0 e^{\mathbf{i}(\Omega_m-\hat{\Omega})t} \quad \frac{H^2}{EJ}Q_0 e^{\mathbf{i}(\Omega_q-\hat{\Omega})t} \quad 0 \quad 0 \quad 0 \quad 0\right] \tag{3.52}$$

and $\mathbf{R}$ represents a 8×8 square complex matrix with elements R_{ij} functions of the frequency parameter ω. The non-zero elements of this matrix are given by

$$R_{1j} = \phi_j(0) + \sum_n \widetilde{E}_n I_{nj}, \qquad j = 1,2,3,4,$$

$$R_{2j} = \phi_j'(0), \qquad j = 1,2,3,4,$$

$$R_{3j} = \phi_j''(1) - \frac{I_0 H}{EJ}\hat{\Omega}^2\phi_j'(1), \qquad j = 5,6,7,8,$$

$$R_{4j} = \phi_j'''(1) + \frac{m_0 H^3}{EJ}\hat{\Omega}^2\phi_j(1), \qquad j = 5,6,7,8,$$

$$R_{5j} = \begin{cases} \phi_j(\nu) + \sum_n \widetilde{E}_n I_{nj} Y_n(\nu), & j = 1,2,3,4, \\ -\phi_j(\nu), & j = 5,6,7,8, \end{cases}$$

$$R_{6j}=\begin{cases}\phi_j'(\nu)+\sum_n \widetilde{E}_n I_{nj} Y_n'(\nu), & j=1,2,3,4,\\ -\phi_j'(\nu), & j=5,6,7,8,\end{cases}$$

$$R_{7j}=\begin{cases}\phi_j''(\nu)+\sum_n \widetilde{E}_n I_{nj} Y_n''(\nu), & j=1,2,3,4,\\ -\phi_j''(\nu), & j=5,6,7,8,\end{cases}$$

$$R_{8j}=\begin{cases}\phi_j'''(\nu)+\sum_n \widetilde{E}_n I_{nj} Y_n'''(\nu), & j=1,2,3,4,\\ -\phi_j'''(\nu), & j=5,6,7,8.\end{cases} \tag{3.53}$$

Only the coefficients $D_j\,(j=1,2,\cdots,8)$ need to be known before we can derive the displacement function $\overline{U}_1$ and $\overline{U}_2$ from equation (3.39).

For the undisturbed condition case, the pressure spatial function $P(x,y)$ takes the form of equation (3.29). Following the procedure as previously discussed, we can derive the same governing equations as equation (3.50) for this undisturbed problem, except that equation (3.49) changes to

$$E_n=\frac{1}{I_n\left[\dfrac{1}{\overline{\kappa}_n^4-\omega^4}-\dfrac{\overline{\lambda}_n}{\gamma\omega^4}\right]},$$

$$\widetilde{E}_n=\frac{-1}{I_n\left[1-\dfrac{\overline{\lambda}_n\left(\overline{\kappa}_n^4-\omega^4\right)}{\gamma\omega^4}\right]}, \tag{3.54}$$

with each $\overline{\lambda}_n^2=\overline{\kappa}_n^2-\dfrac{\omega^4}{\overline{c}^2}$ (different from equation (2.42)).

3.3.2 Characteristic equation describing natural vibrations

In order to study the natural vibration of the system, no external force or moment acts on the system. It is therefore assumed that the horizontal amplitude $w_0=0$ at $x=0$, $y=0$, concentrated exciting force $Q=0$, bending moment $M_z=0$ at $y=H$. From equation (3.52), we obtain

$$\mathbf{f}=\mathbf{0}, \tag{3.55}$$

and equation (3.50) reduces to

$$\mathbf{RD} = \mathbf{0}. \tag{3.56}$$

To determine the natural frequency parameters ω of the coupled system in this linear homogeneous system of algebraic equations, the characteristic eigenvalue equation of the beam-water system is given by

$$det\,\mathbf{R} = 0, \tag{3.57}$$

which is a necessary and sufficient condition of equation (3.56) having a non-zero solution (see Lay (2002)).

3.3.3 Equations describing dynamic responses

As we have confined discussion to a linear system, the responses to all external excitations are equal to the sum of every single response to one excitation. To calculate the dynamic responses of the linear system to some external exciting force or moment, the frequency of the system $\hat{\Omega}$ equals the exciting frequency. From equation (2.48), (2.50) and (2.51), there is only one term in the equations with variable t. To assure the equations are valid, the term involving variable t must be constant. Therefore, we have

$$\hat{\Omega} = \Omega_w, \text{ or } \hat{\Omega} = \Omega_m, \text{ or } \hat{\Omega} = \Omega_q. \tag{3.58}$$

If the exciting frequency is equal to or very close to a natural frequency of the coupled system as defined by equation (3.57), a resonance occurs with the amplitude of the vibration tending to infinity in theory and thus cannot be determined.

For frequencies that satisfy $det\,\mathbf{R} \neq 0$, one solution is obtained by equation (3.50). By knowing the values of the constant D_j ($j = 1,2,\cdots,8$), the vibrations $\overline{U_1}(\xi)$ and $\overline{U_2}(\xi)$ of the beam and $X(x)Y(y)$ of the water pressure p can be calculated using equations (3.39) and (3.29) or (3.30), respectively. The dynamic responses of the beam water system u_1, u_2 and p are derived from variables $U_1(y)$, $U_2(y)$ and $X(x)Y(y)$ by multiplying by $T(t) = e^{\mathrm{i}\Omega_0 t}$, where $\hat{\Omega}_0$ is the exciting frequency.

3.4 Solutions of characteristic equation

As discussed in section 3.3.2, the characteristic eigenvalue equation of the beam-water system is given by equation (3.57). From equations (3.53) and (3.49) or (3.54), we

notice that many non-zero elements R_{ij} of the matrix $\mathbf{R}$ are functions of frequency parameter ω. Therefore, equation (3.57) can be written as

$$det\,\mathbf{R}(\omega) = R_r(\omega) + \mathbf{i}R_i(\omega) = 0, \tag{3.59}$$

where R_r and R_i are the real and imaginary parts of $det\,\mathbf{R}$, respectively.

3.4.1 Undisturbed condition

In the case of an undisturbed condition imposed at infinity, only the real form of the solution is discussed here because only real frequency values exist for a beam water interactive system with undisturbed condition imposed at infinity (See Xing, *et al.* (1997) Appendix A). Under this constraint, all variables u_1, u_2, p and all constants are real or pure imaginary in form, and the determinant $det\,\mathbf{R}(\omega)$ is of real value. The solution of $X(x)$ is given by equations (3.13) and (3.14). The solution of $Y(y)$ is derived from equations (3.21) and (3.22) when free surface waves are neglected and from equations (3.24)-(3.27) when free surface waves are included.

For the case $\hat{\Omega}^2 < 0$, $\hat{\Omega} = \mathbf{i}\Omega$, the exponential solutions of the function $T(t)$ do not represent natural vibration solutions. Thus, it follows that only cases $\hat{\Omega}^2 \geq 0$ need be examined. The case $\hat{\Omega}^2 = 0$ provides a static solution equivalent to rigid mode solutions in structural vibration. However, for the undisturbed condition at infinity there exists no nontrivial static solution associated with $\hat{\Omega}^2 = 0$.

From equations (3.46), (3.53) and (3.54), we notice that all elements R_{ij} of the matrix $\mathbf{R}$ have real values. Therefore, the determinant $det\,\mathbf{R}(\omega)$ is of real value, and equation (3.59) changes to

$$det\,\mathbf{R}(\omega) = R_r(\omega) = 0. \tag{3.60}$$

It is difficult to solve equation (3.60) directly. We use the following numerical approach to find the solutions of frequency parameter ω.

When free surface waves are neglected, the parameters $\hat{\kappa}_n$ given in equation (3.21) are independent of the natural frequency $\hat{\Omega}$ and the latter can be determined by solving

equation (3.60) only. However, when free surface waves are present, the parameters $\hat{\kappa}_n$ determined by equation (3.23) are dependent on the natural frequency $\hat{\Omega}$ and it is therefore necessary to solve equations (3.23) and (3.60) together. Equation (3.23) can be transformed into

$$\hat{\kappa}_n \sin(\hat{\kappa}_n h) + \frac{\hat{\Omega}^2}{g} \cos(\hat{\kappa}_n h) = 0. \tag{3.61}$$

If we assume a function $\Psi(\omega, \hat{\kappa}_n)$ equals to the left hand side of equation (3.61), then equation (3.61) can be written as

$$\Psi(\omega, \hat{\kappa}_n) = 0, \tag{3.62}$$

with $\hat{\Omega}^2 = \omega^4 \Omega_b^2$ as defined in equation (2.42).

Equation (3.62) has the exact form of equation (3.60), which means that we can use the same method to solve both equations.

First, for each value of ω in the range of $0.1 \le \omega \le 10.0$, $\Delta\omega = 0.1$, we calculate the value of $det\,\mathbf{R}(\omega)$. When free surface waves are neglected, the parameters $\hat{\kappa}_n$ is given in equation (3.21). When free surface waves are included, it is known that there exists one root of real value for equation (3.23) for $\hat{\kappa}_n$ in the range of $(\hat{\kappa}_{1n}, \hat{\kappa}_{2n}) = \left(\frac{(2n-1)\pi}{2h}, \frac{n\pi}{h} \right)$, for $\hat{\Omega} > 0$, $n = 1,2,...$ (see Xing, *et al* (1997)), which is the possible root range for $\hat{\kappa}_n$ in each period π for function $tan(\ )$ in equation (3.23). For each interval $(\hat{\kappa}_{1n}, \hat{\kappa}_{2n})$, there is only one root for equation (3.62). Therefore, the continuous function $\Psi(\omega, \hat{\kappa}_n)$ changes signs once within this interval. The values of function $\Psi(\omega, \hat{\kappa}_n)$ at both endpoints $\hat{\kappa}_{1n}$ and $\hat{\kappa}_{2n}$ have opposite signs, and their product is less than zero,

$$\Psi(\omega, \hat{\kappa}_{1n}) \Psi(\omega, \hat{\kappa}_{2n}) < 0. \tag{3.63}$$

For equations like (3.62), especially when it is known that there exists a root in some interval for continuous function $\Psi(\omega, \hat{\kappa}_n)$, the half-interval method or bisection method is used to find the root (see Froberg (1965)). The half-interval method finds a succession of closed intervals, each one being either the left half or the right half of the preceding one, always with the given function having opposite signs at the two endpoints. In this

way, the location of a root is narrowed down to within smaller and smaller intervals. We compute the value of function $\Psi(\omega,\hat{\kappa}_n)$ for the average value of $\hat{\kappa}_{1n}$ and $\hat{\kappa}_{2n}$, i.e., $\hat{\kappa}_n^* = \frac{\hat{\kappa}_{1n}+\hat{\kappa}_{2n}}{2}$. If $\hat{\kappa}_n^*$ satisfies $\Psi(\omega,\hat{\kappa}_n^*)=0$, this $\hat{\kappa}_n^*$ is the solution of equation (3.62). Otherwise $\Psi(\omega,\hat{\kappa}_n^*)>0$ or $\Psi(\omega,\hat{\kappa}_n^*)<0$. If $\Psi(\omega,\hat{\kappa}_{1n})$ or $\Psi(\omega,\hat{\kappa}_{2n})$ has the same sign as $\Psi(\omega,\hat{\kappa}_n^*)$, this means function $\Psi(\omega,\hat{\kappa}_n)$ keeps the same sign in subinterval $(\hat{\kappa}_{1n},\hat{\kappa}_n^*)$ or $(\hat{\kappa}_n^*,\hat{\kappa}_{2n})$ implying, therefore, no root lies in this subinterval and the root is in another subinterval (see illustration in Figure 3.1). Continuing this process dividing the subinterval into half and making sure there is a root in the subinterval, we can find a value of $\hat{\kappa}_n^*$ close enough to make function $\Psi(\omega,\hat{\kappa}_n)$ have a small absolute value, such as $abs(\Psi(\omega,\hat{\kappa}_n))<10^{-5}$, then we can regard this $\hat{\kappa}_n^*$ is the root of equation (3.23).

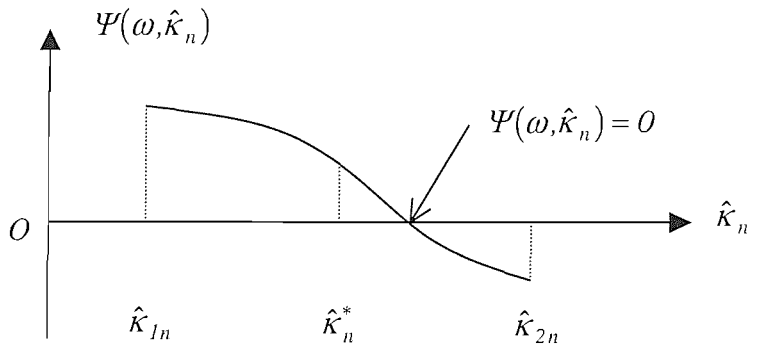

Figure 3.1 Schematic procedure to find roots of function $\Psi(\omega,\hat{\kappa}_n)$ using the half interval method.

Using the half-interval method, we can find roots for each $\hat{\kappa}_n$ with every interval. In order to make calculation possible, one has to truncate all the infinite series of $cos(\hat{\kappa}_n\xi)$ to n_m terms. Calculations show little difference between the results of $n_m=20$ and $n_m=50$. Therefore, all later calculations involving series of $cos(\hat{\kappa}_n\xi)$, $n_m=20$ terms are used in the calculations.

Now for each value of the frequency parameter ω, one can calculate the corresponding $\hat{\kappa}_n$ and other parameters in equations (3.46), (3.48) and (3.54), and in the end derive all the elements R_{ij} of the matrix $\mathbf{R}$ defined in equation (3.53).

With all the elements R_{ij} of the matrix $\mathbf{R}$ known, there are many methods available to calculate $det\,\mathbf{R}(\omega)$. Because there are many calculations involving computing $det\,\mathbf{R}(\omega)$, the calculation of $det\,\mathbf{R}(\omega)$ is required to be efficient using as little memory as possible. In this research, the following method is applied to the calculation of $det\,\mathbf{R}(\omega)$. First, Gauss process, or Gauss-Seidel method, is used to transform the full matrix $\mathbf{R}$ into an upper triangular matrix (for example, see Lay (2002)). Then the product of the main axis elements is equal to $det\,\mathbf{R}(\omega)$.

In order to find roots of the frequency parameter ω in equation (3.60), first we calculate the values of $det\,\mathbf{R}(\omega)$ for ω in the range of $0.1 \le \omega \le 10.0$ with increment of $\Delta\omega = 0.1$, and find those intervals in which function $det\,\mathbf{R}(\omega)$ changes sign. In this first step, one cannot use the half-interval method to find roots because the number of roots in interval $\omega \in [0.1,10.0]$ is unknown and function $det\,\mathbf{R}(\omega)$ may not be continuous. Only for continuous functions with one root in the interval can the half-interval method be used. Because the continuity of function $det\,\mathbf{R}(\omega)$ is unknown, the half-interval method is not used in the calculation of the roots for function $det\,\mathbf{R}(\omega)$. One can try to use the Newton-Raphson method in the small interval to find roots for equation (3.60), but it is not guaranteed that a solution can be found using this method, especially when the function $det\,\mathbf{R}(\omega)$ is not continuous within this interval.

For each interval in which function $det\,\mathbf{R}(\omega)$ changes sign, there may be a root within this interval. We divide the interval evenly into many small subintervals, such as 100 parts, and we calculate the value of function $det\,\mathbf{R}(\omega)$ at each point and find those small subintervals in which function $det\,\mathbf{R}(\omega)$ changes sign. This procedure continues until we find the absolute value of function $det\,\mathbf{R}(\omega)$ is smaller than an imposed error,

such as $|det\,\mathbf{R}(\omega)| < 10^{-5}$, then we accept this value of ω as one of the roots of equation (3.53).

A typical curve illustrating the variation of the value of $det\,\mathbf{R}$ with frequency parameter ω is shown in Figure 3.2. The points at which the determinant $det\,\mathbf{R}$ is zero denote natural frequencies, i.e. 1.68, 3.65 and 6.37 which are the three natural frequencies listed in Table 4.1 ($r_m = 0, r_i = 0$).

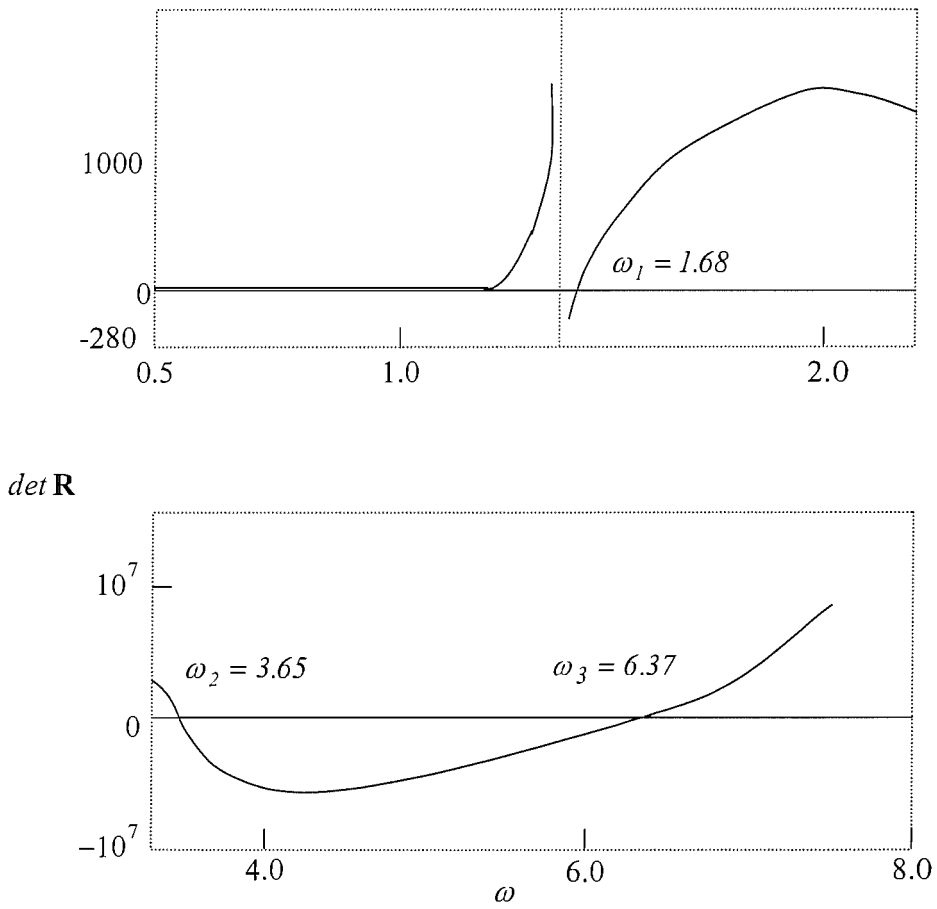

Figure 3.2 A typical curve of $det\,\mathbf{R} \sim \omega$ used to determine the natural frequencies of the beam-water interaction system shown in Figure 2.1.

When solutions $\omega_i (i = 1,2,\cdots,\infty)$ are found for equation (3.57), we can derive the corresponding natural frequency $\Omega_i = \omega_i^2 \Omega_b$. In order to derive the natural mode, (see

Vernon (1967), Wylie (1960)) we first substitute ω_i into equation (3.56), set $D_8 = 1$, or set a certain value for any one D_j ($j = 1,2,\ldots,8$), then we can eliminate one equation in equation (3.56) and calculate the values of the remaining seven values of D_j.

Once knowing all the coefficients D_j ($j = 1,2,\ldots,8$) for a certain frequency parameter ω, one can derive the beam vibration forms $\overline{U}_1(\xi)$ and $\overline{U}_2(\xi)$ from equation (3.39) with coefficients B_n defined in equation (3.48) and water pressure p from equation (3.29) or (3.30) for this natural frequency parameter ω with coefficients $A_n = G_n H^3 / EJ$ obtained from equation (3.48).

The orthogonality relations associated with natural vibration assuming an undisturbed condition imposed at infinity have been discussed by Xing, *et al.* (1997). In a similar manner, the orthogonality relations of the complex natural vibration forms with a Sommerfeld radiation condition imposed at infinity are derived and presented in Appendix B.

3.4.2 Sommerfeld radiation condition

In the case of a Sommerfeld radiation condition imposed at infinity, all functions and constants are of complex values as discussed in section 3.2.

We can use a similar method to search for the roots as in the undisturbed condition case, but now the equation to be solved is equation (3.59), which can be re-written as

$$\begin{cases} R_r(\omega) = 0 \\ R_i(\omega) = 0 \end{cases}. \tag{3.64}$$

When free surface waves are neglected, the parameters $\hat{\kappa}_n$ given in equation (3.21) are of real values and independent of the natural frequency $\hat{\Omega}$ and the latter can be determined by solving equation (3.64) only. However, when free surface waves are present, the complex parameters $\hat{\kappa}_n$ determined by equation (3.23) are dependent on the complex natural frequency $\hat{\Omega}$ and it is therefore necessary to solve equations (3.23) and (3.64) together.

First, we look at equation (3.23), i.e.,

$$tan(\hat{\kappa}_n h) = -\frac{\hat{\Omega}^2}{g\hat{\kappa}_n}. \tag{3.65}$$

When the real part of $\hat{\kappa}_n$ tends to infinity, the real part of the left hand side of equation (3.65) can have any real value within a period of π, and the real part of the right hand side of equation (3.65) tends to zero. Therefore, when the real part of $\hat{\kappa}_n$ is very large, one can expect an infinite set of roots of $\hat{\kappa}_n$ each with large real part and small imaginary part. Again, equation (3.65) can be transformed into equation (3.61) or (3.62), with complex $\hat{\kappa}_n$ and $\hat{\Omega}$.

We apply the method which is used in section 3.4.1 to solve equation (3.64). When free surface waves are neglected, all $\hat{\kappa}_n$ ($n = 1,2,...$) are known from equation (3.21) and only equation (3.64) needs to be solved. One can calculate the value of $det\,\mathbf{R}(\omega)$, and derive its real and imaginary parts R_r and R_i for each point in the range of $-10.0 \le \omega_i \le 10.0$, $0.1 \le \omega_r \le 10.0$, with increments $\Delta\omega_i = 0.1$, $\Delta\omega_r = 0.1$ where $\omega = \omega_r + \mathbf{i}\omega_i$, ω_r and ω_i are the real and imaginary parts of ω respectively. It is noticed that ω and $-\omega$ produce the same natural frequency $\hat{\Omega} = \omega^2\Omega_b$, therefore only positive real part ω_r of ω is calculated.

When free surface waves are present, for a certain complex value of ω, we apply the method used in section 3.4.1 to find roots for $det\,\mathbf{R}(\omega) = 0$ in order to search for roots of $\hat{\kappa}_n$ for equation (3.62). Because now equation (3.62) is of complex value, and there is no possible root interval for us to use in the half-interval method. For a certain complex value of ω, we calculate the complex value of function $\Psi(\omega, \hat{\kappa}_n)$ for each point in the range of $-10.0 \le \hat{\kappa}_{ni} \le 10.0$, $0.1 \le \hat{\kappa}_{nr} \le 100.0$, with increments $\Delta\hat{\kappa}_{ni} = 0.1$, $\Delta\hat{\kappa}_{nr} = 0.1$ where $\hat{\kappa}_n = \hat{\kappa}_{nr} + \mathbf{i}\hat{\kappa}_{ni}$, $\hat{\kappa}_{nr}$ and $\hat{\kappa}_{ni}$ are the real and imaginary parts of $\hat{\kappa}_n$ respectively. It is noticed that $\hat{\kappa}_n$ and $-\hat{\kappa}_n$ do not make a difference in equation $\hat{\lambda}_n^2 = \frac{\hat{\Omega}^2}{c^2} - \hat{\kappa}_n^2$, therefore only the positive real part $\hat{\kappa}_{nr}$ of $\hat{\kappa}_n$ is calculated.

Figures 3.3 and 3.4 illustrate an approach to find the zero of equation (3.64) by drawing figures of functions $R_r(\omega)$ and $R_i(\omega)$. Because ω has complex value, functions

$R_r(\omega)$ and $R_i(\omega)$ now display surfaces instead of curves in the real form solution discussed in section 3.4.1.

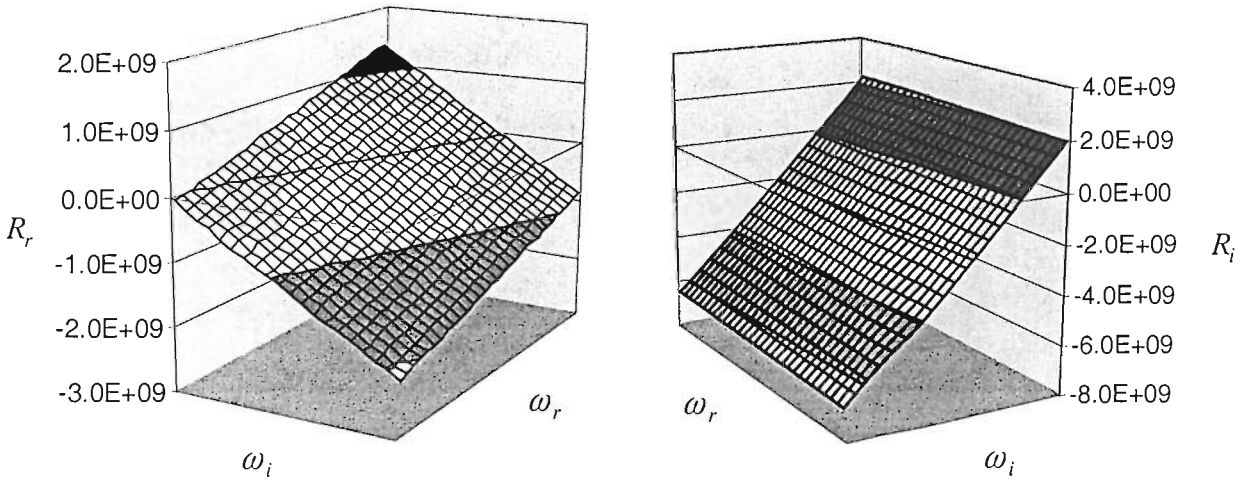

Figure 3.3 Illustration of finding roots for equation (3.64) by drawing figures of functions $R_r(\omega)$ and $R_i(\omega)$.

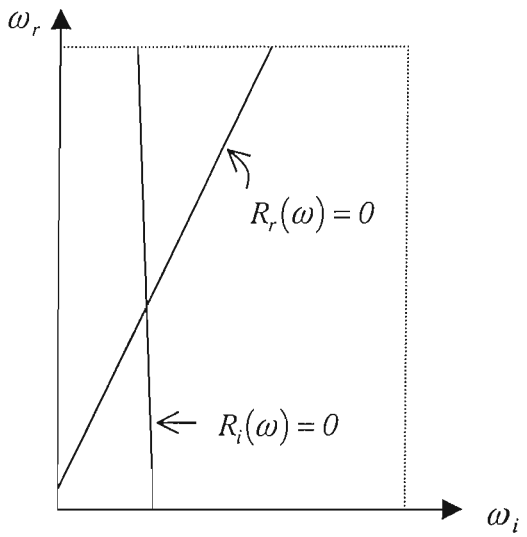

Figure 3.4 Intersection point of curves $R_r(\omega) = 0$ and $R_i(\omega) = 0$ gives the solution of ω for equation (3.64).

When a certain frequency parameter ω_m ($m = 1,2,\cdots,\infty$) is found in equation (3.64), one can derive the corresponding natural frequency $\hat{\Omega}_m = \omega_m^2 \Omega_b$, beam vibration mode shape and water pressure mode shapes by following the steps in section 3.4.1, except that all the functions and constants are complex in this case.

3.5 Solutions of dynamic response equation

As discussed in section 3.3.2, the equation describing the beam-water system under exciting force is given by equation (3.50),

$$\mathbf{RD} = \mathbf{f}, \tag{3.66}$$

with coefficient matrix $\mathbf{R}$, vectors $\mathbf{D}$ and $\mathbf{f}$ defined in equations (3.51), (3.52) and (3.53), respectively.

As we have confined discussion to a linear system, the responses to all external excitations are equal to the sum of every single response to one excitation. The frequency of the system $\hat{\Omega}$ equals the exciting frequency as explained in section 2.4.2, and $\hat{\Omega}$ is not equal to any of the natural frequencies of the beam-water system, otherwise a resonance occurs with the amplitude of the vibration tending to infinity in theory and thus cannot be determined.

For Sommerfeld radiation condition case, pressure p must satisfy Sommerfeld radiation condition, i.e., equation (2.7) or (3.19). And time function $T(t)$ for equation (3.2) must have the form as $T(t) = e^{-i\hat{\Omega}_0 t}$, where $\hat{\Omega}_0$ is the exciting frequency. For undisturbed condition case, time function $T(t)$ has the form as $T(t) = ae^{i\hat{\Omega}_0 t} + be^{-i\hat{\Omega}_0 t}$ and two initial conditions are needed to determine the two constants a and b in equation (3.2).

For frequencies that satisfy $det\,\mathbf{R} \neq 0$, one solution is obtained by solving the linear set of equation (3.66) using the Gauss process. By knowing the values of the constant D_j ($j = 1,2,\cdots,8$), the dynamic responses of the beam water system u_1, u_2 and p are derived from equations (2.19)-(2.21), (2.44), (3.39), and (3.29) or (3.30), i.e., by multiplying variables $U_1(y)$, $U_2(y)$ and $P(x,y)$ respectively by $T(t)$. For undisturbed condition case, we obtain

$$u_1(y,t) = U_1(y)T(t) = H\overline{U}_1(\xi)T(t), \tag{3.67}$$

$$u_2(y,t) = U_2(y)T(t) = H\overline{U}_2(\xi)T(t), \tag{3.68}$$

$$p(x,y,t) = P(x,y)T(t) = \left(\sum_n G_n \cos(\hat{\kappa}_n y)e^{-\lambda_n x}\right)T(t), \tag{3.69}$$

where $T(t) = ae^{i\hat{\Omega}_0 t} + be^{-i\hat{\Omega}_0 t}$, constants a and b can be determined provided knowledge is known of the two initial conditions. For Sommerfeld radiation condition case, the following equations are derived,

$$u_1(y,t) = U_1(y)T(t) = H\overline{U}_1(\xi)T(t) = H\overline{U}_1(\xi)e^{-i\Omega_0 t}, \tag{3.70}$$

$$u_2(y,t) = U_2(y)T(t) = H\overline{U}_2(\xi)T(t) = H\overline{U}_2(\xi)e^{-i\Omega_0 t}, \tag{3.71}$$

$$p(x,y,t) = P(x,y)T(t) = \left(\sum_n G_n \cos(\hat{\kappa}_n y)e^{i\hat{\lambda}_n x}\right)e^{-i\Omega_0 t}. \tag{3.72}$$

Numerical examples are given in Chapters 4 and 5 for natural vibration and dynamic response problems for two-dimensional beam water interaction system subject to undisturbed and Sommerfeld radiation conditions at infinity, respectively.

Chapter 4

System subject to an undisturbed condition

In this Chapter, we discuss the natural vibration and dynamic response of the two-dimensional beam-water interaction system described in Chapter 2, with undisturbed condition imposed at infinity in the water domain, using the equations and methods described in Chapters 2 and 3. Some numerical examples are given.

4.1 Natural vibrations

Xing, *et al* (1997) studied the natural frequencies a beam-water interaction system, without attached top mass or concentrated moment of inertia at the free end of the beam, with undisturbed condition imposed at infinity. In this section, we extend this study by adding an attached top mass with concentrated moment of inertia at the free end of the beam and we investigate the influence of the attachment to the natural frequencies of the beam water system.

By using the theoretical formulations derived in Chapter 2 and the method to solve equation (3.53) in Chapter 3, the parameters required to describe the dynamical behaviour of beam-water systems can be evaluated. In order to compare the present study results with the results given by Xing, *et al* (1997), the same values of parameters are used here. In these calculations, it is assumed that the densities of the beam (concrete) and water are $\rho_s = 2.4 \times 10^3 kg/m^3$ and $\rho_f = 1.0 \times 10^3 kg/m^3$, respectively; the elastic modulus of the beam is $E = 2.94 \times 10^{10} Pa$ and the velocity of sound in water is $c = 1439 m/s$.

The velocity of sound in an incompressible fluid tends to infinity, so that formulations suitable for an incompressible fluid are deduced by substituting $1/c \to 0$ into the equations presented in the previous sections. At the same time the influence of changing other parameters such as the ratio of the concentrated mass to the mass of the beam r_m, the ratio r_i, the depth of the fluid (ν), the ratio H/F (γ) are examined.

Table 4.1 shows the first three frequency parameters ω_1, ω_2, ω_3 assuming compressible water and free surface waves. The three values 1.68, 3.65, 6.37

($r_m = 0, r_i = 0$) are obtained from Figure 3.2 which illustrates how to determine the natural frequencies of the beam-water interaction system.

Table 4.1 The first three frequency parameters ω_1, ω_2, ω_3 assuming compressible water and free surface waves.
($\gamma = 10.0$, $\nu = 0.8$, $r_i = 1$ ($r_i = 0$ when $r_m = 0$))

ith natural frequency ω_i	$r_m = m_0 / (\rho_s HF \times 1)$				
	0.0	1.0	2.0	5.0	10.0
ω_1	1.68	1.24	1.08	0.87	0.73
ω_2	3.65	2.97	2.89	2.83	2.79
ω_3	6.37	5.62	5.51	5.24	4.86

4.1.1 Influence of different mass ratio and different moment of inertia

Tables 4.2-4.4 illustrate the first three natural frequencies for cases: incompressible fluid, constant ν and γ ($\nu = 0.8$, $\gamma = 10.0$) but different mass ratio r_m and different ratio r_i (when $m_0 = 0$, we assume $I_0 = 0$).

Table 4.2 The first natural frequency parameter ω_1 for different concentrated mass and inertia attached to the free end of the beam

	$r_m = m_0 / (\rho_s HF \times 1)$				
$r_i = 10^3 I_0 / m_0 H^2$	0.0	1.0	2.0	5.0	10.0
0.0	1.63	1.21	1.06	0.86	0.73
1.0		1.21	1.06	0.86	0.73
5.0		1.21	1.05	0.86	0.73
10.0		1.20	1.05	0.86	0.73

A comparison of the calculated results shows the following.

(1) Without inclusion of the concentrated inertia ($r_i = 0$), the value of the natural frequency decreases as the ratio r_m increases.

(2) As r_m or r_i increases, the value of the natural frequency decreases. Both of the concentrated mass and moment of inertia play an important role in influencing the behaviour of the dynamical system. In the low frequency region, the concentrated mass is more dominant as confirmed by the predictions presented in Tables 4.2-4.4.

Table 4.3 The second natural frequency parameter ω_2 for different concentrated mass and inertia attached to the free end of the beam

	$r_m = m_0 / (\rho_s HF \times 1)$				
$r_i = 10^3 I_0 / m_0 H^2$	0.0	1.0	2.0	5.0	10.0
0.0	3.65	2.97	2.90	2.86	2.84
1.0		2.96	2.89	2.83	2.78
5.0		2.92	2.83	2.70	2.55
10.0		2.88	2.75	2.55	2.32

Table 4.4 The third natural frequency parameter ω_3 for different concentrated mass and inertia attached to the free end of the beam

	$r_m = m_0 / (\rho_s HF \times 1)$				
$r_i = 10^3 I_0 / m_0 H^2$	0.0	1.0	2.0	5.0	10.0
0.0	6.37	5.71	5.67	5.65	5.65
1.0		5.62	5.51	5.24	4.86
5.0		5.25	4.86	4.22	3.81
10.0		4.86	4.39	3.83	3.56

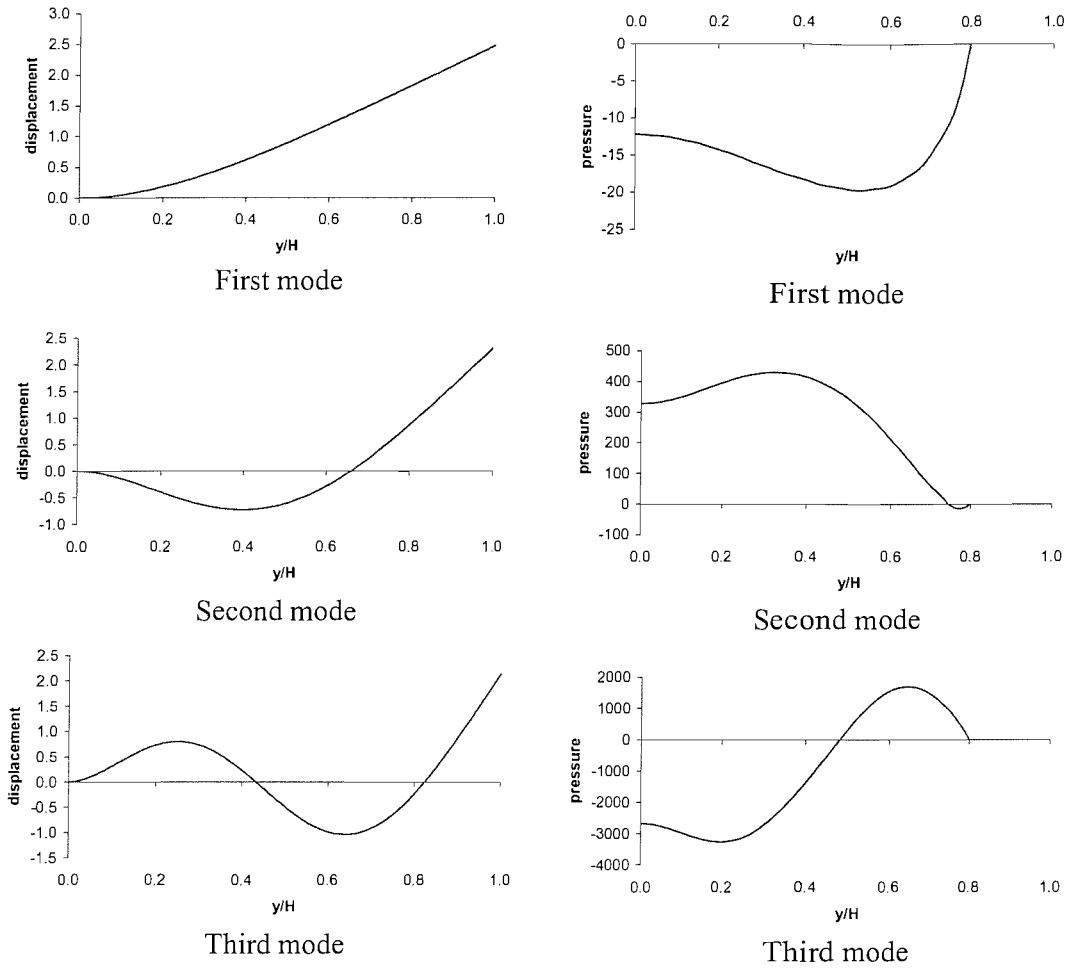

Figure 4.1 The first three modes of dimensionless beam displacement and water pressure assuming compressible water and no free surface waves present ($\gamma = 10.0$, $\nu = 0.8$, $r_m = 0$, $r_i = 0$, $D_g = 1$).

Figure 4.1 shows the first three modes of dimensionless beam displacement ($\overline{U}_1(\xi)$ for $0 < \xi \le \nu$, $\overline{U}_2(\xi)$ for $\nu < \xi \le 1$, $\xi = y/H$) and dimensionless water pressure ($\frac{H^3}{EJ}P(0,y)$, see equation (3.34)), ($\omega_1 = 1.63$, $\omega_2 = 3.65$, $\omega_3 = 6.37$) assuming compressible water but no free surface waves present and without accounting for an attached concentrated tip mass and moment of inertia ($\gamma = 10.0$, $\nu = 0.8$, $r_m = 0$, $r_i = 0$). Figure 4.2 shows the first three modes of dimensionless beam displacement and water pressure modes, ($\omega_1 = 1.21$, $\omega_2 = 2.96$, $\omega_3 = 5.62$) with compressible water but no free

surface waves present and with concentrated tip mass and moment of inertia ($\gamma = 10.0$, $\nu = 0.8$, $r_m = 1$, $r_i = 1$).

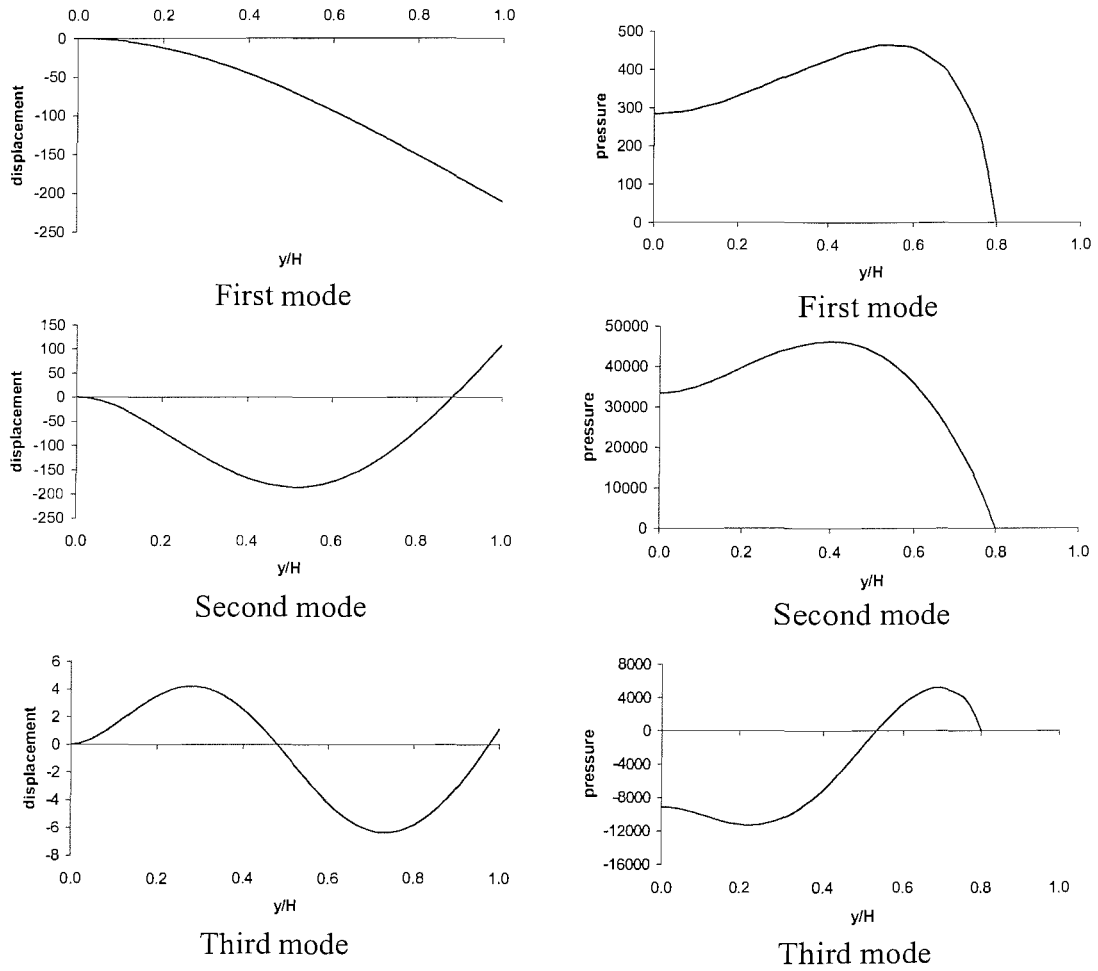

Figure 4.2 The first three beam deflection and water pressure modes assuming compressible water and no free surface waves present ($\gamma = 10.0$, $\nu = 0.8$, $r_m = 1$, $r_i = 1$).

In all the calculations for mode shapes, $D_8 = 1$ is set and substituted into equation (3.56) and the other seven D_j ($j = 1,2,...,7$) values are found by solving the first seven equations in equation (3.56). After knowing all the values of D_j ($j = 1,2,...,8$), we derive the values of dimensionless beam displacement $\overline{U}_1(\xi)$ for $0 < \xi \leq \nu$, $\overline{U}_2(\xi)$ for $\nu < \xi \leq 1$

($\xi = y/H$) from equations (3.39) and (3.48). The dimensionless water pressure is calculated from equations (3.34) and (3.48). The infinite series in equations (3.34) and (3.39) are truncated to the first 20 terms for calculation.

As all the results are derived from setting $D_8 = 1$, the magnitude of the dimensionless beam displacement and water pressure differs greatly from each other. If we multiply by a suitable number to make the maximum beam displacement equal, the corresponding water pressure modes show much larger values for higher order modes than lower modes in both Figures 4.1 and 4.2. This means that to make the higher order beam displacement mode appear with the same amplitude, the water pressure must be much larger.

Comparing these two figures, one can see that the mode shapes with concentrated tip mass and moment of inertia are similar to those without assuming their presence. An obvious difference observed between the two sets of data is that all the mode nodes move towards the free end of the beam when a tip mass and moment of inertia are included. This is because the tip mass changes the mass distribution along the beam.

4.1.2 Influence of different mass ratio in long thin and short thick beams

Tables 4.5-4.7 illustrate and compare the first three natural frequencies of long thin and short thick beams assuming compressible fluid with free surface wave present, a constant depth of fluid and r_i ($\nu = 0.8, r_i = 1$ ($r_i = 0$ when $r_m = 0$)) but different values of γ and r_m.

Table 4.5 The first natural frequency parameter ω_1 for different values of length to breadth ratio γ

	$r_m = m_0/(\rho_s HF \times 1)$				
$\gamma = \rho_f H/(\rho_s F)$	0.0	1.0	2.0	5.0	10.0
0.5	1.82	1.25	1.07	0.87	0.74
10.0	1.63	1.21	1.06	0.86	0.73

These results show the following trends:

(1) As the value of r_m increases, the natural frequency value reduces, and when γ $(=\rho_f H/(\rho_s F))$ increases in value, this reduction becomes more obvious.

(2) As γ increases in value, the determined natural frequency reduces but this reduction is greater in a short thick beam than in a long thin one. It is remembered that in the short thick beam example, beam bending theory is not strictly applicable and a theory incorporating shear effects or a more accurate beam theory is needed. Therefore, this tendency may change with adoption of a more accurate mathematical model. However, from the viewpoint of an engineering approximation, a simple beam bending theory gives a first order approximation to the solution of the dynamical problem.

Table 4.6 The second natural frequency parameter ω_2 for different values of length to breadth ratio γ

	$r_m = m_0/(\rho_s HF \times 1)$				
$\gamma = \rho_f H/(\rho_s F)$	0.0	1.0	2.0	5.0	10.0
0.5	4.69	3.99	3.90	3.77	3.61
10.0	3.65	2.96	2.89	2.83	2.78

Table 4.7 The third natural frequency parameter ω_3 for different values of length to breadth ratio γ

	$r_m = m_0/(\rho_s HF \times 1)$				
$\gamma = \rho_f H/(\rho_s F)$	0.0	1.0	2.0	5.0	10.0
0.5	7.85	6.91	6.68	6.13	5.63
10.0	6.37	5.62	5.51	5.24	4.86

4.1.3 Influence of different mass ratio and different depth of water

Table 4.8 The first natural frequency ω_1 for different values of water depth ratio v

	$r_m = m_0 / (\rho_s HF \times 1)$				
$v = h / H$	0.0	1.0	2.0	5.0	10.0
0.0	1.88	1.25	1.08	0.87	0.74
0.5	1.85	1.24	1.07	0.87	0.74
0.8	1.63	1.21	1.06	0.86	0.73
1.0	1.38	1.14	1.02	0.85	0.73

Tables 4.8-4.10 show the first three natural frequencies derived from an analysis assuming a compressible fluid with free surface wave, constant r_i and γ ($\gamma = 10.0$, $r_i = 1$ ($r_i = 0$ when $r_m = 0$)) but different values of water depth ratio v and r_m.

Table 4.9 The second natural frequency ω_2 for different values of water depth ratio v

	$r_m = m_0 / (\rho_s HF \times 1)$				
$v = h / H$	0.0	1.0	2.0	5.0	10.0
0.0	4.69	3.99	3.91	3.78	3.61
0.5	4.12	3.61	3.56	3.48	3.38
0.8	3.65	2.96	2.89	2.83	2.78
1.0	3.46	2.81	2.70	2.61	2.56

Table 4.10 The third natural frequency ω_3 for different values of water depth ratio v

	$r_m = m_0 / (\rho_s HF \times 1)$				
$v = h / H$	0.0	1.0	2.0	5.0	10.0
0.0	7.85	6.92	6.68	6.14	5.63
0.5	6.83	6.00	5.84	5.48	5.06
0.8	6.37	5.62	5.51	5.24	4.86
1.0	6.22	5.38	5.26	5.05	4.75

It can be seen from this comparison that the natural frequency value corresponding to each mode of the flexible beam-fluid system decreases with increasing ratio ν. The ratio r_m plays a less important role in influencing the natural frequency value as the value ν increases.

4.1.4 Comparison of fluid with and without free surface wave

Table 4.11 shows the first four natural frequencies for the following cases: (1) a compressible fluid with free surface wave present (frequency denoted by ω^{cs}); (2) a compressible fluid with no free surface disturbance present (frequency denoted by ω^{c}); (3) an incompressible fluid with free surface wave present (frequency denoted by ω^{is}). The presented results are relate to values $\nu = 0.8$, $\gamma = 10$, $r_m = 1$ and $r_i = 1$.

Table 4.11 The first four natural frequencies examining the influence of water compressibility and free surface disturbance.

	ω^{cs}	ω^{c}	ω^{is}
ω_1	1.24	1.21	1.24
ω_2	2.97	2.96	2.97
ω_3	5.62	5.62	5.66
ω_4	8.68	8.68	8.39

A comparison of these cases shows that the free surface wave disturbance plays a more dominant role in influencing the natural frequencies of the coupled beam water interaction system in the low frequency region, whereas fluid compressibility is more influential at higher frequencies.

4.1.5 Validation

Laura, *et al.* (1974) and To (1982) both investigated the natural frequencies of a dry beam with a tip mass. They derived similar results for the first three dry beam frequencies $\omega_1 = 1.25$, $\omega_2 = 4.03$, $\omega_3 = 7.13$ corresponding to the parameters we use here $r_i = 0, \nu = 0$, $r_m = 1$ (see Table 4.12). Nagaya (1985) obtained natural frequencies for a

variable cross-section beam with an attached concentrated tip inertia immersed in a fluid. For a uniform beam, Nagaya's results are listed in Table 4.13.

Table 4.12 Comparison of the first three dry beam natural frequencies.

	Laura, *et al* (1974) $r_i = 0, \nu = 0, r_m = 1.$	To (1982) $r_i = 0, \nu = 0, r_m = 1.$	Present results $r_i = 1, \nu = 0, \gamma = 10, r_m = 1.$
ω_1	1.25	1.25	1.25
ω_2	4.03	4.03	3.99
ω_3	7.13	7.13	6.92

Table 4.13 Comparison of the first dry beam natural frequency with different attached mass.

ω_1	Nagaya (1985) $r_i = 0, \nu = 0.$	Present results $r_i = 1, \nu = 0, \gamma = 10.$
$r_m = 1$	1.25	1.25
$r_m = 2$	1.08	1.08

The results in our investigation show good agreement with the resultss by Laura, *et al*, To and Nagaya. It is noticed that the parameters we use here are $r_i = 1$, whilst the results by others are $r_i = 0$, in which the variable $r_i = 10^3 I_0 / m_0 H^2$ represents the influence of moment of inertia of the added top mass. When we take moment of inertia into account, the natural frequencies decrease as the moment of inertia increases. Comparison of the result we have and the other researchers shows this trend. It is seen from Table 4.12 that the natural frequency decreases more obviously in higher order if moment of inertia is included.

4.2 Dynamic responses

From section 3.3, one can derive the dynamic response of the beam-water system by solving equation (3.50). Here we present the dynamic response of the system for two kinds of excitations: a foundation vibration and a free end of the beam forced vibration.

The dynamic response for other excitations can be obtained by solving an equation similar to those presented in equation (3.50).

4.2.1 Foundation vibration

In this section, we consider a forced foundation vibration imposed at the base of the beam, with no other external force or moment acting on the beam-water system, and we investigate the dynamic response of the system. This is to simulate an earthquake.

It is assumed that the foundation has a forced displacement given by

$$u_1(0,t) = w(t) = w_0 e^{i\Omega_w t}. \tag{4.1}$$

In Chapter 3 we show that the corresponding frequency must have the same value as the exciting frequency, $\hat{\Omega} = \Omega_w$, and the dimensionless equations (2.48), (2.50) and (2.51) change to the following forms,

$$\overline{U}_1(0) = \frac{w_0}{H}, \tag{4.2}$$

$$\overline{U}_2''(1) = \frac{I_0 \hat{\Omega}^2 H}{EJ} \overline{U}_2'(1), \tag{4.3}$$

$$\overline{U}_2'''(1) = -\frac{m_0 \hat{\Omega}^2 H^3}{EJ} \overline{U}_2(1). \tag{4.4}$$

Using results derived in Chapters 2 and 3, we formulate the governing equation for this problem. That is, a linear system of algebraic equations in the matrix form as given in equation (3.50)

$$\mathbf{RD} = \mathbf{f}, \tag{4.5}$$

with coefficient matrix $\mathbf{R}$ and vector $\mathbf{D}$ defined in equations (3.53) and (3.51), respectively, and vector $\mathbf{f}$ changed to

$$\mathbf{f}^T = \left[\frac{w_0}{H} \quad 0 \quad 0 \quad 0 \quad 0 \quad 0 \quad 0 \quad 0 \right]. \tag{4.6}$$

Following the steps explained in section 3.5, one can obtain the dynamic response of the system to this foundation vibration as described in equations (3.67)-(3.69). The source code of the developed Fortran program used to solve this dynamic problem is similar to which is shown in Appendix C. The main part of this program for dynamic problem is to use Gauss-Seidel method to solve equation (4.5).

The following discussion represents some numerical examples considered. It is assumed that free surface waves are neglected. Table 4.14 shows the values of $D_j(j=1,\cdots,8)$ when the foundation of the beam is harmonically excited horizontally. Figure 4.3 displays the calculated dimensionless longitudinal beam displacement $\overline{U}_1(\xi)$ for $0 \le \xi \le \nu$ and $\overline{U}_2(\xi)$ for $\nu < \xi \le 1$ from equation (3.39). Figure 4.4 illustrates the predicted dimensionless water pressure along the beam (see equation (3.29)),

$$P(0,y) = \sum_n G_n \cos(\hat{\kappa}_n y) e^{-\lambda_n \times 0} = \sum_n G_n \cos(\overline{\kappa}_n \xi), \tag{4.7}$$

with parameter values $w_0 / H = 0.1$, $\Omega_w = 5 rads/s$, $\gamma = 10$, $\nu = 0$ and 0.8, $r_m = 0$, $r_i = 0$ and $r_m = 1$, $r_i = 1$. The definitions of the parameters γ, ν and r_m are given in the nomenclature and in equation (2.42).

The results show significant differences between the cases involving top mass ($r_m = 1$, $r_i = 1$) and without top mass attached ($r_m = 0$, $r_i = 0$). In the absence of water, the amplitude of the dry beam vibration with top mass included is smaller than without it. This is because the movement of the attached mass consumes part of the mechanical energy of the system. For the beam-water interaction problem, the beam displacement response changes from first vibration mode to second mode when the top mass is added, which means the beam vibration becomes more violently. When the value of r_m increases, the beam displacement reduces whereas the water pressure increases sharply. These calculations suggest that the concentrated moment of inertia has less influence on the dynamic response of the system than the attached mass, as is seen from equations (4.3) and (4.4) if $H > 1m$. However it is observed from Figures 4.3 and 4.4, that the attached mass has a significant effect on the dynamic behaviour of the beam-water interaction system. To ensure an accurate design of such beam-water dynamic interaction systems, both attached mass with concentrated moment of inertia should be taken into account.

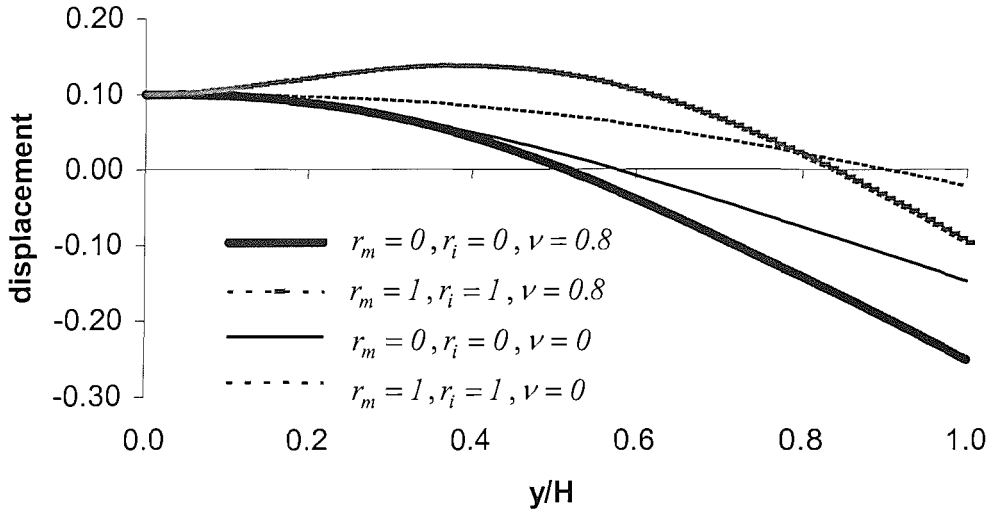

Figure 4.3 Dimensionless longitudinal displacement of the beam caused by foundation vibration for parameter values $w_0 / H = 0.1$, $\Omega_w = 5 rads / s$, $\gamma = 10$, $\nu = 0$ and 0.8, $r_m = 0$, $r_i = 0$ and $r_m = 1$, $r_i = 1$.

Table 4.14 $D_j (j = 1, \cdots, 8)$ with $w_0 / H = 0.1$, $\Omega_w = 5 rads / s$, $\gamma = 10$, $\nu = 0$ and 0.8, $r_m = 0$ and 1.

	$\nu = 0.8$, $r_m = 0$, $r_i = 0$.	$\nu = 0.8$, $r_m = 1$, $r_i = 1$.	$\nu = 0$, $r_m = 0$, $r_i = 0$.	$\nu = 0$, $r_m = 1$, $r_i = 1$.
D_1	5.86E-01	9.92E-01	1.05E-01	5.45E-02
D_2	1.70E-01	4.72E-01	0.0	4.69E-02
D_3	1.40E-01	4.38E-01	-4.67E-03	4.55E-02
D_4	-1.70E-01	-4.72E-01	0.0	-4.69E-02
D_5	-1.26E-01	-4.68E-02	-7.37E-02	-1.01E-02
D_6	-1.13E-01	-2.42E-01	-7.41E-02	-7.20E-02
D_7	-1.26E-01	-5.04E-02	-7.37E-02	-1.14E-02
D_8	-1.13E-01	-5.14E-03	-7.41E-02	-1.96E-02

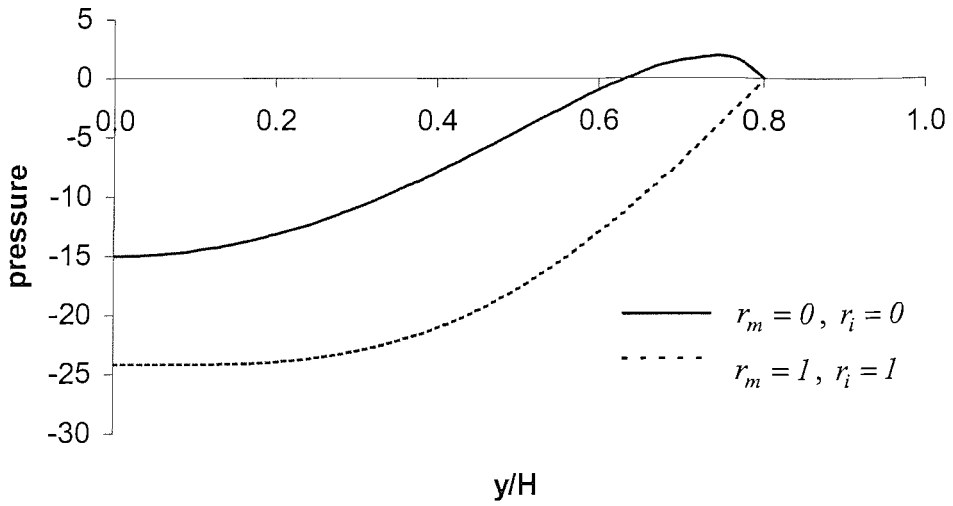

Figure 4.4 Dimensionless water pressure caused by foundation vibration for parameter values $w_0 / H = 0.1$, $\Omega_w = 5 rads/s$, $\nu = 0.8$, $\gamma = 10$, $r_m = 0$, $r_i = 0$ and $r_m = 1$, $r_i = 1$.

From Figure 4.3 and 4.4, we notice that for vibration cases with water ($\nu = 0.8$), displacement for beam without added top mass ($r_m = 0$, $r_i = 0$) shows the first mode whilst displacement for beam with added top mass ($r_m = 1$, $r_i = 1$) shows the second mode. This is because the natural frequencies of the system decrease when top mass is added. The exciting frequency $\Omega_w = 5 rads/s$ is near the first natural frequency of the system for the system without added top mass ($r_m = 0$, $r_i = 0$), and the second natural frequency of the system for the system with added top mass ($r_m = 1$, $r_i = 1$). Yet this exciting frequency does not exactly equal to any natural frequency of the system, therefore the pressure shows the combined frequency effect.

4.2.2 Harmonically excited vibration at the free end of the beam

For the case of a harmonically excited vibration at the free end of the beam, as shown in Figure 2.1, an external force

$$Q(t) = Q_0 e^{i\Omega_q t}, \tag{4.8}$$

acts at this beam position. The responding frequency $\hat{\Omega}$ must be equal to the exciting frequency Ω_q. All the governing equations describing the fluid and solid domain are the same as those presented in Chapter 2 except for modification to the three boundary conditions in equations (2.48) (2.50) and (2.51), which are now given as

$$\overline{U}_1(0) = 0, \tag{4.9}$$

$$\overline{U}_2''(1) = \frac{I_0 \hat{\Omega}^2 H}{EJ} \overline{U}_2'(1), \tag{4.10}$$

$$\overline{U}_2'''(1) = -\frac{m_0 \hat{\Omega}^2 H^3}{EJ} \overline{U}_2(1) + \frac{H^2}{EJ} Q_0, \tag{4.11}$$

Using the results in Chapters 2 and 3, we can write the eight boundary conditions, *i.e.*, equations (4.9), (2.49), (4.10), (4.11), (2.52)-(2.55), in the matrix form,

$$\mathbf{RD} = \tilde{\mathbf{f}}. \tag{4.12}$$

In this equation, both $\mathbf{R}$ and $\mathbf{D}$ have the same form as those given in equations (3.53) and (3.51) and $\tilde{\mathbf{f}}$ represents the vector

$$\tilde{\mathbf{f}}^T = [0 \quad 0 \quad 0 \quad \frac{H^2}{EJ} Q_0 \quad 0 \quad 0 \quad 0 \quad 0]. \tag{4.13}$$

By following the similar procedure described in section 3.5, we derive the dynamic responses of this system.

Table 4.15 $D_j (j = 1, \cdots, 8)$ with $Q_0 = 8.0 \times 10^7 N$, $\Omega_q = 5 rads/s$, $\gamma = 10$, $\nu = 0$ and 0.8, $r_m = 0$, $r_i = 0$ and $r_m = 1$, $r_i = 1$.

	$\nu = 0.8$, $r_m = 0$, $r_i = 0$	$\nu = 0.8$, $r_m = 1$, $r_i = 1$.	$\nu = 0$, $r_m = 0$, $r_i = 0$	$\nu = 0$, $r_m = 1$, $r_i = 1$.
D_1	1.06	4.10E-01	-5.86E-01	-8.58E-02
D_2	7.84E-01	3.03E-01	5.46E-01	8.94E-02
D_3	7.76E-01	3.00E-01	5.86E-01	8.58E-02
D_4	-7.84E-01	-3.03E-01	-5.46E-01	-8.94E-02

D_5	2.03E-01	7.87E-02	7.41E-01	1.08E-01
D_6	-3.36E-01	-1.30E-01	2.62E-02	4.02E-03
D_7	2.03E-01	7.84E-02	7.41E-01	1.10E-01
D_8	2.88E-01	1.11E-01	6.50E-01	9.65E-02

Table 4.15 shows the values of the constants $D_j(j = 1,\cdots,8)$ for different parameters when a forced vibration is applied to the free end of the beam. Free surface waves are neglected. In this example for illustrative purposes, the parameters have value $Q_0 = 8.0\times 10^7 N$, $\Omega_q = 5rads/s$, $\gamma = 10$, $\nu = 0$ and 0.8, $r_m = 0$, $r_i = 0$ and $r_m = 1$, $r_i = 1$.

Figure 4.5 shows the calculated dimensionless longitudinal beam displacement and Figure 4.6 displays the predicted dimensionless water pressure along the beam $P(0,y)$ when an exciting sinusoidal force is applied to the free end of the beam and free surface waves are neglected in the mathematical model, for parameter values $Q_0 = 8.0\times 10^7 N$, $\Omega_q = 5rads/s$, $\gamma = 10$, $\nu = 0$ and 0.8, $r_m = 0$ and 1.

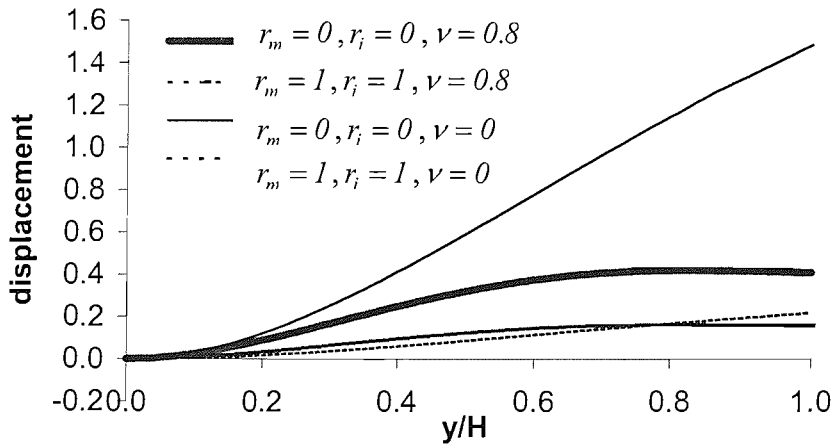

Figure 4.5 Dimensionless longitudinal beam displacement when forced vibration applied to the free end for parameters value $Q_0 = 8.0\times 10^7 N$, $\Omega_q = 5rads/s$, $\gamma = 10$, $\nu = 0$ and 0.8, $r_m = 0$, $r_i = 0$ and $r_m = 1$, $r_i = 1$.

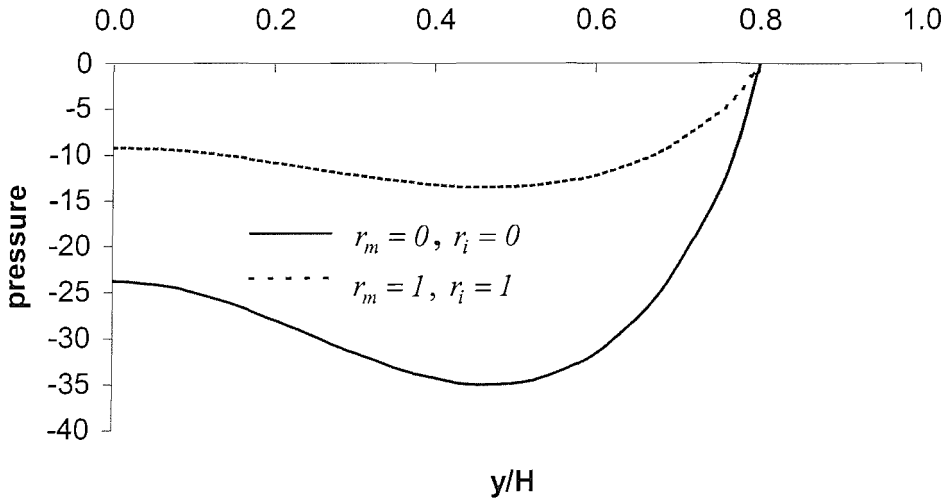

Figure 4.6 Predicted dimensionless water pressure along the beam when forced vibration applied to the free end for parameter values $Q_0 = 8.0 \times 10^7 N$, $\Omega_q = 5 rads/s$, $\gamma = 10$, $\nu = 0.8$, $r_m = 0$, $r_i = 0$ and $r_m = 1$, $r_i = 1$.

These results show that the attached end mass has an important influence in both beam displacement and water pressure. The beam displacement response almost keeps the same shape when top mass added, but its amplitude decreases which means the beam vibration is not as severe as it does without top mass. Therefore, the water pressure is smaller in value. In a similar manner to the first case concluded in section 4.2.1, when the value of r_m increases, the beam displacement decreases and the water pressure clearly decreases as well. This study further indicates that attached top mass and concentrated moment of inertia should be included to derive an exact solution of typical beam-water interaction problems examined herein and to understand the interaction mechanisms.

Chapter 5

System subject to a Sommerfeld radiation condition

To solve wave radiation problems in an infinite domain, Sommerfeld (1949) proposed that a radiation condition be imposed at infinity in the medium. Physically, this represents a disturbance in the water transmitting along the positive x direction with no wave reflected. In order to provide a clear picture of the influence of the Sommerfeld radiation condition on the natural vibration and dynamic response of a two-dimensional elastic beam-water interaction system, sections 5.1 and 5.2 present an investigation of the analytical solutions of the natural frequency of a one-dimensional fluid-mass-spring and a two-dimensional rigid beam-water interaction system, respectively, with the Sommerfeld radiation condition included in the mathematical model. It is shown that natural vibrations of these fluid-structure interaction systems are described by a complex eigenvalue formulation. In later sections, we discuss the natural vibration and dynamic response of the two-dimensional elastic beam-water interaction system.

5.1 Natural vibration of a simple one-dimensional example

Filippi, *et al.* (1999) discussed simple one-dimensional examples in which the Sommerfeld radiation condition was applied. A Fourier transformation method was used to derive the response of a one-dimensional fluid-structure interaction system. In a communication note (Xing (2002)), the natural vibration of a 1-dimensional fluid-structure interaction system subject to Sommerfeld radiation condition was initially discussed. This problem is further investigated in this section. The natural frequencies of a fluid-structure system with imposed Sommerfeld radiation condition at infinity are investigated by using a similar method as described in Chapter 2.

5.1.1 Governing equations

Figure 5.1 shows a linear one-dimensional fluid-structure interaction system. A rigid piston of mass M is connected at the right end wall of a one-dimension semi-infinite long straight channel of section area S by a spring of stiffness K. The left volume of the

channel is filled by a fluid of mass density ρ per unit volume. The fluid is assumed compressible and non-viscous. The origin of the x-axis is located at the natural equilibrium position of the mass. By using the displacement $y(t)$ of the mass and the pressure $p(x,t)$ of the fluid as variables to be determined, the governing equations describing the dynamics of this fluid-structure interaction system are as follows.

Solid structure

$$M\ddot{y} + Ky = -Sp(0,t). \tag{5.1}$$

Fluid domain

$$\frac{\partial^2 p}{\partial x^2} = \frac{1}{c^2}\frac{\partial^2 p}{\partial t^2}, \qquad 0 < x < \infty. \tag{5.2}$$

On the interaction interface

$$\frac{\partial p}{\partial x} = -\rho\frac{\partial^2 y}{\partial t^2}, \qquad x = 0. \tag{5.3}$$

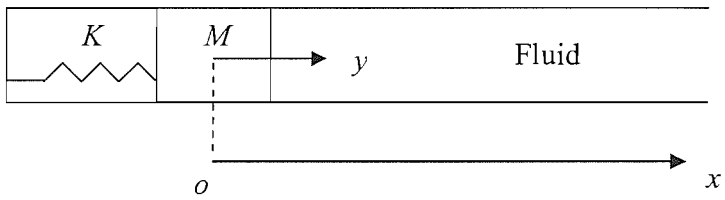

Figure 5.1 A one-dimensional fluid-structure interaction system

Radiation condition on the infinite boundary

The Sommerfeld condition requires the fluid pressure to be described by a form $p(x-ct)$ indicating a wave travels with velocity c along the x direction. Physically, the Sommerfeld condition assumes there exists no wave reflection from the right end of the fluid channel. Therefore, the radiation condition is represented as follows,

$$\frac{\partial p}{\partial x} = -\frac{1}{c}\frac{\partial p}{\partial t}, \qquad x \to \infty. \tag{5.4}$$

Equations (5.1)-(5.3) with equation (5.4) describes an eigenvalue problem formulating the natural vibration of the fluid-solid interaction system.

5.1.2 Eigenvalue solutions of the problem

On using the separation of variable method, it is assumed that

$$p(x,t) = P(x)T(t), \qquad y = XT(t), \tag{5.5}$$

which when substituted into equations (5.1)-(5.4) gives

$$\left(K - \Omega^2 M\right)X = -SP(0), \tag{5.6}$$

$$\ddot{T} + \Omega^2 T = 0, \tag{5.7}$$

$$P'' + \frac{\Omega^2}{c^2}P = 0, \tag{5.8}$$

$$\frac{P'}{P} = -\frac{\dot{T}}{cT}, \qquad x \to \infty, \tag{5.9}$$

$$P' = \rho\Omega^2 X, \qquad x = 0, \tag{5.10}$$

where Ω is a constant to be determined.

Case I: $\Omega^2 = 0$

The solutions of equations (5.7) and (5.8) are given by

$$T(t) = At + B, \tag{5.11}$$

$$P(x) = ax + b, \tag{5.12}$$

where the unknown constants are determined using the boundary conditions. From equation (5.9), it follows that

$$a = 0 = A, \quad P = b, \quad T = B, \tag{5.13}$$

which represents a constant fluid pressure solution given by

$$p = 1, \qquad P = 1, \quad T = 1. \tag{5.14}$$

It also follows from equation (5.6) that the corresponding mass displacement is

$$y = -\frac{1}{K}, \qquad X = -\frac{1}{K}. \tag{5.15}$$

Physically, this solution represents a static constant pressure applied at the infinite right end of the fluid channel.

Case II: $\Omega^2 \neq 0$

From equations (5.7) and (5.8), we obtain solutions of the form

$$T(t) = Ae^{\mathbf{i}\Omega t} + Be^{-\mathbf{i}\Omega t}, \tag{5.16}$$

$$P(x) = ae^{\mathbf{i}\frac{\Omega}{c}x} + be^{-\mathbf{i}\frac{\Omega}{c}x}. \tag{5.17}$$

and the possible solution is

$$P = ae^{\mathbf{i}\frac{\Omega}{c}x}, \quad T = e^{-\mathbf{i}\Omega t}, \quad p = ae^{\mathbf{i}\frac{\Omega}{c}(x-ct)}, \tag{5.18}$$

where $\Omega = \Omega_r + \mathbf{i}\Omega_i$ is an imaginary number. The substitution of equation (5.18) into equations (5.6) and (5.10) produces the corresponding characteristic equation

$$\begin{bmatrix} K - \Omega^2 M & S \\ \rho c \Omega & -\mathbf{i} \end{bmatrix} \begin{Bmatrix} X \\ a \end{Bmatrix} = 0. \tag{5.19}$$

The necessary condition for equation (5.19) to provide a non-zero solution is that the determinant of the coefficient matrix is equal to zero, i.e.,

$$\Omega^2 + 2\eta\mathbf{i}\Omega - \omega^2 = 0. \tag{5.20}$$

where $\omega^2 = K / M$ represents the square of the natural frequency of the mass-spring system and $\eta = \dfrac{S\rho c}{2M}$ represents a damping coefficient. The solution of equation (5.20) is

$$\Omega = \pm\sqrt{\omega^2 - \eta^2} - \mathbf{i}\eta. \tag{5.21}$$

It is noted that one derives the same solution for Ω when assuming $p = ae^{-\mathbf{i}\frac{\Omega}{c}(x-ct)}$.

For the situation $\eta < \omega$, the solution given in equation (5.18) corresponds to mode functions

$$\begin{aligned} P &= \bar{a}e^{\frac{\eta}{c}x}e^{\pm\mathbf{i}\frac{\tilde{\Omega}}{c}x}, \\ T &= e^{-\eta t}e^{\mp\mathbf{i}\tilde{\Omega}t}, \\ p &= \bar{a}e^{\frac{\eta}{c}(x-ct)}e^{\pm\mathbf{i}\frac{\tilde{\Omega}}{c}(x-ct)}, \end{aligned} \tag{5.22}$$

where $\tilde{\Omega} = \sqrt{\omega^2 - \eta^2} > 0$. The solution of the free vibration of the system is represented by the real form

$$p = ae^{\frac{\eta}{c}(x-ct)}\left\{A_1 cos\left[\frac{\tilde{\Omega}}{c}(x-ct)\right] + B_1 sin\left[\frac{\tilde{\Omega}}{c}(x-ct)\right]\right\},$$

$$y = Xe^{-\eta t}\left[A_2 cos\left(\tilde{\Omega}\, t\right) + B_2 sin\left(\tilde{\Omega}\, t\right)\right], \tag{5.23}$$

where the constants a, A_1, B_1, A_2 and B_2 are determined from imposed initial conditions.

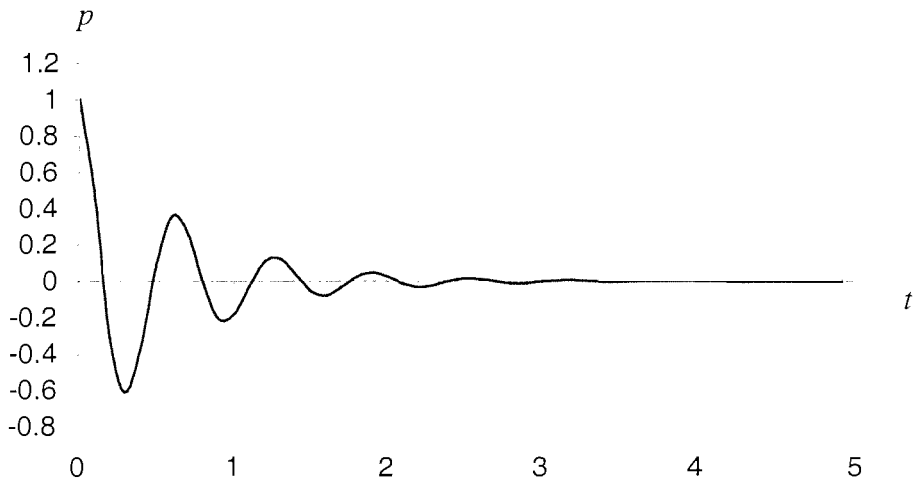

Figure 5.2 Fluid pressure time history at point $x = 0$
($\eta = 1.6$, $\omega = 10.0$, $c = 1439$).

For illustration purpose, values of $a = 1$, $A_1 = 1$, $B_1 = 0$, $A_2 = 1$, $B_2 = 0$ are used in Figures 5.2 and 5.3, which represents the initial condition of the mass at its negative maximum displacement. The value of X is calculated from equation (5.19). Figure 5.2 shows the pressure time history at point $x = 0$, and Figure 5.3 displays the mass displacement time history for the same parameter values $\eta = 1.6$, $\omega = 10.0$, $c = 1439$. It is noted that pressure p and displacement y in Figures 5.2 and 5.3, as well as later in Figures 5.4 and 5.5, are not dimensionless, which have the same dimension as constants a and X, respectively. They can be of any dimension depending on the initial conditions.

For the case of $\eta \geq \omega$, the solution presented in equation (5.18) takes the form

$$P = \bar{a}e^{\frac{\eta}{c}x}e^{\mp\frac{\hat{\Omega}}{c}x},$$

$$T = e^{-\eta t}e^{\pm\hat{\Omega}t},$$

$$p = \bar{a} e^{\frac{\eta}{c}(x-ct)} e^{\mp\frac{\hat{\Omega}}{c}(x-ct)}, \tag{5.24}$$

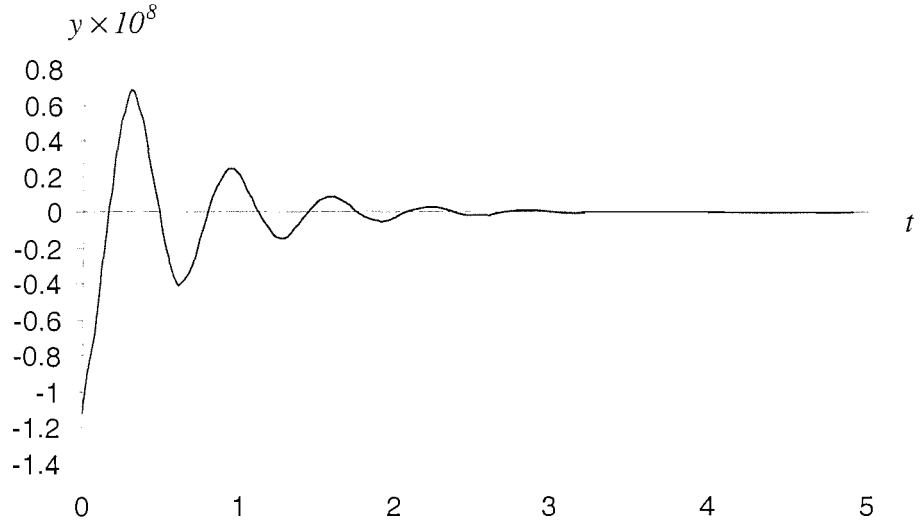

Figure 5.3 Mass displacement time history
($\eta = 1.6$, $\omega = 10.0$, $c = 1439$).

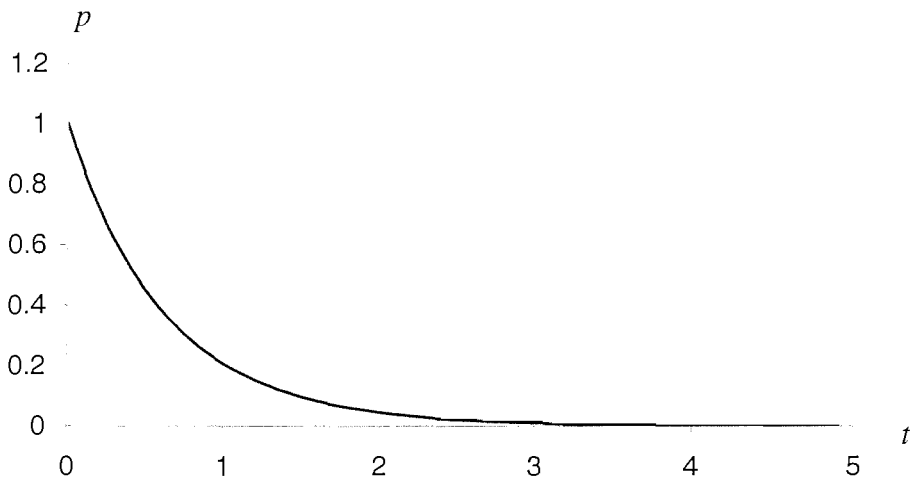

Figure 5.4 Fluid pressure time history at point $x = 0$
($\eta = 1.6$, $\omega = 1.58$, $c = 1439$).

where $\eta > \hat{\Omega} = \sqrt{\eta^2 - \omega^2} > 0$. In this case, the solution describing the free vibration of the system has the real form

$$p = ae^{\frac{\eta}{c}(x-ct)}\left\{A_1 cosh\left[\frac{\hat{\Omega}}{c}(x-ct)\right] + B_1 sinh\left[\frac{\hat{\Omega}}{c}(x-ct)\right]\right\},$$

$$y = Xe^{-\eta t}\left[A_2 cosh\left(\hat{\Omega}\, t\right) + B_2 sinh\left(\hat{\Omega}\, t\right)\right]. \tag{5.25}$$

Figure 5.4 illustrates the fluid pressure variation at point $x = 0$, whereas Figure 5.5 demonstrates the mass displacement time history for the same parameter values $\eta = 1.6$, $\omega = 1.58$, $c = 1439$. For illustration purpose, values of $a = 1$, $A_1 = 1$, $B_1 = 0$, $A_2 = 1$, $B_2 = 0$ are used in Figures 5.4 and 5.5. The value of X is calculated from equation (5.19).

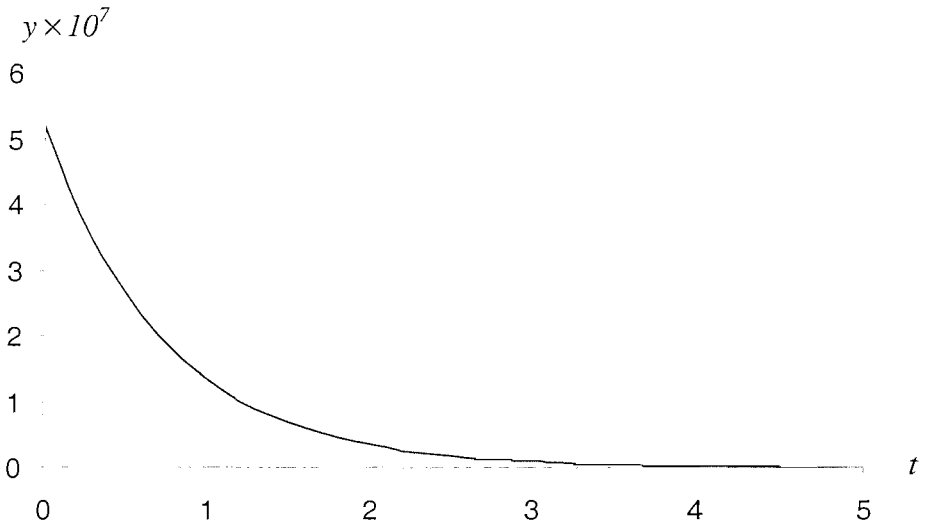

Figure 5.5 Mass displacement time history
($\eta = 1.6$, $\omega = 1.58$, $c = 1439$).

The dynamic behaviour of the fluid-mass-spring interactive system subject to a Sommerfeld condition is similar to a viscous damped free vibration as discussed by Thomson (1988).

5.1.3 Summary

As shown by the solutions presented in equations (5.22) and (5.24), the time function $T(t)$ includes an exponential varying time decaying term. Therefore, the imposition of the Sommerfeld condition contributes to energy dissipating from the system with energy transmitting from the structure to infinity along the x direction. The damping term

$\eta = \frac{S\rho c}{2M}$ is proportional to the travelling wave velocity c and the mass ratio ρ / M. At large travelling wave velocity values, energy transmits faster along the x direction from the structure, and therefore the damping term is increased in value. When the damping term $\eta = \frac{S\rho c}{2M}$ is a value less than the natural frequency ω of the structure, the system is referred to as under-damped and free oscillations of the fluid-structure interaction system are possible. When the damping term $\eta = \frac{S\rho c}{2M}$ is a value larger than the natural frequency ω of the structure, the system is referred to as over-damped and no oscillations of the system are possible. The previous discussion proves and demonstrates that natural vibrations of a fluid-structure interaction system subject to Sommerfeld condition are governed by a complex eigenvalue equation, and therefore a method suitable to solve complex eigenvalue problems has to be used.

5.2 Two-dimensional rigid rod-water interaction system

In this illustrative example, it is assumed that the beam is rigid and supported by a coiled spring of stiffness K attached to the bottom of the beam as illustrated in Figure 5.6. The system is assumed linear and able to rotate through angle θ whose positive direction is clockwise. Therefore, the governing linear differential equations describe small vibrations of the beam.

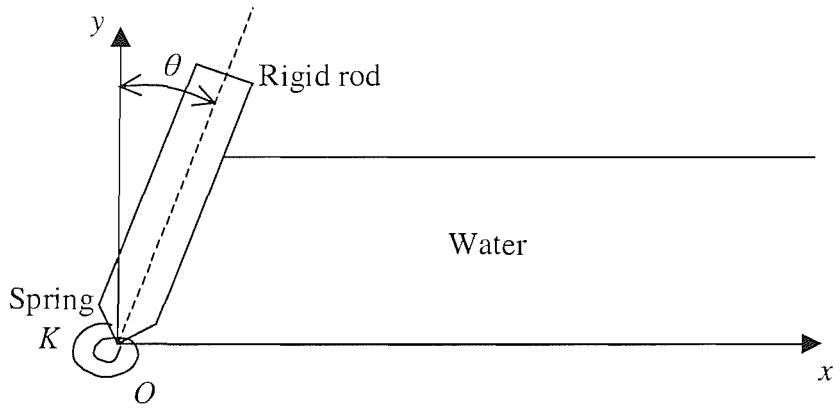

Figure 5.6 Rigid rod-water interaction system

5.2.1 Governing equations

Fluid domain

$$\frac{\partial^2 p}{\partial x^2}+\frac{\partial^2 p}{\partial y^2}=\frac{1}{c^2}\frac{\partial^2 p}{\partial t^2}, \qquad 0<x<\infty, \quad 0<y<h. \tag{5.26}$$

Structure domain

$$J\ddot{\theta}+K\theta=\int_0^h p(0,y,t)Bydy. \tag{5.27}$$

Fluid-structure interaction interface

$$\rho_f y\ddot{\theta}=\frac{\partial p}{\partial x}, \qquad x=0, \qquad 0<y<h. \tag{5.28}$$

Fluid domain boundary conditions

In this investigation a zero free surface wave disturbance is assumed on the free surface,

$$p=0, \qquad \text{at} \quad y=h. \tag{5.29}$$

In a subsequent study (see section 5.3), examining an elastic beam a free surface disturbance is included. It therefore follows that by choosing a suitable stiffness value of the beam, the rigid-free surface disturbance problem can be derived.

On the bottom of the reservoir, assumed impermeable and rigid,

$$\partial p/\partial y=0, \qquad \text{at} \quad y=0. \tag{5.30}$$

At infinity in the water domain, the Sommerfeld radiation condition is assumed in the form

$$p(x,y,t)=P(x,y)e^{-\mathrm{i}\hat{\Omega}t}, \quad P_{,x}-\mathrm{i}\hat{\lambda}P=0, \quad x\to\infty, \tag{5.31}$$

5.2.2 Solutions for $p(x,y,t)$ and $\theta(t)$

By using the separation of variable method, we seek solutions of the pressure p, rotation angle θ in the forms

$$p(x,y,t)=P(x,y)T(t)=X(x)Y(y)T(t), \tag{5.32}$$

$$\theta(t)=\varphi T(t). \tag{5.33}$$

By introducing the following parameters,

$$\bar{x} = x / H, \qquad \bar{y} = y / H, \qquad \omega^2 = \frac{K}{J} T^2,$$

$$T = H / c, \qquad \tilde{g} = \frac{g}{H / T^2}, \qquad \tilde{\rho} = \rho_f / \rho_s,$$

$$J = \frac{\rho_s S H^3}{3}, \qquad \bar{F} = \rho_f g H, \qquad p = \bar{F}\,\bar{p},$$

$$t = T\tau, \qquad \bar{M} = \frac{\bar{F} H^3 T^2}{J}. \tag{5.34}$$

we derive the dimensionless form of equations (5.18)-(5.20) as

$$\frac{\partial^2 \bar{p}}{\partial \bar{x}^2} + \frac{\partial^2 \bar{p}}{\partial \bar{y}^2} = \frac{\partial^2 \bar{p}}{\partial \tau^2}, \tag{5.35}$$

$$\frac{\partial^2 \theta}{\partial \tau^2} + \omega^2 \theta = \bar{M} \int_0^1 \bar{p}(0, \bar{y}, \tau) \bar{B} \bar{y} d\bar{y}, \tag{5.36}$$

$$\frac{\partial \bar{p}}{\partial \bar{x}} = \frac{\rho_f H^2}{\bar{F} T^2} \bar{y} \frac{\partial^2 \theta}{\partial \tau^2} = \frac{H}{g T^2} \bar{y} \frac{\partial^2 \theta}{\partial \tau^2} = \frac{1}{\tilde{g}} \bar{y} \frac{\partial^2 \theta}{\partial \tau^2}, \qquad \text{at } \bar{x} = 0. \tag{5.37}$$

As the water pressure satisfies the same equation as derived for the two-dimensional elastic beam-water problem discussed in Chapters 2 and 3, one can use the results presented in these Chapters. It follows from equations (3.1), (3.2), (3.4) and (3.5) that the functions $T(t)$ and $X(x)$ satisfying equation (5.31) (constant coefficients neglected) are of the form

$$X(\bar{x}) T(\tau) = \begin{cases} 1, & \Omega = 0 = \lambda \\ e^{\mathrm{i}(\lambda \bar{x} - \Omega \tau)}, & \Omega \neq 0 \quad or \quad \lambda \neq 0 \end{cases}. \tag{5.38}$$

When free surface waves are neglected, solutions for $Y(\bar{y})$ expressed in equations (3.21) and (3.22) remain valid and are given by

$$Y(\bar{y}) \equiv 0, \qquad \text{for } \hat{\kappa} = 0 \text{ or } \hat{\kappa} = \mathrm{i}\kappa, \tag{5.39}$$

$$Y_n(\bar{y}) = \cos(\kappa_n \bar{y}), \text{ for } \kappa_n = (2n-1)\pi / 2,\ n = 1,2,3,\cdots, \tag{5.40}$$

$$\lambda_n^2 = \Omega^2 - \kappa_n^2. \tag{5.41}$$

Therefore, the pressure p and rotation angle θ can be expressed as

$$p(x,y,t) = \overline{F}\,\overline{p}(\overline{x},\overline{y},\tau) = \overline{F}\sum_{n=1}^{\infty} A_n e^{\mathrm{i}\lambda\overline{x}} cos(\kappa_n \overline{y}) e^{-\mathrm{i}\Omega\tau}\,, \tag{5.42}$$

$$\theta = \varphi e^{-\mathrm{i}\Omega\tau}\,. \tag{5.43}$$

To calculate pressure p, N terms of the series in equation (5.42) are adopted. This allows equation (5.42) to be re-written in the matrix form,

$$\overline{p}(\overline{x},\overline{y},\tau) = \sum_{n=1}^{N} A_n e^{\mathrm{i}\lambda\overline{x}} cos(\kappa_n \overline{y}) e^{-\mathrm{i}\Omega\tau}$$

$$= e^{-\mathrm{i}\Omega\tau}\left[e^{\mathrm{i}\lambda_1\overline{x}} cos(\kappa_1\overline{y}) \quad \cdots \quad e^{\mathrm{i}\lambda_n\overline{x}} cos(\kappa_n\overline{y}) \quad \cdots \quad e^{\mathrm{i}\lambda_N\overline{x}} cos(\kappa_N\overline{y})\right]\begin{bmatrix} A_1 \\ \vdots \\ A_n \\ \vdots \\ A_N \end{bmatrix}. \tag{5.44}$$

Substituting equations (5.43) and (5.44) into equation (5.36), we obtain

$$\varphi(\omega^2 - \Omega^2) = \overline{M}\int_0^1 \left[\overline{y}cos(\kappa_1\overline{y}) \quad \cdots \quad \overline{y}cos(\kappa_n\overline{y}) \quad \cdots \quad \overline{y}cos(\kappa_N\overline{y})\right]\begin{bmatrix} A_1 \\ \vdots \\ A_n \\ \vdots \\ A_N \end{bmatrix} d\overline{y}$$

$$= \overline{M}\;\overline{E}\;\overline{A}\,, \tag{5.45}$$

where

$$\overline{A} = \begin{bmatrix} A_1 \\ \vdots \\ A_n \\ \vdots \\ A_N \end{bmatrix},\quad \overline{E} = \left[E_1 \quad \cdots \quad E_n \quad \cdots \quad E_N\right],$$

$$E_n = \int_0^1 \overline{y}cos(\kappa_n\overline{y})d\overline{y} = \frac{(-1)^{n+1}2}{(2n-1)\pi} - \frac{4}{(2n-1)^2\pi^2}, \quad n = 1,2,\cdots,N\,.$$

The substitution of equations (5.43) and (5.44) into equation (5.37) gives

$$-\frac{1}{\tilde{g}}\overline{y}\Omega^2\varphi = \mathbf{i}\left[\lambda_1 cos(\kappa_1\overline{y}) \quad \cdots \quad \lambda_N cos(\kappa_N\overline{y})\right]\overline{A}\,. \tag{5.46}$$

Multiplying both sides of equation (5.46) by $Y_n(\bar{y}) = cos(\kappa_n \bar{y})$ and integrating from 0 to 1 with respect to $\bar{y}$ and using the orthogonality relation of the functions $Y_n(\bar{y})$

$$\int_0^1 Y_n(\bar{y}) Y_m(\bar{y}) d\bar{y} = \begin{cases} 0, & m \neq n, \\ \frac{1}{2} + \frac{(-1)^{n+1} 1}{2(2n-1)\pi} = I_n, & m = n, \end{cases} \tag{5.47}$$

we derive the result,

$$\frac{1}{\tilde{g}} \Omega^2 \bar{E}^T \varphi + \mathbf{i} \bar{I}_N \bar{A} = 0, \tag{5.48}$$

where $\bar{E}^T$ is the transpose of vector $\bar{E}$, and

$$\bar{I}_N = \begin{bmatrix} \lambda_1 I_1 & 0 & \cdots & 0 \\ 0 & \lambda_2 I_2 & \cdots & 0 \\ \vdots & \cdots & \ddots & \vdots \\ 0 & \cdots & 0 & \lambda_N I_N \end{bmatrix},$$

$$I_n = \int_0^1 cos^2(\kappa_n \bar{y}) d\bar{y} = \frac{1}{2} + \frac{(-1)^{n+1} 1}{2(2n-1)\pi}, \quad n = 1,2,\cdots,N .$$

Equations (5.45) and (5.48) combine to give the matrix form,

$$\begin{pmatrix} \omega^2 - \Omega^2 & -\bar{M}\ \bar{E} \\ \frac{1}{\tilde{g}} \Omega^2 \bar{E}^T & \mathbf{i} \bar{I}_N \end{pmatrix} \begin{pmatrix} \varphi \\ \bar{A} \end{pmatrix} = 0 . \tag{5.49}$$

To determine the natural frequency parameter Ω of the coupled system described by this linear homogeneous system of algebraic equations, the characteristic eigenvalue equation of the beam-water system is given by

$$\begin{vmatrix} \omega^2 - \Omega^2 & -\bar{M}\ \bar{E} \\ \frac{1}{\tilde{g}} \Omega^2 \bar{E}^T & \mathbf{i} \bar{I}_N \end{vmatrix} = 0 . \tag{5.50}$$

Before deriving the numerical solutions, we analyse and discuss the possible values of the parameters Ω, λ, κ as follows:

1) $\Omega = \Omega_r + \mathbf{i}\Omega_i$, where Ω_r and Ω_i are real numbers. To satisfy the radiation condition, the time function has the form $e^{-\mathbf{i}\Omega t} = e^{-\mathbf{i}(\Omega_r + \mathbf{i}\Omega_i)t} = e^{\Omega_i t} e^{-\mathbf{i}\Omega_r t}$, a negative

real number value of Ω_i produces a decreasing vibration with time because of energy dissipation resulting from imposition of the radiation condition.

2) $\lambda = \lambda_r + \mathbf{i}\lambda_i$, where λ_r and λ_i are real numbers. To satisfy the radiation condition, the water pressure has the form

$$P(x,t) = e^{\mathbf{i}(\lambda x - \Omega t)} = e^{\mathbf{i}(\lambda_r + \mathbf{i}\lambda_i)x} e^{-\mathbf{i}(\Omega_r + \mathbf{i}\Omega_i)t} = e^{-\lambda_i x + \Omega_i t} e^{\mathbf{i}(\lambda_r x - \Omega_r t)}.$$

Furthermore, to produce a travelling wave solution along the x direction, λ_i must be a negative real number and both λ_r and Ω_r, negative or positive at the same time. Therefore, the function $P(x,t)$ has the form $e^{-\lambda_i x + \Omega_i t} e^{\pm \mathbf{i}(\lambda_r x - \Omega_r t)}$ for $\Omega_i < 0$, $\lambda_i < 0$, $\Omega_r > 0$, $\lambda_r > 0$.

For the case when free surface waves are neglected, κ is a real number given by equation (5.40).

After the natural frequency Ω is found by solving equation (5.50), we can evaluate the coefficient parameters φ and A_n $(n = 1,2,...,N)$ by substituting Ω into equation (5.49) and eliminating one of the equations in equation (5.49). Setting $\varphi = 1$ or giving a value to any one of the terms A_n allows solution of the remaining equations and thus we derive a relation between φ and A_n. It follows from equations (5.42) and (5.43) that we can now determine the corresponding water pressure mode and beam rotation angle mode for this natural frequency.

5.2.3 Numerical examples

a) $N = 1$

For the simple case $N = 1$ (N is the number of adopted terms of the series in equation (5.42)), equation (5.50) is of the form

$$\begin{vmatrix} \omega^2 - \Omega^2 & -\overline{M}\, E_1 \\ \dfrac{1}{\tilde{g}}\Omega^2 E_1 & \mathbf{i}\lambda_1 I_1 \end{vmatrix} = 0, \tag{5.51}$$

giving

$$\mathbf{i}\lambda_1 I_1 (\omega^2 - \Omega^2) + \frac{\overline{M}}{\tilde{g}}\Omega^2 E_1^2 = 0. \tag{5.52}$$

to confirm. I.S.

Equation (5.41) for $n = 1$ reduces to

$$\Omega^2 = \lambda_1^2 + \kappa_1^2, \tag{5.53}$$

and the substitution of this equation into equation (5.52) gives

$$-\mathbf{i}I_1\lambda_1^3 + \frac{\overline{M}}{\widetilde{g}}E_1^2\lambda_1^2 + \mathbf{i}I_1\left(\omega^2 - \kappa_1^2\right)\lambda_1 + \frac{\overline{M}}{\widetilde{g}}E_1^2\kappa_1^2 = 0. \tag{5.54}$$

If it is assumed that $\lambda_1 = \mathbf{i}\xi$, equation (5.54) changes into

$$a_3\xi^3 + a_2\xi^2 + a_1\xi + a_0 = 0, \tag{5.55}$$

in which

$$a_3 = I_1,\ a_2 = \frac{\overline{M}}{\widetilde{g}}E_1^2,\ a_1 = I_1\left(\omega^2 - \kappa_1^2\right) = a_3\left(\omega^2 - \kappa_1^2\right),$$

$$a_0 = -\frac{\overline{M}}{\widetilde{g}}E_1^2\kappa_1^2 = -a_2\kappa_1^2,$$

are all real numbers.

If we assume $\xi = \zeta - \dfrac{a_2}{3a_3}$, equation (5.55) transforms into

$$\zeta^3 + \alpha\zeta + \beta = 0, \tag{5.56}$$

where $\alpha = \dfrac{a_1}{a_3} - \dfrac{a_2^2}{3a_3^2}$, $\beta = \dfrac{a_0}{a_3} - \dfrac{a_1a_2}{3a_3^2} + \dfrac{2a_2^3}{27a_3^3}$. The roots of this equation are (see Cohn (1974)):

$$\begin{cases} \zeta_1 = q_1 + q_2 \\ \zeta_2 = \omega_1 \times q_1 + \omega_2 \times q_2, \\ \zeta_3 = \omega_2 \times q_1 + \omega_1 \times q_2 \end{cases} \tag{5.57}$$

where

$$q_1 = \sqrt[3]{-\frac{\beta}{2} + \sqrt{\Delta}} = \sqrt[3]{-\frac{\beta}{2} + \sqrt{\frac{\beta^2}{4} + \frac{\alpha^3}{27}}},$$

$$q_2 = \sqrt[3]{-\frac{\beta}{2} - \sqrt{\Delta}} = \sqrt[3]{-\frac{\beta}{2} - \sqrt{\frac{\beta^2}{4} + \frac{\alpha^3}{27}}},$$

$$\omega_1 = \frac{-1 + \sqrt{3}\mathbf{i}}{2},\ \omega_2 = \frac{-1 - \sqrt{3}\mathbf{i}}{2}\ (\omega_1 \text{ and } \omega_2 \text{ satisfy equation } x^3 - 1 = 0),$$

$$\lambda_1 = \mathbf{i}\xi = \mathbf{i}\left(\zeta - \frac{a_2}{3a_3}\right). \tag{5.58}$$

Here, we find that the determinant

$$\Delta = \frac{\beta^2}{4} + \frac{\alpha^3}{27}$$

$$= \frac{1}{4}\left(\frac{a_0}{a_3} - \frac{a_1 a_2}{3a_3^2} + \frac{2a_2^3}{27a_3^3}\right)^2 + \frac{1}{27}\left(\frac{a_1}{a_3} - \frac{a_2^2}{3a_3^2}\right)^3$$

$$= \frac{1}{4}\left(\frac{a_0^2}{a_3^2} + \frac{a_1^2 a_2^2}{9a_3^4} + \frac{4a_2^6}{27^2 a_3^6} - \frac{2a_0 a_1 a_2}{3a_3^3} + \frac{4a_0 a_2^3}{27a_3^4} - \frac{4a_1 a_2^4}{81a_3^5}\right)$$

$$+ \frac{1}{27}\left(\frac{a_1^3}{a_3^3} - \frac{a_2^6}{27a_3^6} - 3\frac{a_1^2 a_2^2}{3a_3^4} + 3\frac{a_1 a_2^4}{9a_3^5}\right)$$

$$= \frac{a_0^2}{4a_3^2} + \frac{a_1^2 a_2^2}{36a_3^4} - \frac{a_0 a_1 a_2}{6a_3^3} + \frac{a_0 a_2^3}{27a_3^4} + \frac{a_1^3}{27a_3^3} - \frac{a_1^2 a_2^2}{27a_3^4}$$

$$= \frac{1}{a_3^5}\left(\frac{a_0^2 a_3^3}{4} - \frac{a_1^2 a_2^2 a_3}{108} - \frac{a_0 a_1 a_2 a_3^2}{6} + \frac{a_0 a_2^3 a_3}{27} + \frac{a_1^3 a_3^2}{27}\right). \tag{5.59}$$

Furthermore, if we let $\eta = \frac{a_2^2}{a_3^2}$, and write $a_1 = a_3\left(\omega^2 - \kappa_1^2\right)$, $a_0 = -a_2\kappa_1^2$, the determinant is expressible in the form,

$$\Delta = \frac{1}{a_3^5}\left(\frac{a_2^2\kappa_1^4 a_3^3}{4} - \frac{a_3^3\left(\omega^2 - \kappa_1^2\right)^2 a_2^2}{108} - \frac{-a_2^2\kappa_1^2 a_3^3\left(\omega^2 - \kappa_1^2\right)}{6}\right.$$

$$\left. + \frac{-a_2^4\kappa_1^2 a_3}{27} + \frac{a_3^5\left(\omega^2 - \kappa_1^2\right)^3}{27}\right)$$

$$= \eta\left(\frac{\kappa_1^4}{4} - \frac{\left(\omega^2 - \kappa_1^2\right)^2}{108} + \frac{\kappa_1^2\left(\omega^2 - \kappa_1^2\right)}{6}\right) - \eta^2\frac{\kappa_1^2}{27} + \frac{\left(\omega^2 - \kappa_1^2\right)^3}{27}.$$

(5.60)

Again, if we let $s = \omega^2$, this equation transforms into,

$$\Delta = \eta\left(\frac{\kappa_1^4}{4} - \frac{\left(s - \kappa_1^2\right)^2}{108} + \frac{\kappa_1^2\left(s - \kappa_1^2\right)}{6}\right) - \eta^2\frac{\kappa_1^2}{27} + \frac{\left(s - \kappa_1^2\right)^3}{27}. \tag{5.61}$$

This is a third-order polynomial in s with real valued coefficients. By examining the first and second differential of this function with respect to s, we find that

$$\Delta'(s) = \eta\left(-\frac{s-\kappa_1^2}{54}+\frac{\kappa_1^2}{6}\right)+\frac{\left(s-\kappa_1^2\right)^2}{9}, \tag{5.62}$$

$$\Delta''(s) = -\frac{\eta}{54}+\frac{2\left(s-\kappa_1^2\right)}{9}. \tag{5.63}$$

indicating only one turning point $s = \kappa_1^2 + \frac{\eta}{12}$ when $\Delta''(s) = 0$. When s is large enough, $\Delta'(s) > 0$, $\Delta''(s) > 0$, $\Delta(s)$ is an increasing function.

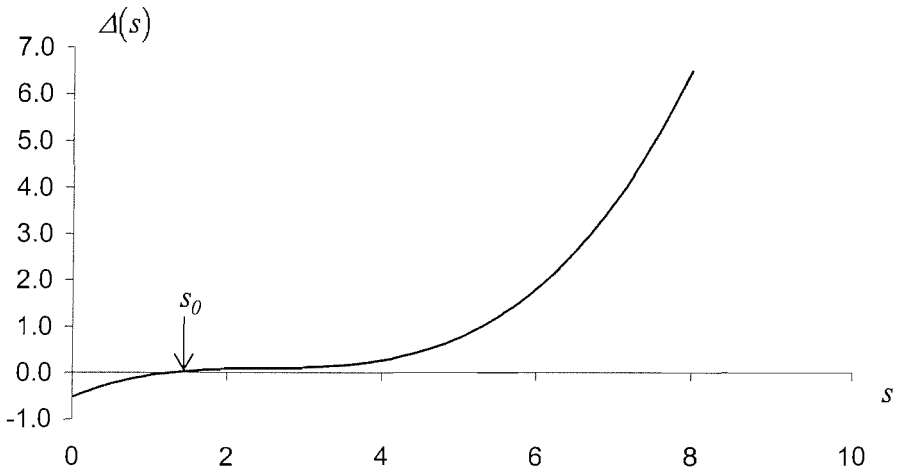

Figure 5.7 Zeros of function $\Delta(s)$

Figure 5.7 illustrates the computed function $\Delta(s)$ in the region $0 \le s \le 8.0$. Figure 5.7 is obtained by connecting each point of the calculated value of function $\Delta(s)$ for each s in the range of $[0,8.0]$ with increment of 0.1. The zero value occurs when $s = s_0 = 1.29$.

We can see from Figure 5.7 that, after $s > s_0$, $\Delta(s)$ is always increasing and therefore $\Delta(s)$ is always positive for $s > s_0$. For positive determinant, there exist one real root and two conjugate complex root solutions to equation (5.56). Similar to the one-dimensional case, the real root solution represents a constant static pressure at infinity, and the two conjugate complex root solutions are the radiation condition solution we are looking for. In Figure 5.7, when $0 < s < s_0$, the determinant $\Delta(s) < 0$, there exist three different real

roots for equation (5.56). But the stiffness K of the spring has a minimum value in order to keep the rigid rod standing upward possible. The value $s = \omega^2 = \frac{K}{J}T^2 = s_0$ represents this minimum value for the structure. Therefore cases for $\Delta(s) < 0$ do not exist.

For the case $\kappa_1 = \frac{\pi}{2}$, $I_1 = \frac{1}{2} + \frac{1}{2\pi}$, $\omega^2 = 2.4$, $\frac{\overline{M}}{\widetilde{g}} = 3.0$, only one solution is found that satisfies the radiation condition and this is given by

$$\begin{cases} \Omega = 1.65 - 0.22\mathbf{i} \\ \lambda_1 = 0.70 - 0.52\mathbf{i} \end{cases}. \tag{5.64}$$

We now can evaluate the coefficient parameters φ and A_1 by substituting Ω and λ_1 into equation (5.49) and eliminating one of the equations in equation (5.49). Setting $\varphi = 1$ or giving a value to A_1 allows solution of the remaining equations and thus we derive a relation between φ and A_1. It follows from equations (5.44) and (5.43) that we can now determine the corresponding dimensionless water pressure $\overline{p}$ mode and beam rotation angle θ mode for this natural frequency.

In the following numerical examples, for $N = 1$, we set $A_1 = 1$, therefore from equation (5.44) the amplitude of dimensionless pressure $\overline{p}$ is 1; for $N = 2$ and $N = 3$, we use $\varphi = 1$, therefore from equation (5.43) the amplitude of rotation angle θ is 1.

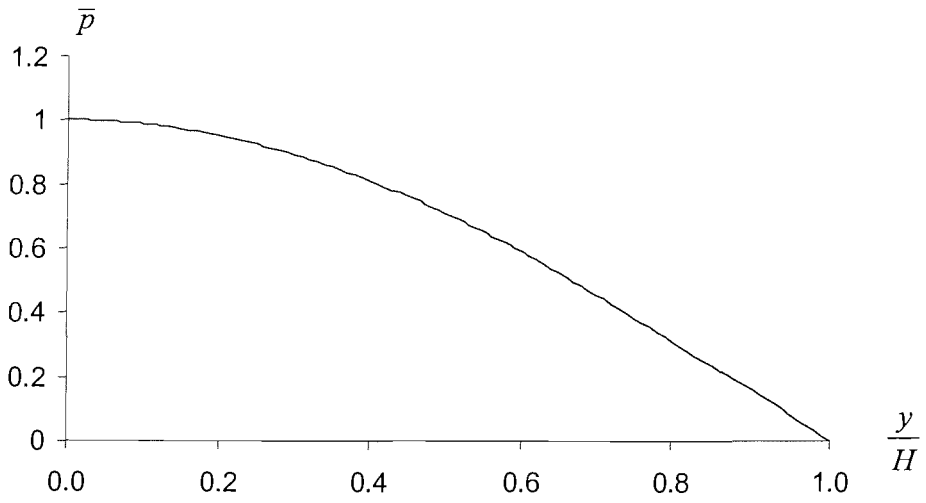

Figure 5.8 Dimensionless water pressure along rigid rod at time $t = 0$.
(Rigid rod-water two-dimension case, $N = 1$)

Figure 5.8 illustrates the dimensionless water pressure along the rigid rod at dimensionless time $\tau = 0$. Figures 5.9 and 5.10 display the time histories of the dimensionless water pressure $\overline{p}$ (at point $x = 0$, $y = 0$) and the rigid rod rotation angle θ for the solution presented in equation (5.64).

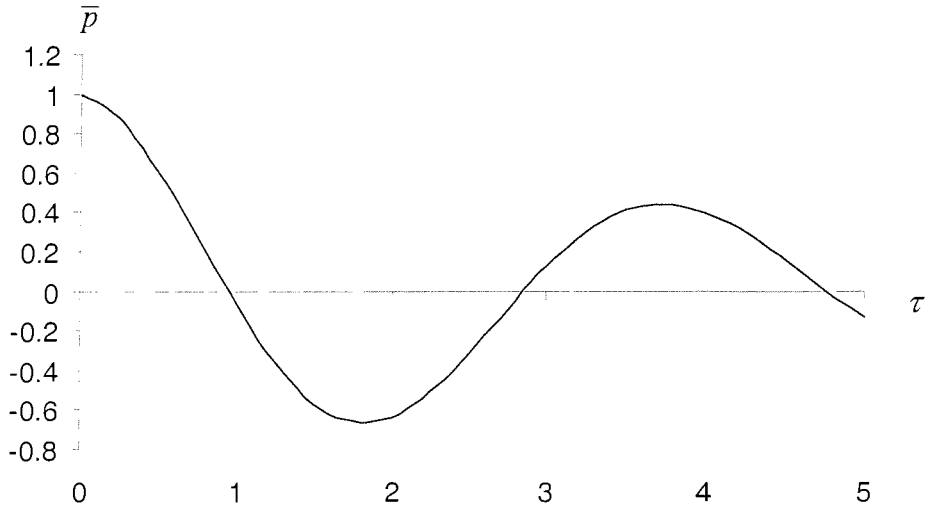

Figure 5.9 Dimensionless water pressure time history at point $x = 0$, $y = 0$.
(Rigid rod-water two-dimension case, $N = 1$)

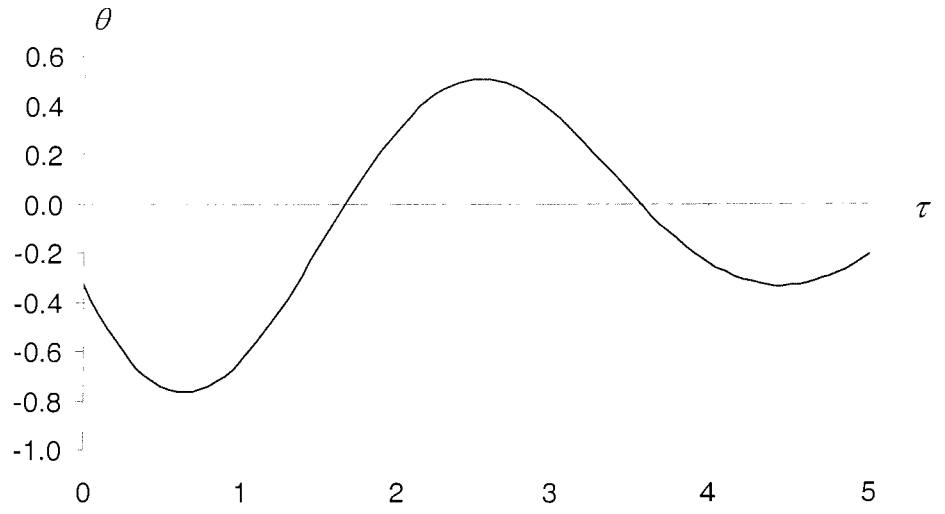

Figure 5.10 Rigid rod rotation angle θ time history.
(Rigid rod-water two-dimension case, $N = 1$)

From Figures 5.9 and 5.10, we see that the solutions are all of oscillatory form.

b) $N = 2$

For the case $N = 2$, equation (5.49) takes the form

$$\begin{vmatrix} \omega^2 - \Omega^2 & -\overline{M}\, E_1 & -\overline{M}\, E_2 \\ \frac{1}{\tilde{g}}\Omega^2 E_1 & \mathbf{i}\lambda_1 I_1 & 0 \\ \frac{1}{\tilde{g}}\Omega^2 E_2 & 0 & \mathbf{i}\lambda_2 I_2 \end{vmatrix} = 0, \tag{5.65}$$

giving

$$-\lambda_1\lambda_2 I_1 I_2\left(\omega^2 - \Omega^2\right) + \mathbf{i}\frac{\overline{M}}{\tilde{g}}\Omega^2\left(\lambda_1 E_2^2 + \lambda_2 E_1^2\right) = 0. \tag{5.66}$$

where

$$\Omega^2 = \lambda_1^2 + \kappa_1^2, \qquad \Omega^2 = \lambda_2^2 + \kappa_2^2. \tag{5.67}$$

To find solutions satisfying equation (5.66), the following method is used. First calculate the values of function $\psi(\Omega) = -\lambda_1\lambda_2 I_1 I_2\left(\omega^2 - \Omega^2\right) + \mathbf{i}\frac{\overline{M}}{\tilde{g}}\Omega^2\left(\lambda_1 E_2^2 + \lambda_2 E_1^2\right)$ for every $\Omega = \Omega_r + \mathbf{i}\Omega_i$ $(-10.0 \le \Omega_r \le 10.0, -10.0 \le \Omega_i \le 10.0)$, adopting a step length of $\Delta\Omega_r = 0.1$ and $\Delta\Omega_i = 0.1$. The function $\psi(\Omega)$ has a complex value, $\psi(\Omega) = \psi_r + \mathbf{i}\psi_i$, where ψ_r and ψ_i are real numbers. We now analyse these terms to find out the small intervals where ψ_r and ψ_i change sign from positive to negative or from negative to positive at the same time. A Newton-Raphson method (see, for example, Froberg 1965) is then used to find solutions for $\psi(\Omega) = 0$ where the sign changes occurred.

For the case $\kappa_1 = \frac{\pi}{2}$, $\kappa_2 = \frac{3\pi}{2}$, $I_1 = \frac{1}{2} + \frac{1}{2\pi}$, $I_2 = \frac{1}{2} - \frac{1}{6\pi}$, $\omega^2 = 2.4$, $\frac{\overline{M}}{\tilde{g}} = 3.0$,

we find only one solution that satisfies the radiation condition, which is given by

$$\begin{cases} \Omega = 1.80 - 0.47\mathbf{i} \\ \lambda_1 = 1.08 - 0.78\mathbf{i} \\ \lambda_2 = 1.92 - 4.38\mathbf{i} \end{cases}. \tag{5.68}$$

We now can evaluate the coefficient parameters φ and A_n $(n = 1,2,...,N)$ by substituting Ω, λ_1 and λ_2 into equation (5.49) and eliminating one of the equations in equation (5.49). Setting $\varphi = 1$ or giving a value to any one of the terms A_n allows

solution of the remaining equations and thus we derive a relation between φ and A_n. It follows from equations (5.44) and (5.43) that we can now determine the corresponding dimensionless water pressure mode and beam rotation angle mode for this natural frequency.

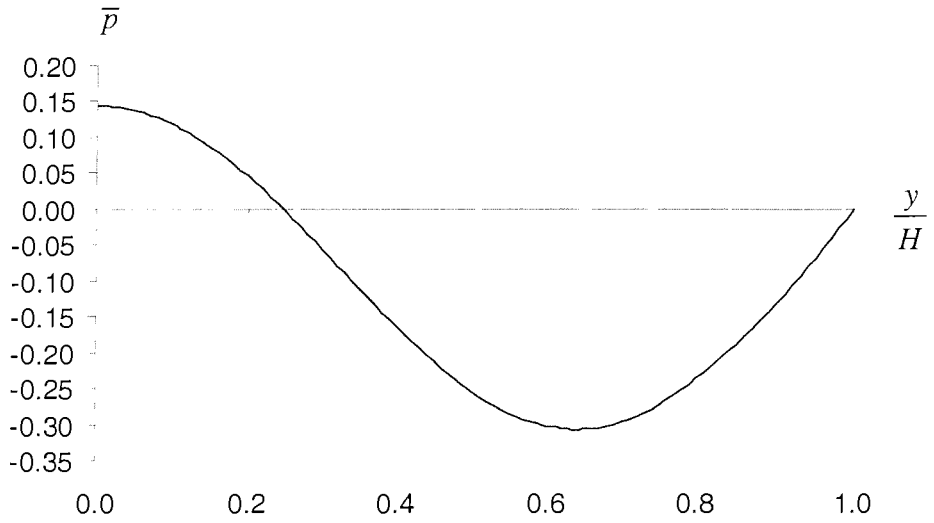

Figure 5.11 Dimensionless water pressure along rigid rod at time $t = 0$.
(Rigid rod-water two-dimension case, $N = 2$)

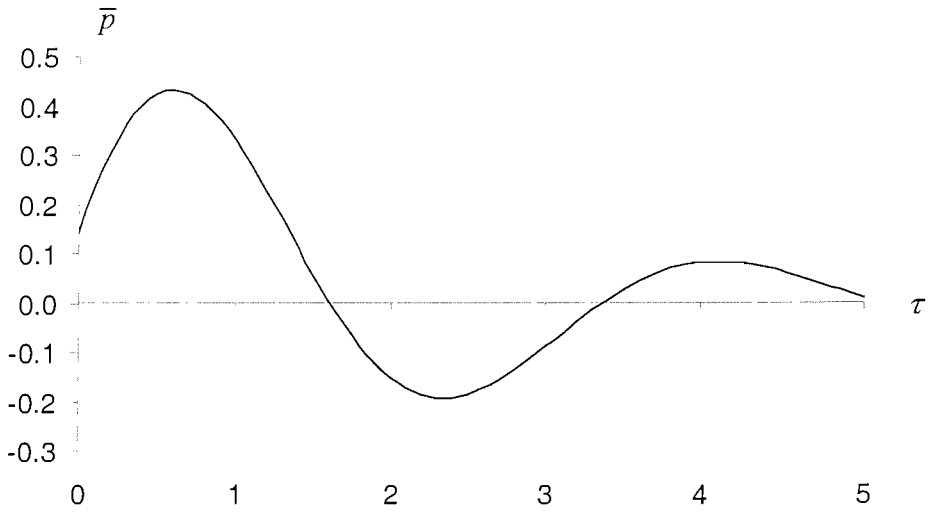

Figure 5.12 Dimensionless water pressure time history at point $x = 0$, $y = 0$.
(Rigid rod-water two-dimension case, $N = 2$)

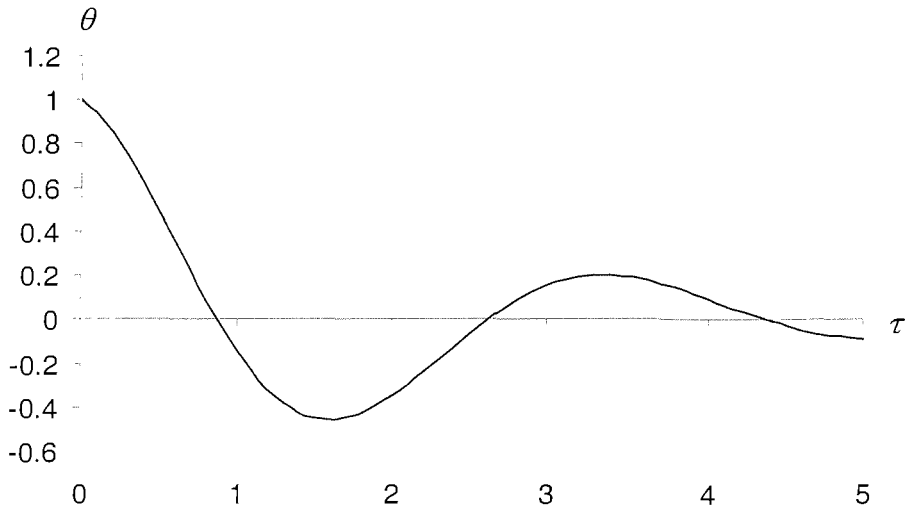

Figure 5.13 Rigid rod rotation angle θ time history.
(Rigid rod-water two-dimension case, $N = 2$)

Figure 5.11 shows the dimensionless water pressure acting along the rigid rod at dimensionless time $\tau = 0$. Figures 5.12 and 5.13 display the time histories of the dimensionless water pressure $\bar{p}$ (at point $x = 0$, $y = 0$) and the rigid rod rotation angle θ for the solution presented in equation (5.68).

c) $N = 3$

Using a similar method to the one developed for $N = 2$ case, we derive solutions for the case $N = 3$ adopting the values $\kappa_1 = \frac{\pi}{2}$, $\kappa_2 = \frac{3\pi}{2}$, $\kappa_3 = \frac{5\pi}{2}$, $I_1 = \frac{1}{2} + \frac{1}{2\pi}$, $I_2 = \frac{1}{2} - \frac{1}{6\pi}$, $I_3 = \frac{1}{2} + \frac{1}{10\pi}$, $\omega^2 = 2.4$, $\frac{\overline{M}}{\tilde{g}} = 3.0$ for illustrative purposes. Only one solution is found as given by

$$\begin{cases} \Omega = 1.55 - 1.03 \times 10^{-4}\mathbf{i} \\ \lambda_1 = 6.16 \times 10^{-4} - 0.26\mathbf{i} \\ \lambda_2 = 3.59 \times 10^{-5} - 4.45\mathbf{i} \\ \lambda_3 = 2.21 \times 10^{-5} - 7.70\mathbf{i} \end{cases} . \tag{5.69}$$

Figure 5.14 illustrates the dimensionless water pressure along the rigid rod at dimensionless time $\tau = 0$. Figures 5.15 and 5.16 display the time histories of the

dimensionless water pressure $\overline{p}$ (at point $x=0,\ y=0$) and the rigid rod rotation angle θ for the solution presented in equation (5.69).

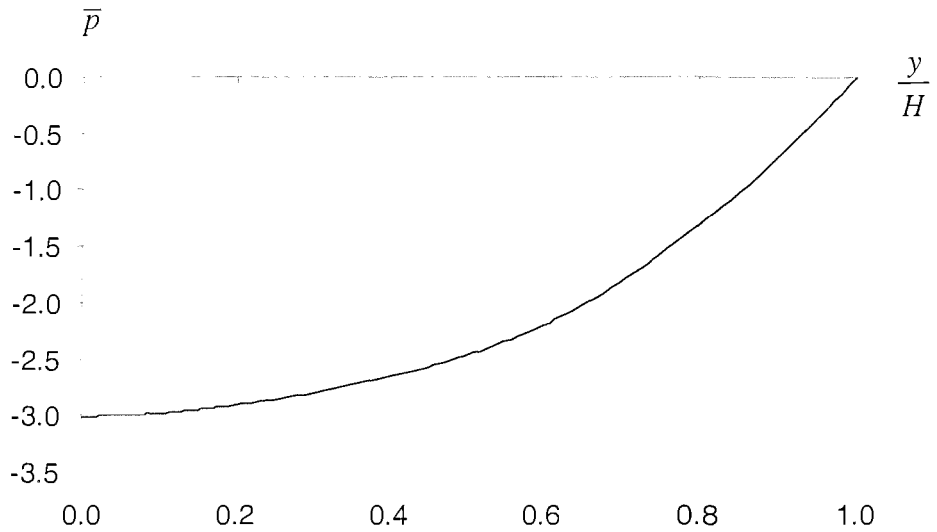

Figure 5.14 Dimensionless water pressure along rigid rod at time $t=0$.
(Rigid rod-water two-dimension case, $N=3$)

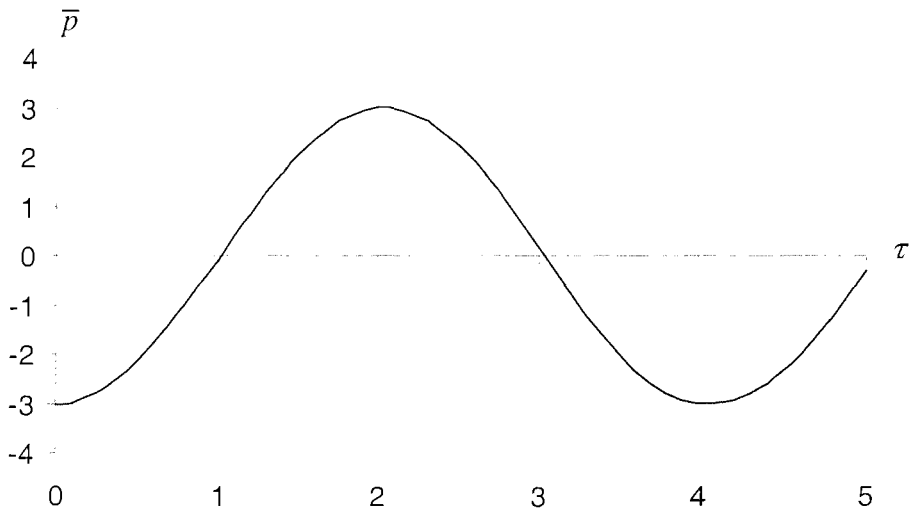

Figure 5.15 Dimensionless water pressure time history at point $x=0,\ y=0$.
(Rigid rod-water two-dimension case, $N=3$)

From equation (5.50) we derive the water pressure distribution along the beam. Like the one-dimensional case, the dynamic behaviour of the beam-water interaction system subject to the Sommerfeld radiation condition is similar to a viscous damped free

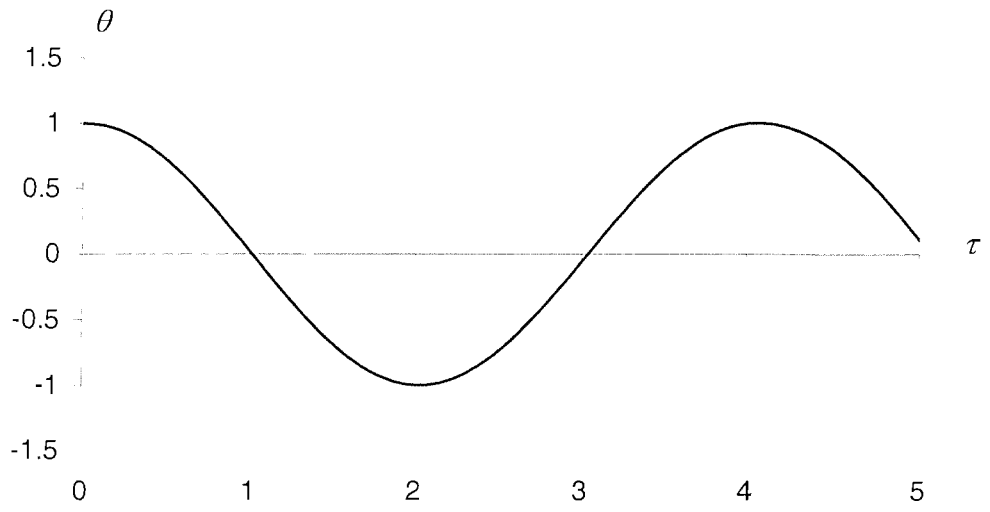

Figure 5.16 Rigid rod rotation angle θ time history.
(Rigid rod-water two-dimension case, $N = 3$)

vibration. It is also noticed that only one natural frequency is found for the rigid beam water interaction system. The beam has one degree of freedom while the fluid is a continuum with an infinite number of frequencies. It is noted that the number of degree of freedom in the fluid (*i.e.* $N = 1$, $N = 2$, $N = 3$, etc) does not affect the number of the natural frequencies of the system. However, this number affects the accuracy of the results, which is observed from Figures 5.8-5.16. For more accurate results, higher retained term number N is needed.

5.3 Two-dimensional elastic beam-water system

5.3.1 Natural vibration

Using the results derived in Chapters 2 and 3, the natural frequency of the two-dimensional elastic beam-water interaction system can be obtained by solving equation (3.59).

The orthogonality relations associated with natural vibration assuming an undisturbed condition imposed at infinity have been discussed by Xing, *et al.* (1997). In a similar manner, the orthogonality relations of the complex natural vibration forms with a

Sommerfeld radiation condition imposed at infinity are derived and presented in Appendix B.

A Fortran language program was written to solve equation (3.59) which is included in Appendix C together with flow charts.

In these illustrative calculations, it is assumed that the densities of the beam (concrete) and water are $\rho_s = 2.4 \times 10^3 kg/m^3$ and $\rho_f = 1.0 \times 10^3 kg/m^3$, respectively. The elastic modulus of the beam is $E = 2.94 \times 10^{10} Pa$ and the velocity of sound in water is $c = 1439 m/s$.

From Section 5.1, it is observed that when damping exists, the frequency of the interaction system is complex and its real part has a slightly smaller value but very close to the undamped natural frequency and its imaginary part has a very small value when the damping coefficient is small.

In Chapter 4 we derived the first three natural frequencies $\omega_1 = 1.21$, $\omega_2 = 2.96$, $\omega_3 = 5.62$ associated with an elastic-beam water interaction problem assuming parameter values $\gamma = 10.0$, $\nu = 0.8$, $r_m = 1$, $r_i = 1$ with no free surface wave disturbance present. At infinity, an undisturbed condition was imposed. For a Sommerfeld radiation condition existing at infinity and with the same system parameters, because of the complex nature of the fluid-structure interaction system, it is now expected that the natural frequencies are of complex value.

To solve equation (3.59), firstly, we use a method similar to the one used in Chapter 4. We portion the frequency domain into small intervals, e.g. $A < \omega_r \le 1.0 + A$, $A = 0,1,2,3,\cdots$, $-0.1 \le \omega_i \le 0.1$ (ω_r and ω_i are the real and imaginary parts of eigenfrequency ω, respectively), and we compute the value of $det\,\mathbf{R}$ at 100×200 points ($\Delta\omega_r = 0.01$, $\Delta\omega_i = 0.001$) and detect the possible root region where the signs of R_r and R_i in equation (3.59) change. We find the exact roots using a Newton-Raphson method within those small intervals. For the parameters chosen, solutions of the illustrative fluid-structure interaction system are,

$$\omega_1 = 1.21 + 1.62 \times 10^{-11}\mathbf{i},$$

$$\omega_2 = 2.96 + 3.96 \times 10^{-12}\mathbf{i},$$

$$\omega_3 = 5.62 + 1.83 \times 10^{-10}\mathbf{i}, \tag{5.70}$$

allowing the natural frequency of the system to be evaluated from the relation

$$\Omega = \Omega_b \times \omega^2 = \Omega_b \times \left[\left(\omega_r^2 - \omega_i^2\right) + 2\omega_r\omega_i\mathbf{i}\right], \tag{5.71}$$

where $\Omega_b = \left[EJ / \left(\rho_s F H^4\right)\right]^{1/2}$ represents the frequency parameter of the dry beam.

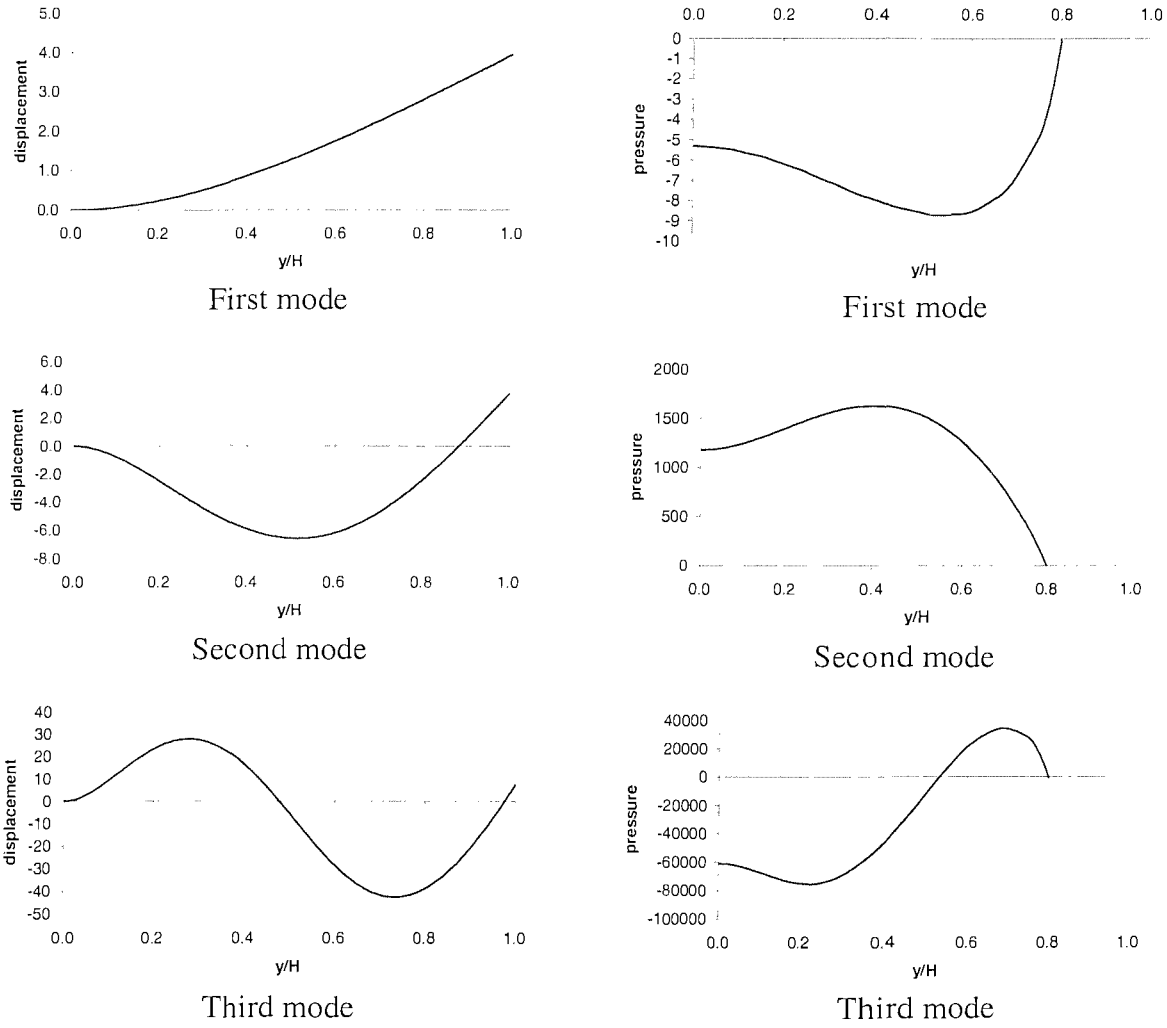

Figure 5.17 The first three modes of dimensionless beam displacement and water pressure of elastic beam-water interaction system excluding free surface waves.

Figure 5.17 displays the first three modes of dimensionless beam displacement and water pressure of the elastic beam-water interaction system excluding free surface waves. It is observed that all three frequencies have real component values which are close to the

natural frequency values when an undisturbed condition is imposed at infinity. Their corresponding imaginary component values are all very small and the associated mode shapes are the same as those presented in Chapter 4.

When free surface waves are included in the mathematical model, equations (3.23) and (3.59) are coupled equations and they need solving at the same time to derive the natural frequencies of the beam water interaction system subject to a Sommerfeld radiation condition imposed at infinity. Using a similar method to the one applied to solve equation (3.59) alone when free surface waves are excluded, for each given value of ω we can obtain a series of κ_n, $n = 1,2,3,\cdots$, and therefore the value of $det\,\mathbf{R}$ is derived. For demonstration purposes, only the first two modes of beam displacement and water pressure of the elastic beam-water interaction system are presented in Figure 5.18. For the parameters chosen, solutions of the illustrative fluid-structure interaction system are,

$$\omega_1 = 1.23 + 4.78 \times 10^{-5}\mathbf{i},$$

$$\omega_2 = 2.72 - 2.30 \times 10^{-5}\mathbf{i}. \tag{5.72}$$

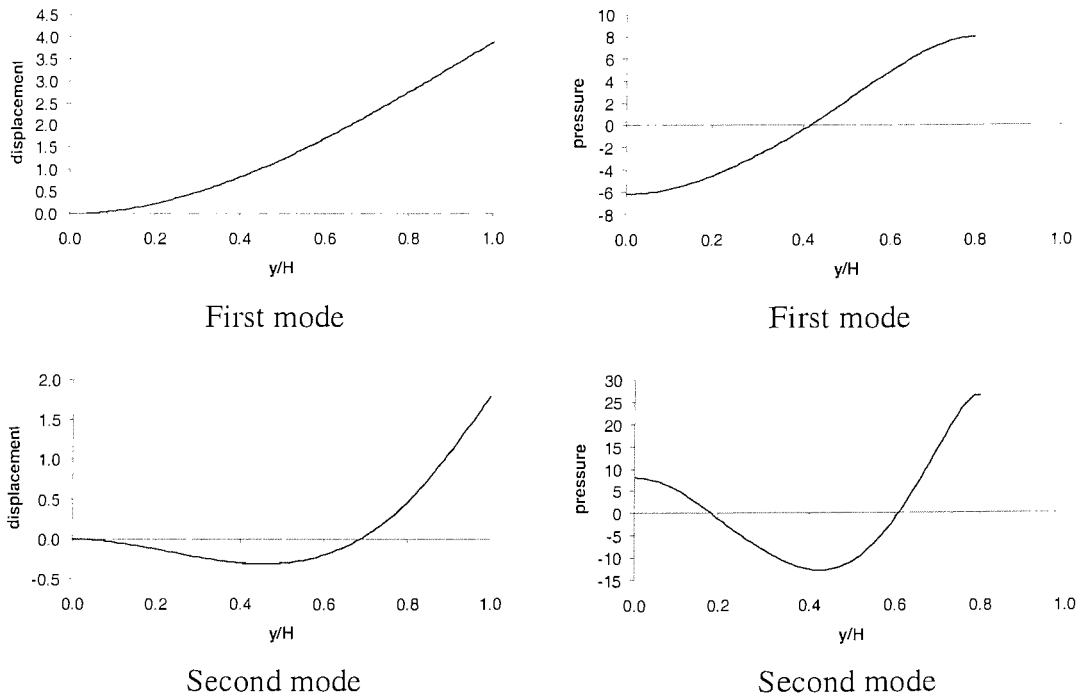

Figure 5.18 The first two modes of dimensionless beam displacement and water pressure of elastic beam-water interaction system including free surface waves.

The corresponding natural frequencies of beam water interaction system subject to an undisturbed condition imposed at infinity with free surface waves included are $\omega_1 = 1.24$, $\omega_2 = 2.97$. It can be seen that with free surface waves included, the influence of the Sommerfeld radiation condition on the natural frequencies of the beam water interaction system is that the natural frequencies are of complex values with small imaginary components compared to their real components but additionally slightly changes the real components of the natural frequencies.

The pressure mode shape in Figures 5.17 and 5.18 are quite different because Figure 5.17 shows the results for the case without free surface wave, and the water pressure on the surface is zero. Figure 5.18 shows the results for the case with free surface wave including, and the water pressure on the surface is not zero.

5.3.2 Dynamic response

(1) Foundation vibration

All the equations are the same as those derived in section 4.3.1 except that all the constants and coefficients are of complex values. Table 5.1 presents the calculated complex values of the constants $D_j(j = 1,\cdots,8)$ when a foundation vibration is present. In the following numerical examples we assume parameter values $\gamma = 10$, $\nu = 0.8$, $\Omega_w = (5,0)$, $w_0 / H = 0.1$, $r_m = 0$, $r_i = 0$ and $r_m = 1$, $r_i = 1$ for illustrative purposes.

Table 5.1 $D_j\ (j = 1,\cdots,8)$ in the case of foundation vibration with $\Omega_w = (5,0)$, $w_0 / H = 0.1$, $\gamma = 10$, $\nu = 0.8$.

	$r_m = 0$, $r_i = 0$	$r_m = 1$, $r_i = 1$
D_1	(2.93E-01,-8.52E-02)	(4.96E-01,-2.36E-01)
D_2	(2.93E-01,8.52E-02)	(4.96E-01,2.36E-01)
D_3	(-1.51E-02,-2.56E-18)	(-1.69E-02,-1.20E-17)
D_4	(1.55E-01,1.44E-17)	(4.55E-01,2.40E-16)
D_5	(-6.28E-02,5.64E-02)	(-2.34E-02,1.21E-01)

D_6	(-6.28E-02,-5.64E-02)	(-2.34E-02,-1.21E-01)
D_7	(-1.19E-01,-3.07E-17)	(-2.78E-02,-2.68E-17)
D_8	(-6.39E-03,-1.98E-19)	(-2.26E-02,5.93E-19)

These numerical results show that both the dimensionless displacement and water pressure are represented by complex values with a very small magnitude imaginary part in comparison to the real part. For example, the real part displacement is of order 0.1, whereas the imaginary part displacement is of order 6×10^{-17}. Physically these variables are real values and because of their smallness it is assumed that their imaginary part contributions are caused by numerical error and therefore should be zero.

Figures 5.19 and 5.20 show the real part component for the dimensionless beam deflection and dimensionless water pressure, respectively, when a harmonic foundation vibration is present. When compared to the results associated with an undisturbed boundary condition at infinity described in Chapter 4, the displacements and water pressure are of very similar shape distributions along the beam, but the amplitudes of the beam vibration are slightly smaller for the Sommerfeld radiation condition than those for

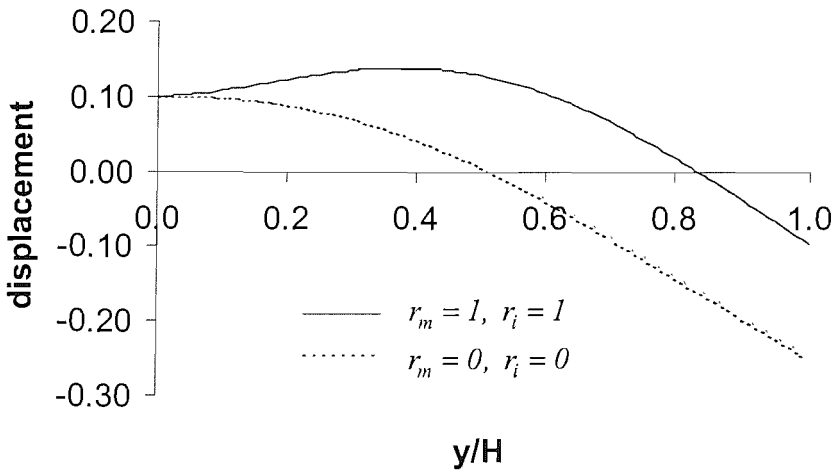

Figure 5.19 Real part of dimensionless beam displacement with $\Omega_w = (5,0)$, $w_0 / H = 0.1$, $\gamma = 10$, $\nu = 0.8$, $r_m = 0,\ r_i = 0$ and $r_m = 1,\ r_i = 1$ (Foundation vibration case).

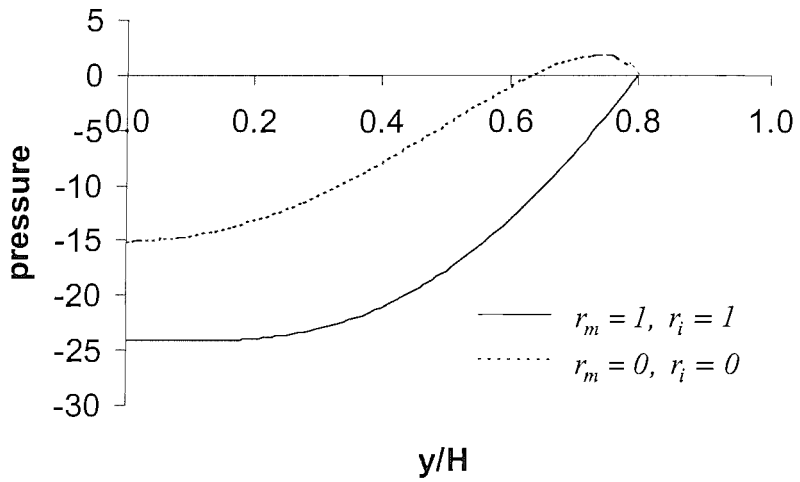

Figure 5.20 Real part of dimensionless water pressure with $\Omega_w = (5,0)$, $w_0 / H = 0.1$, $\gamma = 10$, $\nu = 0.8$, $r_m = 0$, $r_i = 0$ and $r_m = 1$, $r_i = 1$ (Foundation vibration case).

the undisturbed condition. This is because the radiation condition allows energy to dissipate from the system to infinity, so the system's mechanical energy is lower in the radiation condition than in the undisturbed condition causing reduced beam vibration amplitudes. As discussed in Chapter 4, the attachment of a top mass with inertia decreases the natural frequencies of the system which makes a significant difference in beam vibration and water pressure amplitudes. This is demonstrated by the changes occurring in the first and second modes. When the value of r_m increases, the beam displacement reduces whereas the water pressure increase sharply.

As observed from Figures 5.19 and 5.20, the attached mass with concentrated moment of inertia has a big effect on the dynamic behaviour of the beam-water interaction system. Therefore, to develop accurate designs of systems involving beam-water dynamic interaction problems, both attached mass and concentrated moment of inertia should be taken into account.

(2) Harmonically excited vibration at the free end of the beam

The governing equations describing the dynamical behaviour in the fluid and solid domains for a beam harmonically excited at the free end remain unchanged to those as

presented in Section 4.2.2 except that all functions and constants and coefficients are of complex values.

Table 5.2 presents the calculated complex values of constants $D_j(j=1,\cdots,8)$ when a forced sinusoidal vibration occurs at the free end of the beam. In the numerical examples the following parameters are used: $\gamma = 10$, $\nu = 0.8$, $\Omega_0 = (5,0)$, $Q_0 = 8.0\times 10^7 N$, $r_m = 0$, $r_i = 0$ and $r_m = 1$, $r_i = 1$.

Table 5.2 $D_j\ (j=1,\cdots,8)$ in the case of free end forced vibration with $\Omega_0 = (5,0)$, $Q_0 = 8.0\times 10^7 N$, $\gamma = 10$, $\nu = 0.8$.

	$r_m = 0$, $r_i = 0$	$r_m = 1$, $r_i = 1$
D_1	(5.29E-01,-3.92E-01)	(2.05E-01,-1.52E-01)
D_2	(5.29E-01,3.92E-01)	(2.05E-01,1.52E-01)
D_3	(-4.16E-03,-1.72E-17)	(-1.63E-03,-7.22E-18)
D_4	(7.80E-01,1.99E-16)	(3.02E-01,7.64E-17)
D_5	(1.02E-01,1.68E-01)	(3.93E-02,6.49E-02)
D_6	(1.02E-01,-1.68E-01)	(3.93E-02,-6.49E-02)
D_7	(2.46E-01,-9.53E-17)	(9.48E-02,-1.70E-17)
D_8	(-4.25E-02,1.70E-17)	(-1.64E-02,7.19E-19)

Again these numerical results show that both displacement and water pressure are represented by complex values with a very small magnitude imaginary part in comparison to the real part. Physically these variables are real values and because of their smallness it is assumed that their imaginary part contributions are caused by numerical error and therefore should be zero.

Figures 5.21 and 5.22 show the real part components of the dimensionless beam deflection and the dimensionless water pressure for the system under a free end forced external action. Compared to the presented results for the undisturbed case in Chapter 4, the beam displacements and water pressure are of similar shape distribution along the

beam, but the amplitudes of the beam vibration are slightly smaller in value in the Sommerfeld radiation condition than those determined for the undisturbed condition. The reasons for this are discussed in Section 5.4.1. The addition of a top mass increases the values of the beam displacement and water pressure, whereas the effect of the concentrated moment of inertia at the free end of the beam has the opposite influence.

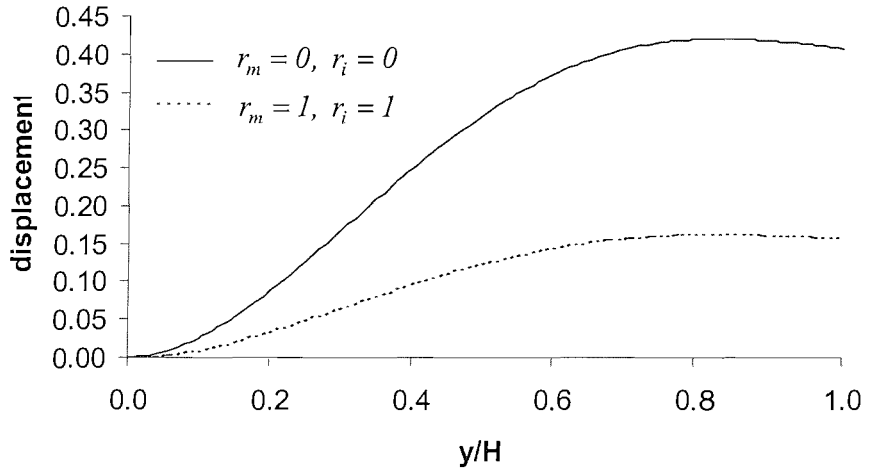

Figure 5.21 Real part of dimensionless beam displacement with $\Omega_0 = (5,0)$, $Q_0 = 8.0 \times 10^7 N$, $\gamma = 10$, $\nu = 0.8$, $r_m = 0$, $r_i = 0$ and $r_m = 1$, $r_i = 1$. (Free end forced vibration case)

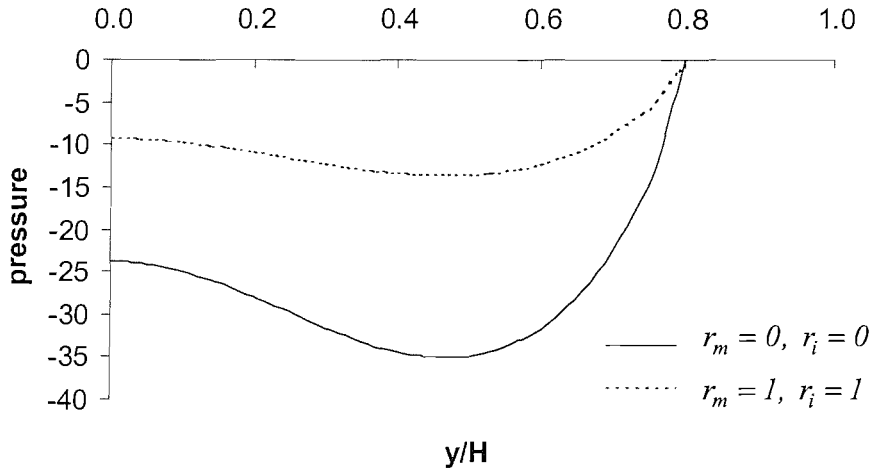

Figure 5.22 Real part of dimensionless water pressure with $\Omega_0 = (5,0)$, $Q_0 = 8.0 \times 10^7 N$, $\gamma = 10$, $\nu = 0.8$, $r_m = 0$, $r_i = 0$ and $r_m = 1$, $r_i = 1$. (Free end forced vibration case)

The calculated results show little difference between the dynamic behaviour of the beam-water interaction system subject to a Sommerfeld radiation condition or an undisturbed condition when a free end forced vibration is imposed. This result suggests that for simple beam-water interaction problems, we can implement an undisturbed condition at infinity instead of the Sommerfeld radiation condition, and derive a very good approximate solution with reduced analytical and computational effort.

Chapter 6

Numerical analysis of a two dimensional nonlinear beam water interaction system

6.1 Introduction

In this chapter, a coupled iterative scheme, referred to as a partitioned procedure (see, for example, Bathe (2001)), is used to calculate the nonlinear dynamic responses of a beam-water interaction system. This scheme solves the fluid flow equations for the last calculated structural configuration before the forces along the fluid structure interface are calculated. The application of these forces in the structural model allows evaluation of the incremental structural displacements that are applied to the fluid model and the process between structure and fluid continues until convergence of the load/time behaviour is reached. In previous preliminary numerical investigations (Xing *et al.* (2002, 2003)), the structure was treated as a rigid body undergoing large motions so that ideas and concepts were clarified before considering a fully flexible solid. This chapter continues the above study by examining the behaviour of structures through a nonlinear beam–water interaction system. The beam is assumed to undergo a large rigid motion and small elastic deformation. This research uses a fluid solver code which is briefly discussed in Appendix D and was described, validated and used in investigations performed by Xing *et al.* (2002, 2003) and Price and Chen (2005).

6.2 Governing equations

Figure 6.1 illustrates the two-dimensional beam-water interaction system under examination and models a simple flap wavemaker. The bottom and left-hand-side wall of the towing tank are impermeable. The length of the tank is L and depth of water h when the flap is upright, and the volume of water is hL. The flap is modelled by a uniform elastic beam of density ρ_s and length $H(>h)$. It is assumed the fluid is incompressible and its density is represented by ρ_f. Point O' denotes the position of the attachment of the beam to the tank's base where a spring of stiffness C_k acts. The beam rotates about

O' and a clockwise rotation denotes a positive angle θ. Point A represents a position on the beam at distance $H/2$ from O'. In the beam's vertical upward position, the spring is in its natural state with no deformation. At time $t=0$, the elastic beam is pulled to an initial rotation angle θ_0 by an external force and released to undergo a free vibration. If necessary, the external force can be applied continuously and the fluid-structure interaction process investigated. However, here only the free vibration interaction is examined.

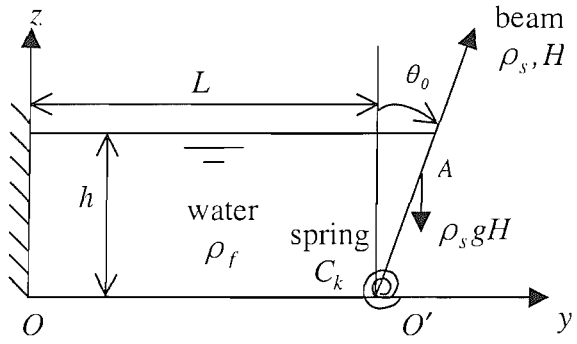

Figure 6.1 A beam water interaction system idealising a simple wavemaker.

6.2.1 Dynamic equations of solid

The motion of the beam is a combination of a large rigid rotation about point O' and small deformation along the beam. The deformation in the beam's axial direction caused by the component of gravity is assumed negligible and therefore neglected. To define the dynamics at a point on the beam, two variables in the form of a rigid rotation angle θ and deflection of the beam w are specified. For a small deformation, we assume that all the deflections are perpendicular to the mid-face axis of the undeformed beam and the length of the beam remains constant H (i.e. no elongation of the beam). Figure 6.2 illustrates the beam displaced and deflected. In order to derive the motion of the beam, we introduce the material frame of reference coordinate system $O'-YZ$ attached to the beam. This allows the transformation between the unit coordinate vectors of the moving frame $O'-YZ$ and the fixed spatial coordinate system $O-yz$ to be defined as

$$\mathbf{a} = \mathbf{i}\cos\theta - \mathbf{j}\sin\theta, \tag{6.1}$$

$$\mathbf{b} = \mathbf{i}\sin\theta + \mathbf{j}\cos\theta. \tag{6.2}$$

Taking the time derivative of equations (6.1) and (6.2), we obtain

$$\dot{\mathbf{a}} = \dot{\theta}\,(-\mathbf{i}\,sin\theta - \mathbf{j}cos\theta) = -\dot{\theta}\,\mathbf{b}, \tag{6.3}$$

$$\dot{\mathbf{b}} = \dot{\theta}\,(\mathbf{i}\,cos\theta - \mathbf{j}sin\theta) = \dot{\theta}\,\mathbf{a}. \tag{6.4}$$

By assuming the deflection of the beam is small (i.e. $\partial w/\partial Z << \theta_0$) and perpendicular to the $O'Z$ axis, the position vector of an arbitrary point Z on the beam relative to $O'-YZ$ at time t can be written in the vector form,

$$\mathbf{R} = w\mathbf{a} + Z\mathbf{b}. \tag{6.5}$$

The first and second order time derivatives of this vector are given by

$$\dot{\mathbf{R}} = \left(\dot{w} + Z\dot{\theta}\right)\mathbf{a} - w\dot{\theta}\,\mathbf{b}, \tag{6.6}$$

$$\ddot{\mathbf{R}} = \left(\ddot{w} + Z\ddot{\theta} - w\dot{\theta}^2\right)\mathbf{a} - \left(w\ddot{\theta} + 2\dot{w}\dot{\theta} + Z\dot{\theta}^2\right)\mathbf{b}. \tag{6.7}$$

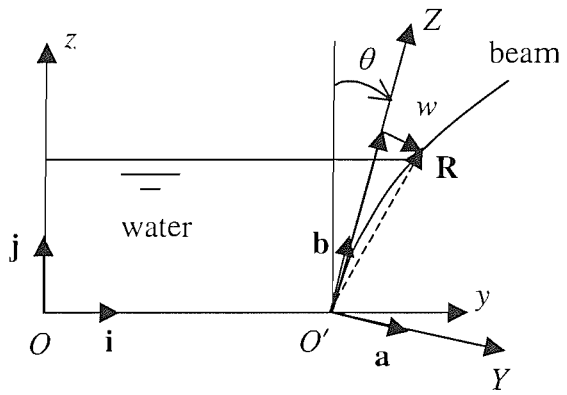

Figure 6.2 Beam displacement in material (Y,Z) and spatial (y,z) coordinate reference systems

Let us now examine the small element of beam shown in Figure 6.3 with mass centre at position $\mathbf{R}$. External and internal forces act on the element such as water pressure pdZ, gravity $\rho_s g dZ$, shearing force V and bending moment M. The positive directions of these forces are shown in Figure 6.3.

The application of Newton's law of motion to element dZ gives

$$\rho_s dZ \cdot \ddot{\mathbf{R}} = \left(pdZ - \frac{\partial V}{\partial Z}dZ\right)\mathbf{a} + \rho_s g dZ(\mathbf{a}\,sin\theta - \mathbf{b}cos\theta). \tag{6.8}$$

By assuming all forces act in the $O'Y$ direction and summing moments about any point on the upward face of the element, we find that

$$\frac{\partial M}{\partial Z} = V\,, \tag{6.9}$$

where the term associated with $(dZ)^2$ and rotation of the element dZ about its centre of mass are neglected.

The bending moment is related to the curvature by the constitutive relation

$$M = EJ\frac{\partial^2 w}{\partial Z^2}\,, \tag{6.10}$$

where EJ denotes the flexural rigidity of the beam.

On substituting equations (6.6), (6.7), (6.9) and (6.10) into equation (6.8), and assuming the unit vector **a** is orthogonal to unit vector **b**, we derive the relationships

$$\frac{\partial^2}{\partial Z^2}\left(EJ\frac{\partial^2 w}{\partial Z^2}\right) + \rho_s\left(\ddot{w} + Z\ddot{\theta} - w\dot{\theta}^2\right) = p + \rho_s g\sin\theta\,, \tag{6.11}$$

$$Z\dot{\theta}^2 = g\cos\theta - w\ddot{\theta} - 2\dot{w}\dot{\theta}\,, \tag{6.12}$$

in the directions of **a** and **b**, respectively.

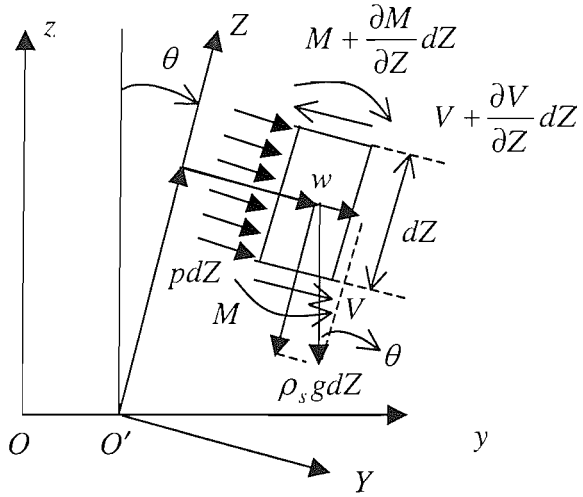

Figure 6.3 Forces acting on a small element of flexible beam

For the case of constant flexural rigidity EJ, equation (6.11) reduces to

$$EJ\frac{\partial^4 w}{\partial Z^4} + \rho_s\left(\ddot{w} + Z\ddot{\theta} - w\dot{\theta}^2\right) = p + \rho_s g\sin\theta\,. \tag{6.13}$$

Equations (6.11) and (6.12) or equations (6.13) and (6.12) are the two coupled equations governing the dynamics of the elastic beam assuming a large rigid rotation angle θ and a small elastic deflection.

To these coupled equations, boundary conditions must be introduced before solution can take place. It is assumed that no concentrated force or moment acts at the free end $(Z = H)$ of the beam. The base of the beam is simply supported. The spring at $Z = 0$ provides a concentrated moment that prevents the beam from falling down. The boundary conditions applicable to the wavemaker are given by

$$w(0) = 0, \qquad EJ\frac{\partial^2 w(0)}{\partial Z^2} = C_k\left(\theta + \frac{\partial w(0)}{\partial Z}\right),$$

$$\frac{\partial^2 w(H)}{\partial Z^2} = 0, \qquad \frac{\partial^3 w(H)}{\partial Z^3} = 0. \tag{6.14}$$

If we substitute equation (6.12) into equation (6.13), and multiply it by Z before integrating with respect to Z from 0 to H, we obtain

$$I\ddot{\theta} + \int_0^H \left(EJ\frac{\partial^4 w}{\partial Z^4} + \rho_s \ddot{w}\right) Z dZ - \int_0^H \rho_s w\left(g\cos\theta - 2\dot{w}\dot{\theta}\right) dZ$$

$$= \int_0^H \left(p + \rho_s g \sin\theta\right) Z dZ, \tag{6.15}$$

where $I = \int_0^H \rho_s\left(Z^2 + w^2\right) dZ$ denotes the moment of inertia of the elastic beam. An application of the boundary conditions gives

$$\int_0^H EJ\frac{\partial^4 w}{\partial Z^4} Z dZ = EJ\frac{\partial^3 w}{\partial Z^3} Z\Big|_0^H - \int_0^H EJ\frac{\partial^3 w}{\partial Z^3} dZ = -EJ\frac{\partial^2 w}{\partial Z^2}\Big|_0^H$$

$$= C_k\left(\theta + \frac{\partial w(0)}{\partial Z}\right). \tag{6.16}$$

Thus equation (6.15) becomes:

$$I\ddot{\theta} + \left(\int_0^H 2\rho_s w\dot{w} dZ\right)\dot{\theta} + C_k\left(\theta + \frac{\partial w(0)}{\partial Z}\right) + \int_0^H \rho_s \ddot{w} Z dZ$$

$$-\rho_s g\left(\frac{H^2}{2}\sin\theta + \int_0^H w dZ\cos\theta\right) = \int_0^H pZ dZ. \tag{6.17}$$

The static equilibrium position of this system is obtained by solving the two coupled equations derived from equations (6.13) and (6.17) with all time derivatives set to zero.

6.2.2 Fluid flow equations

This research uses the fluid code described by Price and Chen (2005) as the viscous fluid solver, which had been previously used for investigations by Xing *et al* (2002, 2003). The fluid flow equations and fluid representation are attached in Appendix D.

6.2.3 Beam-water interface boundary conditions

The boundary condition applicable on the beam water interface is the no slip condition, where the displacement and velocity of the water particles are the same as those on the wet surface of the beam. The boundary condition imposed by the beam on the interface is the force acting on the wet surface of the beam caused by the water pressure. That is, after substitution from equations (6.1) and (6.2), we find that on the

Solid:

$$p = p(y,z), \text{ where } \mathbf{R} = w\mathbf{a} + Z\mathbf{b} = (y-L)\mathbf{i} + z\mathbf{j}. \tag{6.18}$$

Water:

$$n_i u_j = \dot{w}, \text{ and } (y-L)\mathbf{i} + z\mathbf{j} = \mathbf{R} = w\mathbf{a} + Z\mathbf{b}. \tag{6.19}$$

6.2.4 Static equilibrium position of the system

For simplicity, let us assume that an equilibrium position exists when the flap is at position $\theta = \beta_0$ (see Figure 6.1), no deflections occur, and the water depth is $\tilde{h}$. Furthermore, when the beam is vertical with zero deformation, it is assumed the system is at a zero potential position. The potential of the whole beam-water interaction system at arbitrary rotation θ, assuming the spring is linear, is

$$\Pi(\theta) = \frac{1}{2}C_k\theta^2 - \rho_s g\frac{H^2}{2}(1-\cos\theta) + f(\theta), \tag{6.20}$$

where $f(\theta)$ represents an increment of the water potential given by

$$f(\theta) = \int_0^{\tilde{h}}\int_0^{L+z\tan\theta}\rho_f g z dy dz - \frac{\rho_f g L h^2}{2} = \rho_f g\left(\frac{\tilde{h}^2 L}{2} + \frac{\tilde{h}^3\tan\theta}{3} - \frac{h^2 L}{2}\right). \tag{6.21}$$

As the volume of water remains constant, it follows that

$$\frac{\tilde{h}^2 \sin\theta}{2} + \tilde{h}L = hL, \tag{6.22}$$

giving

$$\tilde{h} = \frac{L}{\sin\theta}\left(\pm\sqrt{1+2\alpha\sin\theta} - 1\right), \tag{6.23}$$

where $\alpha = h/L < 1$, and we choose the positive solution. For small rotation angle θ, using Taylor series to expand $\tilde{h}$ and neglecting higher order terms, we obtain

$$f(\theta) = \rho_f g h^2 L\left(\left(1-\frac{\alpha}{2}\sin\theta\right)^2\left(\frac{1}{2} - \frac{\alpha\tan\theta}{3}\left(1-\frac{\alpha}{2}\sin\theta\right)\right) - \frac{1}{2}\right). \tag{6.24}$$

The static equilibrium position $\theta = \beta_0$ is determined by solving the following variation equation,

$$\delta\Pi(\theta) = 0. \tag{6.25}$$

This equation represents the total contribution of the rotation moment due to water pressure, the gravity acting on the beam and the twisting of the spring at point O'. That is,

$$C_k\beta_0 - \rho_s g\frac{H^2}{2}\sin\beta_0 - \int_0^{\tilde{h}/\cos\beta_0}\rho_f g\left(\tilde{h} - Z\cos\beta_0\right)ZdZ = 0. \tag{6.26}$$

For small β_0 this equation can be linearised giving

$$C_k\beta_0 - \rho_s g\frac{H^2}{2}\beta_0 - \rho_f g\frac{\tilde{h}^3}{6} = 0, \tag{6.27}$$

from which the equilibrium position is determined as

$$\beta_0 = \frac{\rho_f g\dfrac{\tilde{h}^3}{6}}{C_k - \rho_s g\dfrac{H^2}{2}}. \tag{6.28}$$

This equilibrium position is stable only if the following condition is satisfied,

$$\delta^2\Pi(\beta_0) > 0. \tag{6.29}$$

From equations (6.20), (6.21) and inequality (6.29), the stable condition for the beam water system is given by the inequality

$$C_k > \rho_s g \frac{H^2}{2} cos\beta_0 + f''(\beta_0). \tag{6.30}$$

Usually $f''(\theta)$ is small compared to $\rho_s g \frac{H^2}{2} cos\beta_0$ when θ is a small value. Under this assumption, the equilibrium position $\theta = \beta_0$ is stable if

$$C_k > \rho_s g \frac{H^2}{2}. \tag{6.31}$$

From equation (6.28) and inequality (6.31), it is observed that when the twisting stiffness of the spring C_k is large enough satisfying inequality (6.31) the beam-water interaction system has a stable static equilibrium position at $\theta = \beta_0 > 0$.

6.3 Numerical scheme of study

6.3.1 Solid representation

The beam is discretised into n_m uniform two-node Hermite beam elements. For a single element, a deflection is represented by

$$w_n^e(\xi) = \sum_{i=1}^{4} N_i(\xi) x_{ni}^e = \mathbf{N}\mathbf{x}_n^e, \tag{6.32}$$

$$\mathbf{x}_n^e = [w_n \quad \varphi_n \quad w_{n+1} \quad \varphi_{n+1}]^T, \tag{6.33}$$

$$\mathbf{N} = [N_1 \quad N_2 \quad N_3 \quad N_4], \tag{6.34}$$

where

$$N_1(\xi) = 1 - 3\xi^2 + 2\xi^3, \qquad N_2(\xi) = (\xi - 2\xi^2 + \xi^3)\chi,$$

$$N_3(\xi) = 3\xi^2 - 2\xi^3, \qquad N_4(\xi) = (\xi^3 - \xi^2)\chi,$$

$$\xi = \frac{Z - Z_n}{\chi}, \qquad \chi = \frac{H}{n_m}, \qquad 0 \le \xi \le 1.$$

An expansion of equations (6.12) and (6.13) produces the equivalent matrix forms:

$$\mathbf{K}\mathbf{x} + \mathbf{M}(\ddot{\mathbf{x}} - \mathbf{x}\dot{\theta}^2) + \mathbf{I}_z\ddot{\theta} + \mathbf{C}\theta = \mathbf{P}_1, \tag{6.35}$$

$$\mathbf{M}(\mathbf{x}\ddot{\theta} + 2\dot{\mathbf{x}}\dot{\theta}) + \mathbf{I}_z\dot{\theta}^2 = \mathbf{P}_2, \tag{6.36}$$

where

$$\mathbf{K} = \mathbf{G}_1^T \mathbf{K}_c \mathbf{G}_1 + \sum_e \mathbf{G}_n^T \mathbf{K}^e \mathbf{G}_n, \qquad \mathbf{M} = \sum_e \mathbf{G}_n^T \mathbf{M}^e \mathbf{G}_n,$$

$$\mathbf{x} = \sum_e \mathbf{G}_n^T \mathbf{x}_n^e \mathbf{G}_n, \qquad \mathbf{P}_1 = \sum_e \mathbf{G}_n^T \mathbf{P}_1^e \mathbf{G}_n,$$

$$\mathbf{I}_z = \sum_e \mathbf{G}_n^T \mathbf{I}_n^e \mathbf{G}_n, \qquad \mathbf{P}_2 = \sum_e \mathbf{G}_n^T \mathbf{P}_2^e \mathbf{G}_n, \qquad \mathbf{C}_s = C_k \frac{d\mathbf{N}^T(0)}{\chi d\xi},$$

$$\mathbf{K}^e = \int_0^l \frac{EJ}{\chi^3} \left(\frac{d^2\mathbf{N}}{d\xi^2}\right)^T \left(\frac{d^2\mathbf{N}}{d\xi^2}\right) d\xi, \qquad \mathbf{K}_c = C_k \frac{d\mathbf{N}^T(0)}{\chi d\xi} \cdot \frac{d\mathbf{N}(0)}{\chi d\xi},$$

$$\mathbf{M}^e = \int_0^l \rho_s \mathbf{N}^T \mathbf{N} d\xi, \qquad \mathbf{I}_n^e = \int_0^l \rho_s \chi (n-1+\xi) \mathbf{N}^T d\xi,$$

$$\mathbf{P}_1^e = \int_0^l \mathbf{N}^T (p + \rho_s g \sin\theta) \chi d\xi, \qquad \mathbf{P}_2^e = \int_0^l \mathbf{N}^T \rho_s g \cos\theta \chi d\xi,$$

$$\mathbf{C} = \mathbf{G}_1^T \mathbf{C}_s \mathbf{G}_1, \qquad \mathbf{G}_1 = (1 \quad 1 \quad 1 \quad 1 \quad 0 \quad \cdots \quad 0).$$

Spatial and time discretisations are accomplished using the Newmark scheme, which basically consists of a Taylor series formulation using a quadratic expansion (see Bathe (1982)). The right hand side of equations (6.35) and (6.36) represent the total force acting upon the structure. The force relating to the fluid flow pressure is obtained from the flow solver at $t = t_{n+1}$ and a suitable criterion adopted to terminate the iterative process.

6.4 Numerical examples

To investigate the fluid-beam interaction system shown in Figure 6.1, for illustration purposes, the following parameters are used: $\rho_f = 1.0 \times 10^3 kg \cdot m^{-3}$, $h = 1m$, $H = 2m$, $L = 15m$.

From physical reasoning, we assume that the mass of the beam is much less than the mass of water and therefore neglect nonlinear gravity effects acting on the beam. Non-linearity influences arise in the description of the supporting spring and fluid flows. There is no spring element in the structure solver. In order to numerically simulate the twisting spring as shown in Figure 6.4, a combination of a simply supported beam QS and two identical trusses FQ and GS with suitable chosen boundary constraints is used to produce only a concentrated rotation moment about point O'. In the two-dimensional

structure calculations, points F and G in Figure 6.4 are fixed, and point O' has only one degree of freedom of rotation.

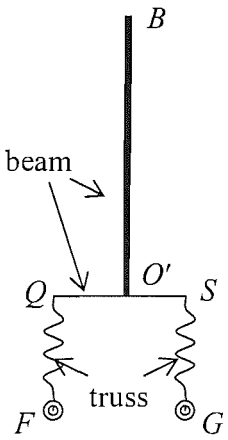

Figure 6.4 Numerical model for twisting spring

In the simulations, the beam is initially statically located at a position of $\theta_0 = 0.2rads$ and then released. The dynamic process involved in the beam-water interaction is calculated. The densities of beams $O'B$, QS and two trusses FQ, GS are $\rho_b = 7.8 \times 10^3 kg \cdot m^{-3}$ (steel), $\rho_q = 7.8 \times 10^3 kg \cdot m^{-3}$ (steel) and $\rho_g = 5.6 \times 10^3 kg \cdot m^{-3}$, respectively. The Young's modulus of beam QS and two trusses FQ, GS are $E_q = 2.0 \times 10^{11} N \cdot m^{-2}$ and $E_g = 7.1 \times 10^{10} N \cdot m^{-2}$. (The density and Young's modulus for the two trusses are artificially chosen for illustrative purpose and they can be changed.) For the elastic beam $O'B$, its Young's modulus is $E_b = 2.0 \times 10^{10} N \cdot m^{-2}$. This value is artificially increased to $E_b = 2.0 \times 10^{13} N \cdot m^{-2}$ to simulate a rigid beam $O'B$.

For the nonlinear spring case, all parameters given previously remain unchanged except that the Young's modulus E_g is assumed to have the nonlinear properties defined as

$$E_g = \begin{cases} 4.0 \times 10^5 N \cdot m / rad & |\varepsilon| \le 0.1 \\ 1.2 \times 10^6 N \cdot m / rad & 0.1 < |\varepsilon| \le 0.2 \\ 7.0 \times 10^8 N \cdot m / rad & 0.2 < |\varepsilon| \le 0.4 \\ 7.1 \times 10^{10} N \cdot m / rad & 0.4 < |\varepsilon| \le 0.7 \end{cases}, \tag{6.37}$$

where ε is the strain of the trusses.

Before each calculation, we first use the structure solver to calculate the first vibration period of the structure. For the rigid beam structure and elastic beam structure with linear springs the first periods of vibration are $T_r = 0.89s$ and $T_e = 1.73s$, respectively. For nonlinear spring cases, the first vibration periods for rigid beam and elastic beam structures are $T_{rn} = 0.88s$ and $T_{en} = 1.72s$, respectively. Subsequently, we use the dimensionless time $\bar{t} = t / T_0$ in the calculations, where T_0 represents the first vibration period of the structure of the studied case. Each chosen incremental time step is $\Delta\bar{t} = 0.01$, and at time $\bar{t} = 1.0$ the system vibrates over the first vibration period of the structure.

In the numerical iteration process for each case, the structure and fluid domains are calculated by structure and fluid solvers, respectively. For the structure solver, in order to calculate the movement of a structure, the external forces, i.e., the water pressure forces along the beam in these cases, need to be known for the whole time history of each step. For the fluid solver, in order to calculate the movement of the fluid, the displacements and velocities of the moving boundary on the beam-water interface need to be known for the whole time history of each step.

In the first step, we use the fluid solver to calculate the water pressure $\mathbf{f}_I^0$ by assuming the beam does not move and stays at its initial position $\mathbf{u}_I^0$ (subscript denotes the step number and superscript defines the iteration number within this step). The structure solver is then used to compute the displacements $\mathbf{u}_I^1$ and velocities $\mathbf{v}_I^1$ of some points on the beam, assuming that the external forces keep the value of $\mathbf{f}_I^0$ within the time history of this step. Then we use the fluid solver to calculate the water pressure forces $\mathbf{f}_I^1$ by assuming the beam configuration changes from initial position $\mathbf{u}_I^0$ and $\mathbf{v}_I^0 = \mathbf{0}$ to the next step displacements $\mathbf{u}_I^1$ and velocities $\mathbf{v}_I^1$. By assuming the external forces linearly change from $\mathbf{f}_I^0$ to $\mathbf{f}_I^1$ within the time step, we can calculate the displacements $\mathbf{u}_I^2$ and velocities $\mathbf{v}_I^2$ of the points on the beam. This iteration procedure continues until $\left|\mathbf{u}_I^{m+1} - \mathbf{u}_I^m\right| < error$ (error chosen as 1.0×10^{-5}). When the structure

configuration does not change within this time step, the next step calculation begins. Usually the first step takes much more iterations to reach convergence condition than other steps.

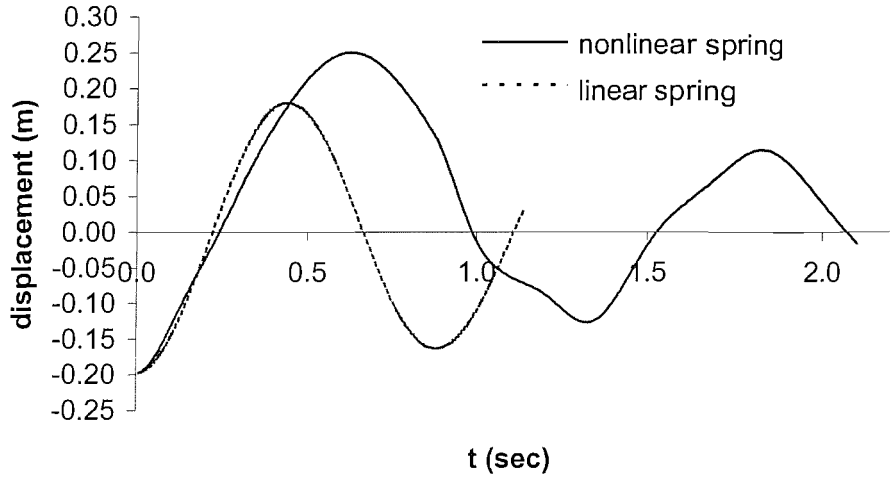

Figure 6.5 Displacement time history at point A during simulation ($\theta_0 = 0.2rads$, linear and nonlinear spring, rigid beam $O'B$)

Figures 6.5 and 6.6 show the time histories of the displacement of point A of the rigid and the elastic beam, respectively. Point A is a point on the half length of the beam (see Figure 6.1). Figures 6.7 and 6.8 display the time evolutions of the water pressure at point O'. In Figures 6.5-6.8, real time t is used instead of the dimensionless time $\bar{t}$ because the time scale T_0 is different for each case.

The calculations take much time, such as for the rigid beam linear spring case, it takes five to ten hours for the first step (calculated at UNIX workstation, 300Mhz processor, 128MB RAM) then about one hour for each time step $\Delta\bar{t} = 0.01$. The calculations were carried out on a workstation. Therefore, we terminate the calculation when one period is observed or when the vibration becomes stable. The more complicated the case, the more time steps are required in the calculation. Longer time responses are necessary for the nonlinear spring case than linear spring case, and an increased number of time steps for the elastic beam case than for the rigid beam case.

It is observed from Figure 6.5 that the displacement response of the rigid beam system supported by the linear spring is a damped oscillation. The period of this free vibration of the beam water system is $T = 0.90sec = 1.01T_r$ which approximately agree

with the predictions of the rigid beam-water interaction system investigated by Xing *et al.* (2003), where an idealised rigid beam model is used.

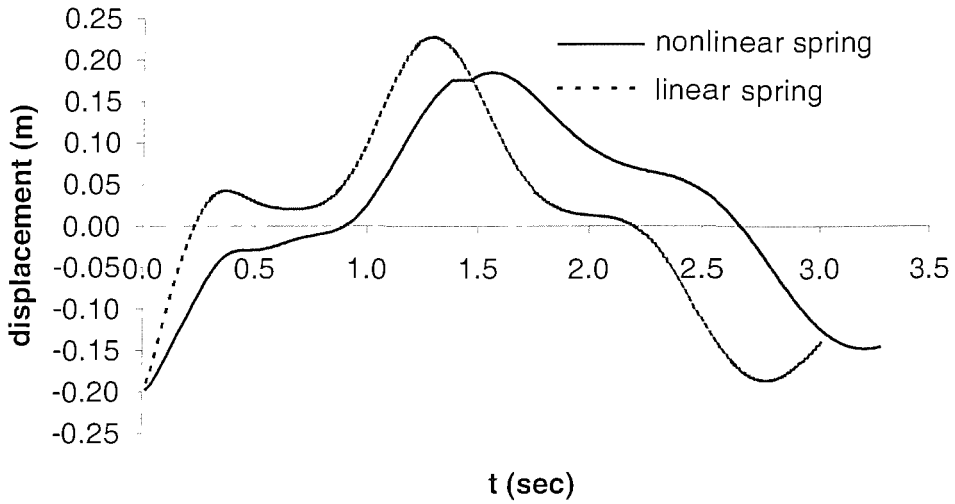

Figure 6.6 Displacement time history at point A during simulation ($\theta_0 = 0.2rads$, linear and nonlinear spring, elastic beam $O'B$)

It is found from Figure 6.7 that the water pressure follows a damping shaped profile but its characteristic does not follow a typical, simple damped oscillation form although the initial rotation angle is not large ($\theta_0 = 0.2rads$). This may arise because of the modelling of the fluid field in which viscous effects are included in the numerical model.

In Figure 6.7, the curve for the last few time steps for linear spring case is not smooth. The pressure is still rising but much slower than previous. The calculation for this case is well over one period of the structure's first natural vibration period without water.

We see large variation for rigid beam cases and small variation for elastic beam cases between linear and nonlinear spring cases for displacement between Figure 6.5 and 6.6 and for pressure between Figure 6.7 and 6.8. The reason is that the vibration along the elastic beam absorbs a significant part of the mechanic energy of the system. And the nonlinear spring is a soft spring which also delay the reaction of the system.

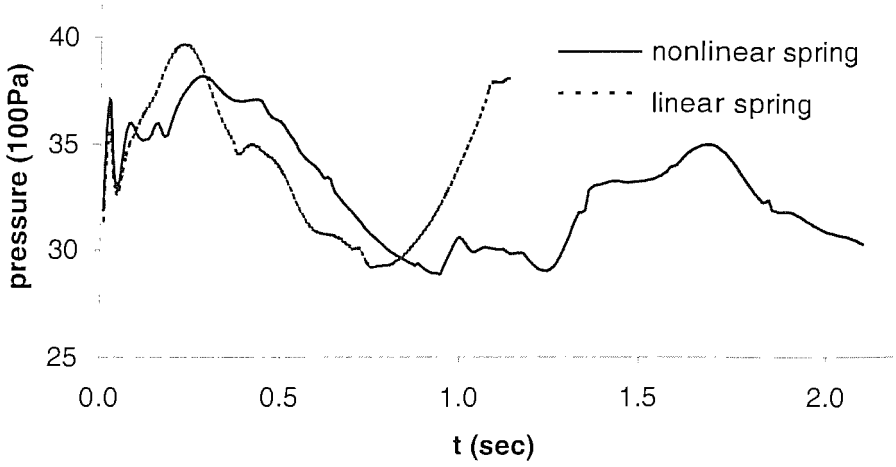

Figure 6.7 Pressure forces time history at point O' during simulation ($\theta_0 = 0.2rads$, linear and nonlinear spring, rigid beam $O'B$)

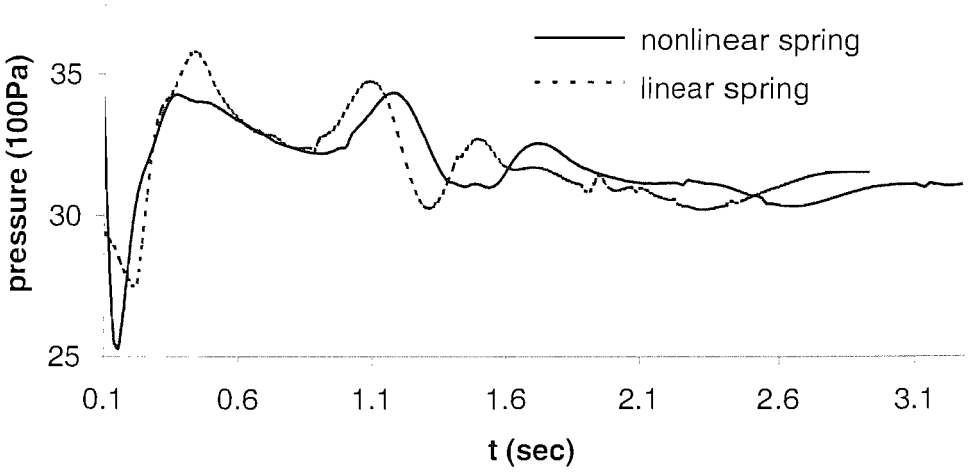

Figure 6.8 Pressure forces time history at point O' during simulation ($\theta_0 = 0.2rads$, linear and nonlinear spring, elastic beam $O'B$)

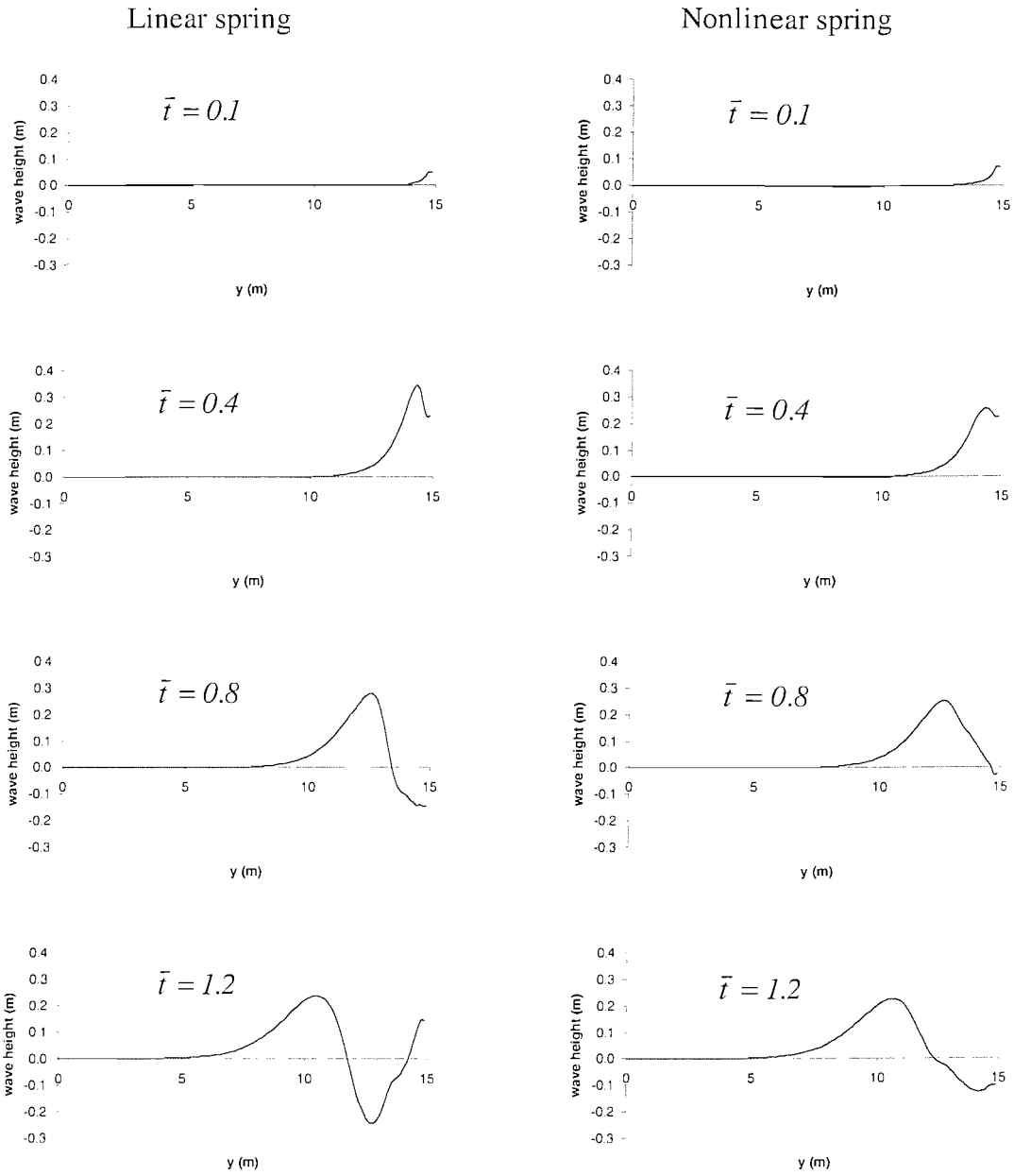

Figure 6.9 Free surface wave height disturbance along tank at dimensionless time $\bar{t} = 0.1$, 0.4, 0.8, 1.2 for rigid beam, linear and nonlinear spring cases, $\theta = 0.2 rad$.

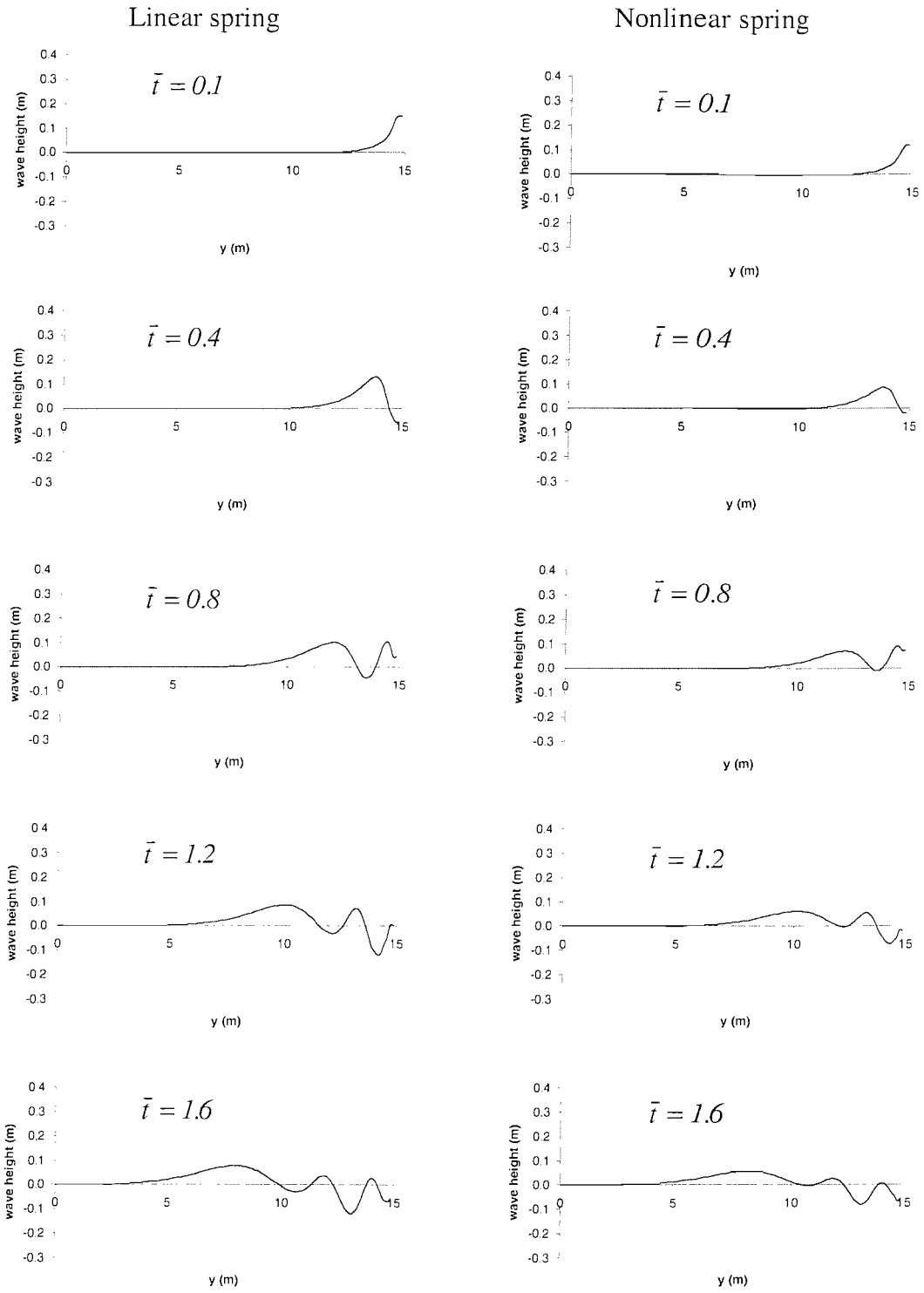

Figure 6.10 Free surface wave height disturbance along tank at dimensionless time $\bar{t} = 0.1$, 0.4, 0.8, 1.2, 1.6 for elastic beam, linear and nonlinear spring cases, $\theta = 0.2 rad$.

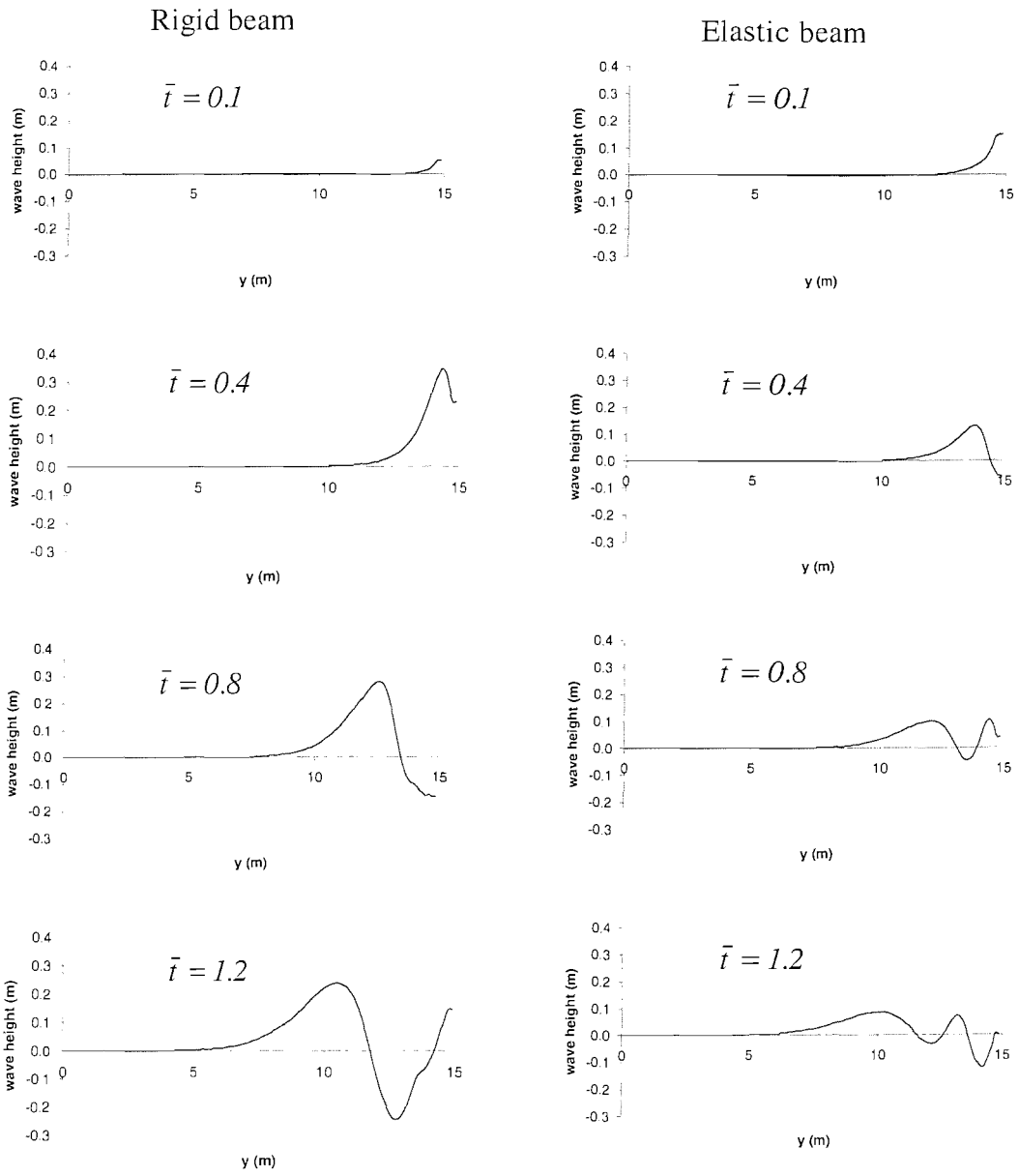

Figure 6.11 Free surface wave height disturbance along tank at dimensionless time $\bar{t} = 0.1$, 0.4, 0.8, 1.2 for rigid and elastic beams, linear spring case, $\theta = 0.2rad$.

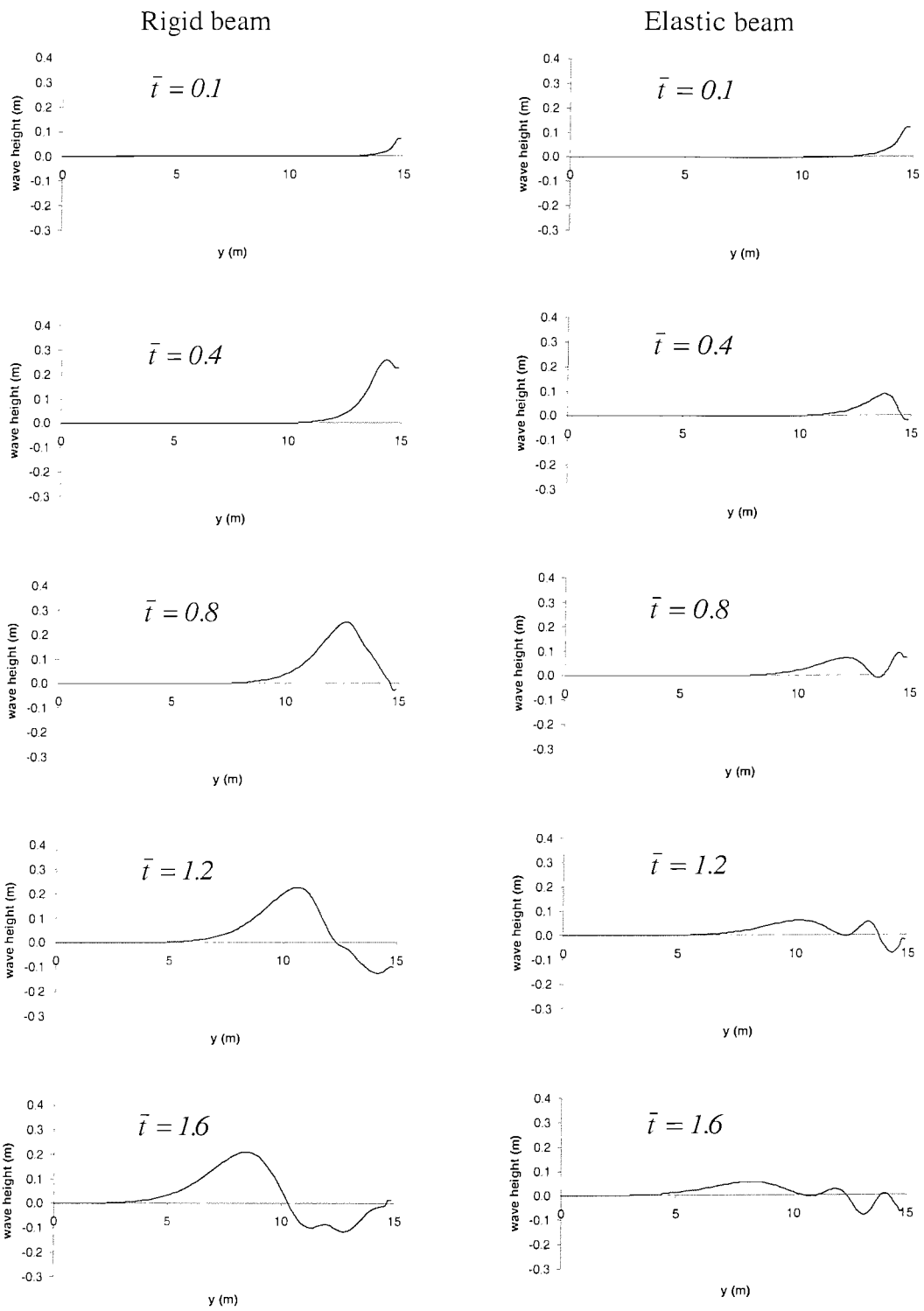

Figure 6.12 Free surface wave height disturbance along tank at dimensionless time $\bar{t} = 0.1$, 0.4, 0.8, 1.2, 1.6 for rigid and elastic beams, nonlinear spring case, $\theta = 0.2rad$.

A very obvious difference between the rigid and elastic beam systems is observed in Figures 6.6 and 6.8, where oscillations appear with higher frequency content and the dynamic responses of the beam-water interaction system are affected by the dynamic characteristics of the elastic beam. One vibration period ends when point A returns to its initial position or the direction of the velocity of point A changes twice. The actual vibration period for the elastic beam water system is $T = 2.79 sec$ compared with $T_e = 1.73 sec$ for elastic beam structure system in air ($\bar{t} = T / T_e = 1.6$). For the rigid beam case, the equivalent period is $T = 0.90 sec = 1.01 T_r$. These results demonstrate the influence of fluid-structure interactions when the complexity of the system increases.

For the initial rotation angle used herein, the nonlinear spring is weaker than the linear one, and therefore it is seen from Figures 6.5 - 6.8 that the vibration period for the nonlinear system is longer than that for the linear one. The effect of the nonlinearity of the supporting spring on the vibration period and response curves for the elastic beam is more obvious than for the rigid beam.

The free surface wave height disturbances along the towing tank are shown in Figures 6.9-6.12. The left hand side of Figures 6.9 - 6.12 denotes the fixed boundary for the water and the right hand side represents the beam which is the wave-maker. In these Figures, the horizontal axis describes the length along the towing tank, and the vertical axis defines the free surface wave height under the assumption that the free surface height is zero at its initial position.

The dynamic processes in both the rigid and elastic beam systems show damped oscillations, but the amplitudes of the responses for the elastic beam system reduce faster than those for the rigid beam system. This is because the elastic beam has deflection movement as well as rigid rotation and these dissipate more efficiently mechanical energy than a single rigid rotation movement as in the case of a rigid beam.

The free surface wave height profiles for both rigid and elastic beam $O'B$ with linear spring are shown in Figures 6.9 and 6.10 and the nonlinear spring cases are shown in Figures 6.11 and 6.12. Here the first vibration period of the structure is chosen as a characteristic time and corresponding dimensionless times are used.

Similar to the displacement responses described previously, the wave height decreases more in value for the elastic beam system than the rigid one. It is also observed

that non-linearity of the spring has more influence on free surface wave height disturbance for the rigid beam system than the elastic one and the free surface wave height amplitudes for the nonlinear spring case are smaller than those predicted for the linear spring systems.

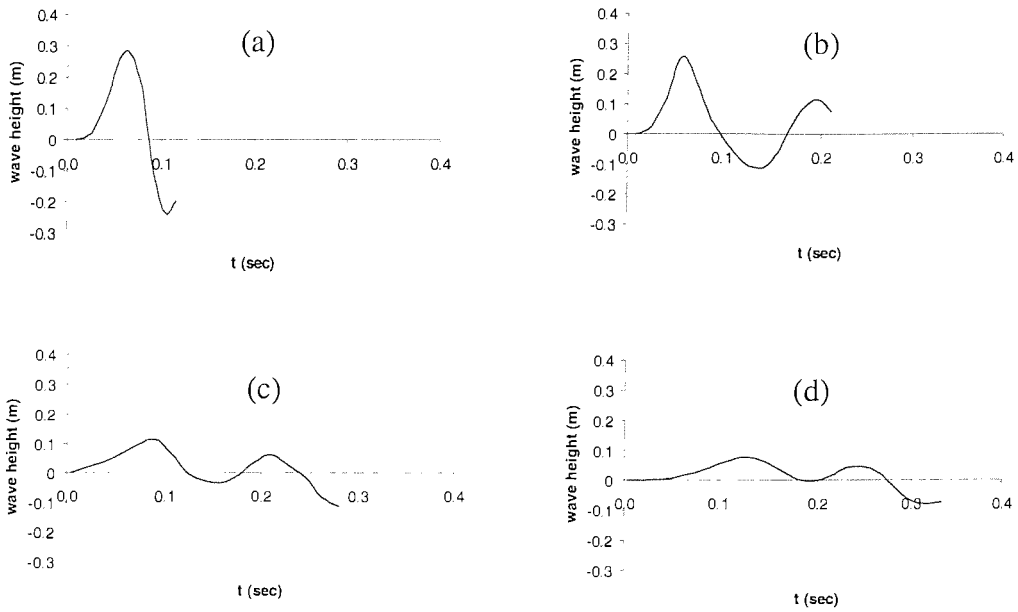

Figure 6.13 Wave height disturbance time history at two metres away from the wave-maker. (a) rigid beam, linear spring; (b) rigid beam, nonlinear spring; (c) elastic beam, linear spring; (d) elastic beam, nonlinear spring.

Figure 6.13 shows the wave height disturbance time history at a point in the water surface two metres away from the wave-maker, i.e., at point $(13.0,1.0)$ in the fixed spatial coordinate system $O-yz$ (the wave-maker is based at point $(15.0,0)$) for rigid and elastic beam, linear and nonlinear spring cases. It is assumed that the original wave height is zero when the system is static. Calculation time for elastic beam cases is longer than rigid beam ones and nonlinear spring cases is longer than linear spring cases. It is seen that the wave height for elastic beam cases is much lower than the rigid beam cases.

In Figure 6.13 the maximum of wave height for elastic beam cases is around $0.1m$, whilst the one for rigid beam cases is around $0.3m$ (the water depth $h = 1m$).

These calculations show that although the initial rotation angle $\theta_0 = 0.2rads$ is not large, the free surface wave height amplitude is quite large compared to the water depth ($h = 1m$), especially in the rigid beam cases in which the largest wave height amplitude recorded is about $0.35m$. This indicates that the dynamic process occurring in the beam-water interactive system is nonlinear.

Further calculations show that for a rotation angle $\theta_0 = 0.5rads$, separation between beam and water occurs as well as an increase in determined wave height of approximately $0.6m$, which caused difficulty in calculations using the current computer code. To solve this problem requires the mathematical model to include possible fluid-structure separation in simulations of the fluid-structure interface as well as accounting for shallow water affects.

There is no readily available experimental data or other independently determined results to compare with this particular study. The only available results to compare are given in the investigation by Xing, *et al* (2003) in which a spring-rigid beam-water system was studied. Because the structure and fluid solvers are both proven to be effective in separate structure or fluid domain (see Price and Chen (2005)) cases, the only added problem is the fluid-structure interface. This problem is solved by iterative procedures to ensure convergence is achieved at every step.

Chapter 7
Conclusions and further research work

The present research study concentrates on the natural characteristics and dynamic responses of beam-water interaction systems in both linear and nonlinear cases. Linear problems are discussed in Chapters 2 to 5, and the dynamic response of a nonlinear beam-water system presented in Chapter 6. Chapter 1 explains the background to this research and includes a brief review of research investigations relating to beam-water interaction problems involving natural frequency and dynamic responses of linear and nonlinear systems. Chapter 2 derives the governing equations in a variable separation form to evaluate the natural frequency and dynamic response of a linear beam-water interaction system with an attached mass with moment of inertia at the free end of the beam subject to an undisturbed or Sommerfeld radiation condition at infinity in the water domain. Chapter 3 discusses the numerical method to solve the equations developed in Chapter 2. Chapter 4 studies the natural frequency of the system and its dynamic responses subject to a horizontal foundation vibration and a free end forced vibration of the beam-water interaction system with undisturbed condition imposed at infinity. Chapter 5 investigates the effect of the Sommerfeld radiation condition imposed at infinity on the natural frequency and dynamic response of the fluid-structure systems. A one-dimensional spring-mass-water system, a two-dimensional spring-rigid rod-water system and the beam-water interaction system presented in Chapter 5 are included in this investigation. Complex values of frequency are derived in these cases, indicating that the introduction of a Sommerfeld radiation condition produces energy dissipation from the system and its dynamic behaviour is similar to characteristics observed in a viscously damped free vibration. Calculations show little difference between the dynamic responses of the beam water system with imposed undisturbed or Sommerfeld radiation condition at infinity, though the latter significantly increase computational and analysis effort. In Chapter 6, an iterative procedure is used to calculate the dynamical responses of a nonlinear beam-water interaction system which simulates a flap wave maker. The

influence of structural elasticity in the dynamic response of the whole system and the influence of nonlinearity of the structure in the dynamic response are mainly studied.

7.1 Conclusions

The following conclusions are drawn from these investigations, which provide guidelines to deal with some beam-water interaction problems in engineering.

1) For linear systems, the attached mass with moment of inertia has significant influence in the dynamical responses of the beam-water interaction system. The natural frequency of the system decreases when the value of attached mass or moment of inertia increases.
2) The imposed Sommerfeld radiation condition at infinity on a fluid-structure interaction system produces an energy dissipation from the system through the fluid even though there is no damping contribution considered in the fluid and structure. The natural frequencies of the system are of complex values of which the real component values are close to the corresponding natural frequency values determined when an undisturbed condition is imposed at infinity and the imaginary component values are very small representing a damping mechanism. This first derivation of the natural frequency for a two-dimensional fluid-structure interaction problem with radiation condition imposed at infinity provides support to physical intuition of energy dissipation from this non-conserving energy mechanism. The results derived in Chapter 5 provide an understanding of how the Sommerfeld radiation condition affects the natural vibration and dynamic response of the system. The number of degrees of freedom adopted in defining the behaviour of the fluid does not affect the number of system frequencies.
3) Dynamic responses of linear beam-water interaction systems for horizontal foundation vibration and free end forced vibration are investigated for both imposed undisturbed or radiation condition. The results show significant differences between the cases with and without attached mass and concentrated moment of inertia, therefore they should be taken into account in design studies where applicable (e.g., offshore structures with significant top weight component). Numerical examples

show little difference between dynamic responses of the beam-water interaction systems with undisturbed or Sommerfeld radiation condition imposed at infinity. This result indicates that for some simple fluid-structure interaction problems, the undisturbed condition at infinity may be applied instead of the Sommerfeld radiation condition and reasonable results achieved with a decrease in theoretical analyssi and computational effort.

4) The governing equations describing the nonlinear dynamics of a beam undergoing a large rigid rotation about its base and small elastic deformation are developed, which are transferred into numerical equations using a mixed finite element – finite difference model. The iterative method developed demonstrates an effective and practical approach to solve strongly coupled structure-water interaction problems by using a FEA solver in the structural analysis of a beam and a finite difference solver for the fluid dynamics.

5) From the numerical simulations of this beam-water interaction system adopting rigid or elastic beam, linear or nonlinear spring, the following points summarise findings.

   a) Significant differences are observed between dynamic responses of rigid and elastic beam systems. Therefore a cautious approach should be used when treating a flexible structure as a rigid body since error may ensue and physical behaviour missed or wrongly represented. A fluid-structure interaction analysis is necessary to safeguard the investigator from such pitfalls.

   b) As a result of the deflection deformation of the elastic beam, the amplitudes of dynamic responses of beam displacement, fluid pressure and free surface wave height decrease in value faster than those for the rigid beam system. The dynamic response amplitudes of elastic beam-water system are smaller than those corresponding to the rigid beam-water system.

   c) The nonlinearity of the spring has more influence in the rigid beam system than in the elastic beam system for the cases studied. This is because the supporting spring is the only element to constrain the rigid rotation of the beam.

   d) Even for small initial rotation angles, the responses of the elastic beam-water interaction system are nonlinear in character.

To summarise, it is concluded that the mathematical model and analytical methods investigated, developed and the results obtained in this thesis provide an important contribution to the study of the dynamics of beam-water interaction systems by providing new insights into the mechanisms arising when different boundary conditions are imposed in the mathematical model.

7.2 Further research work

Further research investigations will focus on the dynamic behaviour of more complicated fluid-structure interaction problems.

Firstly, in this study, the boundary conditions of the beam are fixed-free or simply supported-free. If we want to use the beam-water model to simulate a long thin ship floating on water, free-free boundary condition should be applied to the structure. The dynamic behaviour of a free-free elastic beam-water system will be investigated. The governing equations are the same, but the boundary conditions are different.

Secondly, the nonlinear effect caused by gravity due to the large rotation movement of the beam is not included in the present numerical study. From equations (6.11), (6.12) and (6.17), we can see the governing equations of the structure become much more complicated, and the nonlinearity of the dynamic behaviour of the system may be more visible. The structure solver code needs to be updated with the gravity effect being considered. This basic study provides the foundation to develop a general mathematical model to tackle a wide range of fluid-structure interaction problems and to assess the importance or otherwise of different assumptions introduced into the model allowing comparison with physical reality.

References:

- Anderson, W. K. and Bonhaus, D. L. 1994 An implicit upwind algorithm for computing turbulent flows on unstructured grids, *Computers and Fluids*, **23**(1), 1-21.
- Arens, T. 1999 The scattering of plane elastic waves by a one-dimensional periodic surface, *Math. Meth. Appl. Sci.*, **22**, 55-72.
- Attwood, E. L. and Pengelly, H. S. 1922 *Theoretical naval architecture*, Longmans, Green & Co, London.
- Baldwin, B. S. and Barth, T. J. 1991 A one-equation turbulence transport model for high Reynolds number wall bounded flows, *AIAA* 91-0610.
- Bathe, K. J. 1982 *Finite element procedures in engineering analysis*, Prentice-Hall Inc., Englewood Cliffs, USA.
- Bathe, K. J. (Editor) 2001 *Proceedings of First MIT Conference on Computational Fluid and Solid Mechanics*, 12-15 June, 2001, Cambridge, Massachussetts, USA.
- Baysal, O., Fouladi, K. and Lessard, V. R. 1991 Multigrid and upwind viscous flow solver on three dimensional overlapped and embedded grids, *AIAA Journal*, **29**(6), 903-910.
- Bergan, P. G., Mollestad, E. and Sandsmark, N. 1985 Non-linear static and dynamic response analysis for floating offshore structures, *Engineering Computations*, **2**(1), 13-20.
- Bishop, R. E. D. and Price, W. G. 1979 *Hydroelasticity of ships*, Cambridge University Press.
- Bourgin, A. 1953 *The design of dams*, Sir Isaac Pitman & Sons, LTD, London.
- Casagrande, A. 1973 *Embankment dam engineering: Casagrande volume*, Wiley, New York.
- Chang, J. Y. and Liu, W. H. 1989 Some studies on the natural frequencies of immersed restrained column, *Journal of Sound and Vibration*, **130**(3), 516-524.
- Cohn, P. M. 1974 *Algebra*, Wiley, London.
- Courant, R. and Hilbert, D. 1962 *Methods of mathematical physics*, Interscience, New York.

- Drews, J. E. and Horst, P. 2001 Fluid-structure interaction of high lift devices at low Mach numbers, *Computational Fluid and Solid Mechanics*, (ed. Bathe, K. J.), 1139-1142, Elsevier Science.
- Eatock Taylor, R. 1981 A review of hydrodynamic load analysis for submerged structures excited by earthquakes, *Engineering Structures*, **3**, 131-139.
- Evans, J. H. 1975 *Ship structural design concepts*, Cornell Maritime Press, Inc., Cambridge, Maryland.
- Filippi, P., Habault, D., Lefebvre, J. P. and Bergassoli, A. 1999 *Acoustics basic physics, theory & methods*, Academic Press, San Diego.
- Frink, N. T. 1996 Assessment of an unstructured grid method for predicting 3-D turbulent viscous flows, *AIAA* 96-0292.
- Froberg, C. E. 1965 *Introduction to numerical analysis*, Addison-Wesley Publishing Co, Reading.
- Hairer, E., Nrsett, S. P. and Wanner, G. 1987 *Solving ordinary differential equations I*, Springer-Verlag, Berlin.
- Hirsch, C. 1988 *Numerical computation of internal and external flows*, John Wiley & Sons, Chichester.
- Jansen, R. B. 1988 *Advanced dam engineering for design, construction and rehabilitation*, Van Nostrand Reinhold.
- Kao, K. H., Liou, M. S. and Chow, C. Y. 1994 Grid adaptation using chimera composite overlapping meshes, *AIAA Journal*, **32**(5), 942-949.
- Koomullil, R. P. and Soni, B. K. 1999 Flow simulation using generalized static and dynamic grids, *AIAA Journal*, **37**(12), 1551-1557.
- Kroyer, R. 2001 On some aspects of fluid-structure interaction analysis with respect to aeroelasticity on industrial applications, *Computational Fluid and Solid Mechanics*, (ed. Bathe, K. J.), 1272-1277, Elsevier Science.
- Kuang, Z. and Cao, G. 1993 Dynamic response of fluid-single leg gravity platform-soil interaction system, *China Ocean Engineering*, **7**(2), 187-195.
- Kwak, D., Chang, J. L. C., Shanks, S. P. and Chakravarthy, S. R. 1986 A three-dimensional incompressible Navier-Stokes flow solver using primitive variables, *AIAA Journal*, **24**(1), 390-396.

- Laura, P. A. A., Pombo, J. L. and Susemihl, E. A. 1974 A note on the vibrations of a clamped-free beam with a mass at the free end, *Journal of Sound and Vibration*, **37**(2) 161-168.
- Laura, P. A. A. and Gutierrez, R. H. 1986 Vibrations of an elastically restrained cantilever beam of varying cross section with a tip mass of finite length, *Journal of Sound and Vibration*, **108**(1) 123-131.
- Lay, D. C. 2002 *Linear algebra and its applications*, third edition, Addison-Wesley Publishing Co., Reading.
- Leonards, G. A. (editor) 1987 *Dam failures: Proceedings of the International Workshop of Dam Failures*, 6-8 August 1985, Purdue University, Elsevier, Amsterdam.
- Matthies, H. G. and Steindorf, J. 2001 How to make weak coupling strong. *Computational Fluid and Solid Mechanics*, (ed. Bathe, K. J.), 1317-1319, Elsevier Science.
- Mok, D. P., Wall, W. A. and Ramm, E. 2001 Accelerated iterative substructuring schemes for instationary fluid-structure interaction, *Computational Fluid and Solid Mechanics*, (ed. Bathe, K. J.), 1325-1328, Elsevier Science.
- Nagaya, K. 1985 Transient response in flexure to general uni-directional loads of variable cross-section beam with concentrated tip inertias immersed in a fluid, *Journal of Sound and Vibration*, **99**(3), 361-378.
- Nagaya, K. and Hai, Y. 1985 Seismic response of underwater members of variable cross section, *Journal of Sound and Vibration*, **103**(1), 119-138.
- Novozhilov, V. V. 1961 *Theory of elasticity*, Pergamon Press, New York.
- Pippard, A. B. 1978 *The physics of vibrations*, Volume 1, Cambridge University Press, London.
- Popov, E. P. 1968 *Introduction to mechanics of solids*, Prentice Hall, Inc., Englewood Cliffs, USA.
- Pramila, A. 1986 Sheet flutter and the interaction between sheet and air, *TAPPI-Journal* **69**, 70-74.
- Pramila, A. 1987 Natural frequencies of a submerged axially moving band, *Journal of Sound and Vibration* **113**(1), 198-203.

- Price, W. G. and Chen, Y. G. 2005 A simulation of free surface waves for incompressible two-phase flows using a curvilinear level set formulation, *International Journal for Numerical Methods in Fluids* (in press).
- Price, W. G. and Xing, J. T. 2000 A mixed finite element – finite difference method for nonlinear fluid-solid interaction dynamics, *ICTAM 2000 – 20th International Congress of Theoretical and Applied Mechanics*, pp.216, 27 Aug-2 Sept 2000, Chicago, Illinois, USA.
- Roe, P. L., 1981, Approximate Riemann solvers, parameter vectors and difference scheme, *Journal of Computational Physics*, **43**, 357-372.
- Rogers, S. E., Kwak, D. and Kiris, C. 1991 Steady and unsteady solutions of the incompressible Navier-Stokes equations, *AIAA Journal*, **29**(4), 603-610.
- Shen, Q. X., Cai, R. Q., Chen, Y. G. and Chen, Z. G. 1996 Solution of viscous flow around ships using flux-difference splitting upwind difference scheme, *Journal of Hydrodynamics*, series A **11**(4), 372-384.
- Sommerfeld, A. 1949 *Partial differential equations in physics*, Academic, New York.
- Takahashi, K. 1980 Eigenvalue problem of a beam with a mass and spring at the end subjected to an axial force, *Journal of Sound and Vibration*, **71**(3), 453-447.
- Thomson, W. T. 1988 *Theory of vibration with applications*, third edition, Prentice, London.
- To, C. W. S. 1982 Vibration of a cantilever beam with a base excitation and tip mass, *Journal of Sound and Vibration*, **83**(4), 445-460.
- Townsend, A. A. 1980 Response of sheared turbulence to additional distortion, *Journal of Fluid Mechanics*, **98**(1), 171-191.
- Uscilowska, A. and Kolodziej, J. A. 1998 Free vibration of immersed column carrying a tip mass, *Journal of Sound and Vibration*, **216**(1), 147-157.
- Vernon, J. B. 1967 *Linear vibration theory: generlized properties and numerical methods*, Wiley, New York.
- Westermo, B. D. 1981 Dynamic response of elastic cyliners in fluid layer, *ASCE J Eng Mech Div*, **107**(1), 187-205.
- Wylie, C. R., Jr. 1960 *Advance engineering mathematics*, second edition, McGraw-Hill Book Company, Inc., New York.

- Xing, J. T. 2002 Natural vibrations of a 1-dimensional fluid-structure interaction system subject to Sommerfeld radiation condition, Communication note, L/28/02, 6 August, 2002.
- Xing, J. T., Price, W. G., Pomfret, M. J. and Yam, L. H. 1997 Natural vibration of a beam-water interaction system, *Journal of Sound and Vibration*, **199**(3), 491-512.
- Xing, J. T. and Price, W. G. 2000 Theory of non-linear elastic ship-water interaction dynamics, *Journal of Sound and Vibration*, **230**(4), 877-914.
- Xing, J. T., Price, W. G. and Chen, Y. G. 2002 A numerical simulation of nonlinear fluid-rigid structure interaction problems, *Proceedings of the ASME International Mechanical Engrg Congress & Exposition*, ISBN: 0791816931, Volume 3 (CD-ROM), Session AMD-12A, Paper IMECE2002-32534, 1-10, November 17-22, 2002, New Orleans, USA.
- Xing, J. T., Price, W. G. and Chen, Y. G. 2003 A mixed finite element – finite difference method for nonlinear fluid – structure interaction dynamics, Part I: fluid - rigid structure interaction, *Proc. R. S. Lond. A*, **459**, 2399-2430.
- Zhang, H. and Bathe, K. J. 2001 Direct and iterative computing of fluid flows fully coupled with structures, *Computational Fluid and Solid Mechanics*, (ed. Bathe, K. J.), 1440-1443, Elsevier Science.
- Zhao, S., Xing, J. T. and Price, W. G. 2002 Natural vibration of a flexible beam-water coupled system with a concentrated mass attached at the free end of the beam, *Proc Instn Mech Engrs, Part M: J Engineering for the Maritime Environment*, **216**, 145-154.
- Zienkiewicz, O. C. and Taylor, R. L. 1989 *The finite element method*, fourth edition, Volume 1, McGraw-Hill, New York.
- Zienkiewicz, O. C. and Taylor, R. L. 1991 *The finite element method*, fourth edition, Volume 2, McGraw-Hill, New York.

Appendix A

Application of separation of variable method

For equation (2.1)

$$\frac{\partial^2 p}{\partial x^2}+\frac{\partial^2 p}{\partial y^2}=\frac{1}{c^2}\frac{\partial^2 p}{\partial t^2}, \qquad 0<x<\infty,\ 0<y<h. \tag{A.1}$$

where c denotes the velocity of sound in water, we assume the pressure has the form

$$p(x,y,t)=P(x,y)T(t)=X(x)Y(y)T(t). \tag{A.2}$$

Substituting equation (A.2) into equation (A.1) and divide both sides of the equation by $X(x)Y(y)T(t)$, we obtain

$$\frac{1}{X(x)Y(y)T(t)}\left(\frac{\partial^2 p}{\partial x^2}+\frac{\partial^2 p}{\partial y^2}\right)=\frac{1}{X(x)Y(y)T(t)}\frac{1}{c^2}\frac{\partial^2 p}{\partial t^2},$$

$$\frac{1}{X(x)Y(y)T(t)}\left(\frac{\partial^2\left(X(x)Y(y)T(t)\right)}{\partial x^2}+\frac{\partial^2\left(X(x)Y(y)T(t)\right)}{\partial y^2}\right)=\frac{1}{X(x)Y(y)T(t)}\frac{1}{c^2}\frac{\partial^2\left(X(x)Y(y)T(t)\right)}{\partial t^2}$$

$$\frac{1}{X(x)Y(y)T(t)}\left(\frac{\partial^2 X(x)}{\partial x^2}Y(y)T(t)+\frac{\partial^2 Y(y)}{\partial y^2}X(x)T(t)\right)=\frac{X(x)Y(y)}{X(x)Y(y)T(t)}\frac{1}{c^2}\frac{\partial^2 T(t)}{\partial t^2},$$

$$\frac{X''(x)}{X(x)}+\frac{Y''(y)}{Y(y)}=\frac{1}{c^2}\frac{\ddot{T}(t)}{T(t)}. \tag{A.3}$$

In equation (A.3), the three terms in the equation are functions of variables x, y and t, respectively. This equation stands only if all the terms in this equation are constants. Therefore, We assume that

$$\frac{X''(x)}{X(x)}=-\hat{\lambda}^2, \tag{A.4}$$

$$\frac{Y''(y)}{Y(y)}=-\hat{\kappa}^2, \tag{A.5}$$

$$\frac{\ddot{T}(t)}{T(t)}=-\hat{\Omega}^2, \tag{A.6}$$

and from equation (A.3), the three constants $\hat{\lambda}$, $\hat{\kappa}$ and $\hat{\Omega}$ satisfy the following equation,

$$\hat{\lambda}^2 + \hat{\kappa}^2 = \frac{\hat{\Omega}^2}{c^2}, \tag{A.7}$$

or in another form used in Chapter 2,

$$\hat{\lambda}^2 = \frac{\hat{\Omega}^2}{c^2} - \hat{\kappa}^2. \tag{A.8}$$

Equations (A.4)-(A.6) can therefore be expressed in the following forms,

$$X'' + \hat{\lambda}^2 X = 0, \tag{A.9}$$

$$Y'' + \hat{\kappa}^2 Y = 0, \tag{A.10}$$

$$\ddot{T} + \hat{\Omega}^2 T = 0. \tag{A.11}$$

Appendix B

Orthogonality relations of the complex natural vibration forms

The orthogonality relations associated with natural vibration assuming an undisturbed condition imposed at infinity have been discussed by Xing, *et al.* (1997). In a similar manner, the orthogonality relations of the complex natural vibration forms with a Sommerfeld radiation condition imposed at infinity are derived as follows:

A solution is assumed in the form $p(x,y,t)=P(x,y)T(t)$, $u_1(y,t)=U_1(y)T(t)$ and $u_2(y,t)=U_2(y)T(t)$, where $T(t)=e^{-\mathrm{i}\hat{\Omega}t}$. The substitution of this solution into equations (4.70)-(4.77) and (4.79)-(4.82) gives

$$P_{,ii}+\frac{\hat{\Omega}^2}{c^2}P=0, \tag{B.1}$$

$$P_{,y}(x,0)=0, \tag{B.2}$$

$$P(x,h)=0, \qquad \text{with the free surface waves neglected,} \tag{B.3}$$

or

$$P_{,y}-\frac{\hat{\Omega}^2}{g}P=0, \qquad \text{with the free surface waves included,} \tag{B.4}$$

$$P_{,x}-\mathrm{i}c\hat{\Omega}P=0, \qquad x\to\infty, \tag{B.5}$$

$$P_{,x}=\rho_f\hat{\Omega}^2U_1, \qquad x=0, \tag{B.6}$$

$$EJU_1^{(4)}(y)-\rho_sFU_1(y)=-P(0,y), \qquad 0<y<h, \tag{B.7}$$

$$EJU_2^{(4)}(y)-\rho_sFU_2(y)=0, \qquad h<y<H, \tag{B.8}$$

$$U_1(0)=0, \tag{B.9}$$

$$U_1'(0)=0, \tag{B.10}$$

$$EJU_2''(H)=I_0\hat{\Omega}^2U_2'(H), \tag{B.11}$$

$$EJU_2'''(H)=-m_0\hat{\Omega}^2U_2(H), \tag{B.12}$$

$$U_1(h)=U_2(h), \tag{B.13}$$

$$U_1'(h) = U_2'(h), \tag{B.14}$$

$$U_1''(h) = U_2''(h), \tag{B.15}$$

$$U_1'''(h) = U_2'''(h). \tag{B.16}$$

For convenience, a tensor index i $(i = 1,2)$ is used to represent x and y, respectively, and $(\ )_{,ii} = (\ )_{,11} + (\ )_{,22}$; $(\ )_{,x} = \partial(\ )/\partial x$; $(\ )_{,y} = \partial(\ )/\partial y$. In the same way, a set of equations satisfied by the conjugate solution $p^* = P^*T^*$, $u_1^* = U_1^*T^*$, $u_2^* = U_2^*T^*$ can be derived, which is similar to the set satisfied by solution $p = PT$, $u_1 = U_1T$, $u_2 = U_2T$ but with all complex quantities replaced by their corresponding conjugate quantities. These equations are as follows.

$$P_{,ii}^* + \frac{\left(\hat{\Omega}^*\right)^2}{c^2} P^* = 0, \tag{B.17}$$

$$P_{,y}^*(x,0) = 0, \tag{B.18}$$

$$P^*(x,h) = 0, \qquad \text{with the free surface waves neglected,} \tag{B.19}$$

or

$$P_{,y}^* - \frac{\left(\hat{\Omega}^*\right)^2}{g} P^* = 0, \qquad \text{with the free surface waves included,} \tag{B.20}$$

$$P_{,x}^* - \mathbf{i}c\hat{\Omega}^* P^* = 0, \qquad x \to \infty, \tag{B.21}$$

$$P_{,x}^* = \rho_f \left(\hat{\Omega}^*\right)^2 U_1^*, \qquad x = 0, \tag{B.22}$$

$$EJU_1^{*(4)}(y) - \rho_s F U_1^*(y) = -P(0,y), \qquad 0 < y < h, \tag{B.23}$$

$$EJU_2^{*(4)}(y) - \rho_s F U_2^*(y) = 0, \qquad h < y < H, \tag{B.24}$$

$$U_1^*(0) = 0, \tag{B.25}$$

$$U_1^{*\prime}(0) = 0, \tag{B.26}$$

$$EJU_2^{*\prime\prime}(H) = I_0\left(\hat{\Omega}^*\right)^2 U_2^{*\prime}(H), \tag{B.27}$$

$$EJU_2^{*\prime\prime\prime}(H) = -m_0\left(\hat{\Omega}^*\right)^2 U_2^*(H), \tag{B.28}$$

$$U_1^*(h) = U_2^*(h), \tag{B.29}$$

$$U_1^{*'}(h) = U_2^{*'}(h), \tag{B.30}$$

$$U_1^{*''}(h) = U_2^{*''}(h), \tag{B.31}$$

$$U_1^{*'''}(h) = U_2^{*'''}(h). \tag{B.32}$$

It is assumed that $\hat{\Omega}_n$ and $\hat{\Omega}_m^*$ are two different natural frequencies and P_n, U_{1n}, U_{2n} and P_m^*, U_{1m}^*, U_{2m}^* the corresponding natural vibration forms satisfying equations (B.1)-(B.16) and their conjugate equations (B.17)-(B.32). For these solutions, we consider three pairs of equations (B.1), (B.7), (B.8) and their conjugate equations (B.17), (B.23), (B.24). The multiplication of these equations by their conjugate form of solution and integrating over the water domain and structure region in conjunction with subtraction of the integration of their conjugate equations gives,

$$\begin{aligned} 0 = & \int_\Gamma \left[(B.1) \times P_m^* - (B.17) \times P_n \right] d\Gamma \\ & + \int_0^h \left[(B.7) \times \rho_f \left(\hat{\Omega}_m^* \right)^2 U_{1m}^* - (B.23) \times \rho_f \hat{\Omega}_n^2 U_{1n} \right] dy \\ & + \int_h^H \left[(B.8) \times \rho_f \left(\hat{\Omega}_m^* \right)^2 U_{2m}^* - (B.24) \times \rho_f \hat{\Omega}_n^2 U_{2n} \right] dy , \end{aligned} \tag{B.33}$$

where Γ represents the domain of water with its boundary S.

Substituting equations (B.1), (B.7), (B.8), (B.17), (B.23) and (B.24) into equation (B.33), we obtain

$$\begin{aligned} 0 = & \frac{\hat{\Omega}_n^2 - \left(\hat{\Omega}_m^* \right)^2}{c^2} \int_\Gamma P_n P_m^* d\Gamma + \int_\Gamma \left(P_{n,ii} P_m^* - P_n P_{m,ii}^* \right) d\Gamma \\ & + EJ\rho_f \int_0^h \left(U_{1n}^{(4)} U_{1m}^* \left(\hat{\Omega}_m^* \right)^2 - U_{1m}^{*\,(4)} U_{1n} \hat{\Omega}_n^2 \right) dy \\ & + \rho_f \int_0^h \left(P_n(0,y) U_{1m}^* \left(\Omega_m^* \right)^2 - P_m^*(0,y) U_{1n} \hat{\Omega}_n^2 \right) dy \\ & + EJ\rho_f \int_h^H \left(U_{2n}^{(4)} U_{2m}^* \left(\hat{\Omega}_m^* \right)^2 - U_{2m}^{*\,(4)} U_{2n} \hat{\Omega}_n^2 \right) dy . \end{aligned} \tag{B.34}$$

By using Green's theorem, it follows that

$$\int_{\Gamma}\left(P_{n,ii}P_m^* - P_n P_{m,ii}^*\right)d\Gamma = \int_S \left(P_{n,i}P_m^* - P_n P_{m,i}^*\right)\eta_i dS$$

$$= -\int_0^h \left(P_{n,x}(0,y)P_m^*(0,y) - P_n(0,y)P_{m,x}^*(0,y)\right)dy$$

$$-\int_0^\infty \left(P_{n,y}(x,0)P_m^*(x,0) - P_n(x,0)P_{m,y}^*(x,0)\right)dx$$

$$+\int_0^\infty \left(P_{n,y}(x,h)P_m^*(x,h) - P_n(x,h)P_{m,y}^*(x,h)\right)dx$$

$$+\lim_{x\to\infty}\int_0^h \left(P_{n,x}(x,y)P_m^*(x,y) - P_n(x,y)P_{m,x}^*(x,y)\right)dy\,. \qquad \text{(B.35)}$$

The second integration term of equation (B.35) equals zero when we consider boundary condition equations (B.2) and (B.18). Applying the other boundary condition equations (B.3)-(B.6), (B.19)-(B.22), we can simplify equation (B.35) into the following form,

$$\int_{\Gamma}\left(P_{n,ii}P_m^* - P_n P_{m,ii}^*\right)d\Gamma = \beta\frac{\hat{\Omega}_n^2 - \left(\hat{\Omega}_m^*\right)^2}{g}\int_0^\infty P_n(x,h)P_m^*(x,h)dx - J_{mn}(0) + J_{mn}(\infty), \qquad \text{(B.36)}$$

where

$$J_{mn}(x) = \int_0^h \left[P_m^*(x,y)P_{n,x}(x,y) - P_{m,x}^*(x,y)P_n(x,y)\right]dy\,, \qquad \text{(B.37)}$$

$$J_{mn}(0) = \rho_f \int_0^h \left(P_n(0,y)U_{1m}^*\left(\Omega_m^*\right)^2 - P_m^*(0,y)U_{1n}\hat{\Omega}_n^2\right)dy\,, \qquad \text{(B.38)}$$

$$J_{mn}(\infty) = \lim_{x\to\infty} J_{mn}(x)$$

$$= -\mathbf{i}c\left(\hat{\Omega}_n - \hat{\Omega}_m^*\right)\lim_{x\to\infty}\int_0^h P_m^*(x,y)P_n(x,y)dy\,, \qquad \text{(B.39)}$$

$$\beta = \begin{cases} 0 & \text{with the free surface wave neglected} \\ 1 & \text{with the free surface wave included} \end{cases}. \qquad \text{(B.40)}$$

Integrating by parts for the third and fifth terms in equation (B.34), we derive

$$\int_0^h \left(U_{1n}^{(4)}U_{1m}^*\left(\hat{\Omega}_m^*\right)^2 - U_{1m}^{*\,(4)}U_{1n}\hat{\Omega}_n^2\right)dy = \left(\left(\hat{\Omega}_m^*\right)^2 - \Omega_n^2\right)\int_0^h U_{1n}''U_{1m}^{*\,\prime\prime}\,dy$$

$$+\left(\hat{\Omega}_m^*\right)^2\left[U_{1n}'''U_{1m}^* - U_{1n}''U_{1m}^{*\,\prime}\right]_0^h - \Omega_n^2\left[U_{1n}U_{1m}^{*\,\prime\prime\prime} - U_{1n}'U_{1m}^{*\,\prime\prime}\right]_0^h, \qquad \text{(B.41)}$$

$$\int_h^H \left(U_{2n}^{(4)} U_{2m}^* \left(\hat{\Omega}_m^*\right)^2 - U_{2m}^{*\,(4)} U_{2n} \hat{\Omega}_n^2 \right) dy = \left(\left(\hat{\Omega}_m^*\right)^2 - \Omega_n^2 \right) \int_h^H U_{2n}'' U_{2m}^{*\,''} dy$$

$$+ \left(\hat{\Omega}_m^*\right)^2 \left[U_{2n}''' U_{2m}^* - U_{2n}'' U_{2m}^{*\,'} \right]_h^H - \Omega_n^2 \left[U_{2n} U_{2m}^{*\,'''} - U_{2n}' U_{2m}^{*\,''} \right]_h^H . \quad \text{(B.42)}$$

The sum of the boundary terms in these two equations reduces to zero when boundary condition equations (B.9)-(B.16), (B.25)-(B.32) are taken into account.

The substitution of equations (B.36)-(B.42) into equation (B.34) gives

$$\left(\left(\hat{\Omega}_m^*\right)^2 - \Omega_n^2 \right) \left\{ \frac{1}{c^2} \int_\Gamma P_n P_m^* d\Gamma + EJ\rho_f \left[\int_0^h U_{1n}'' U_{1m}^{*\,''} dy + \int_h^H U_{2n}'' U_{2m}^{*\,''} dy \right] \right.$$

$$\left. + \frac{\beta}{g} \int_0^\infty P_n(x,h) P_m^*(x,h) dx \right\} = J_{mn}(\infty) , \quad \text{(B.43)}$$

which has the same form as derived by Xing, *et al.* (1997) for an undisturbed condition imposed at infinity, with the exception that in this equation $J_{mn}(\infty) \neq 0$ (see equation (4.155)) for the Sommerfeld radiation condition case whereas for the undisturbed condition case $J_{mn}(\infty) = 0$. The substitution of equation (B.39) into equation (B.43) gives

$$\left(\hat{\Omega}_m^* - \Omega_n \right) \left\{ \left(\hat{\Omega}_m^* + \Omega_n \right) \left(\frac{1}{c^2} \int_\Gamma P_n P_m^* d\Gamma + EJ\rho_f \left[\int_0^h U_{1n}'' U_{1m}^{*\,''} dy + \int_h^H U_{2n}'' U_{2m}^{*\,''} dy \right] \right. \right.$$

$$\left. \left. + \frac{\beta}{g} \int_0^\infty P_n(x,h) P_m^*(x,h) dx \right) - \mathrm{i}c \lim_{x \to \infty} \int_0^h P_m^*(x,y) P_n(x,y) dy \right\} = 0 . \quad \text{(B.44)}$$

For two different frequencies ($m \neq n$), there exists the following orthogonality relation associated with natural vibration, *i.e.*

$$\left(\hat{\Omega}_m^* + \Omega_n \right) \left(\frac{1}{c^2} \int_\Gamma P_n P_m^* d\Gamma + EJ\rho_f \left[\int_0^h U_{1n}'' U_{1m}^{*\,''} dy + \int_h^H U_{2n}'' U_{2m}^{*\,''} dy \right] \right.$$

$$\left. + \frac{\beta}{g} \int_0^\infty P_n(x,h) P_m^*(x,h) dx \right) - \mathrm{i}c \lim_{x \to \infty} \int_0^h P_m^*(x,y) P_n(x,y) dy = 0 . \quad \text{(B.45)}$$

Appendix C

Flow chart and source program for linear problems

C.1 Flow chart

Figure C1 shows the flow chart for the programs developed to solve equation (3.52). Namely,

$$det\,\mathbf{R}(\omega) = R_r(\omega) + \mathbf{i}R_i(\omega) = 0. \tag{C1}$$

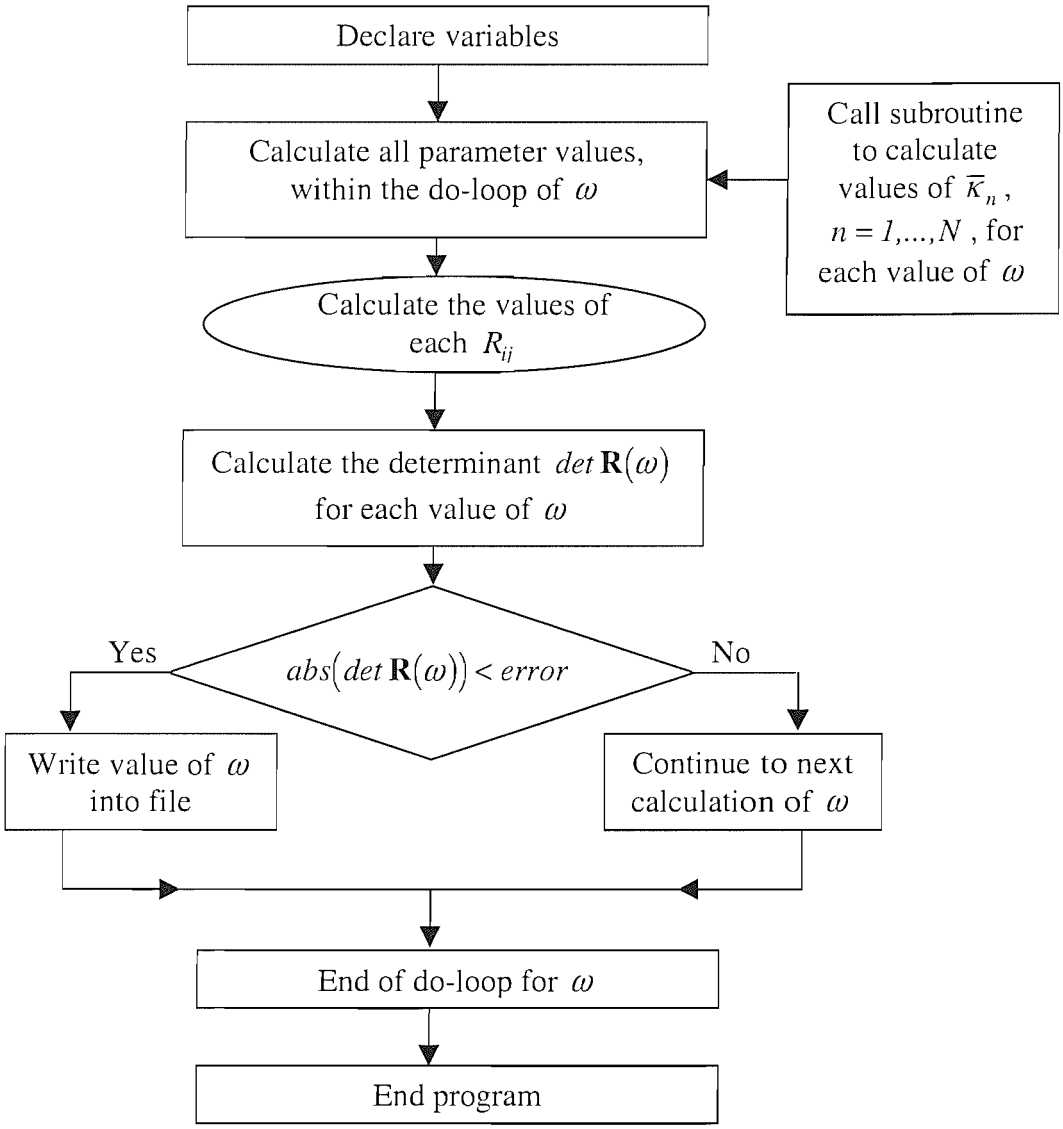

Figure C.1 Flow chart illustrating approach to determine the natural frequency of the linear system.

The developed source program calculates the natural frequency of the linear two-dimensional beam-water interaction system with Sommerfeld radiation condition imposed at infinity. For the undisturbed condition cases, the structure of the program is the same, except that the beam functions are different and the variables are of real values.

The source program allows solution of problems without free surface disturbances. For cases which include free surface wave, $\hat{\kappa}_n$ from the free surface wave disturbance equation (3.23) is unknown, and it needs to be solved for every frequency parameter $\hat{\Omega}$ or ω. As discussed in section 3.3.1, equation (3.23) can be re-written as equation (3.61), which has the same form as equation (C1). Therefore, we can use the same method to find the natural frequency to evaluate roots for $\hat{\kappa}_n$. The subroutine to find roots for $\hat{\kappa}_n$ is mostly the same as developed in the source program to search for the natural frequency parameter ω, so there is no need to show this subroutine.

To evaluate dynamic responses, the array $R(8,8)$ changes to $R(8,9)$, and the additional terms $R(*,9)$ are used to store the non-zero terms on the right hand side of equation (3.50). The Gauss-Seidel method is used to reduce the full matrix $\mathbf{R}$ in equation (3.50) into an upper-triangular matrix, as shown in the source program. It is noted that in the program software the Gauss-Seidel method is used to derive the determinant of the matrix $\mathbf{R}$, but in programs to calculate the dynamic responses, the Gauss-Seidel method is used to solve equation (3.50) with full rank coefficient matrix $\mathbf{R}$.

To derive the natural modes for beam displacement and water pressure responses, the program is the same as those to derive dynamic responses, except that now the natural frequency ω_i is substituted into the coefficient matrix $\mathbf{R}$ reducing its rank reduces to 7 from 8. For convenience of calculation, we assume $D_8 = 1$, or set a certain value for any one of D_j ($j = 1,2,\ldots,8$). This allows elimination of the last equation in equation (3.50) simplifying calculation to the values of the remaining seven D_j. The corresponding beam displacement and water pressure variables are determined from equations (3.67)-(3.69) for this particular frequency ω_i.

C.2 Source program to find the natural frequency with undisturbed condition imposed at infinity.

```
!************************************
! HERE Kn=(2n-1)PI/2h, no disturbance on free
surface
!************************************

program new4
!-------------------------------------------------------------
!** now change all real and complex (8) into (4)
to save memory and space.
!
! main program begin, calculate natural freq of
beam-water sys.
!-------------------------------------------------------------
    IMPLICIT NONE
!
    REAL::WR,WI,DW,WR0,WI0,dwr,dwi

INTEGER::I,J,NUM,N1,N2,N0,NUMr,NUMi,N
s,Nt,Nx,ii,Nx0
          COMPLEX::W,SRR,WS
!
    OPEN(16,FILE='KESI1.DAT')
    OPEN(20,FILE='RESULTS.DAT')
    OPEN(30,FILE='kn.dat')

    OPEN(10,FILE='rootbackup.DAT')
    OPEN(35,FILE='ROOT.DAT')
    OPEN(45,FILE='ROOT-NEWTON.DAT')
            OPEN(71,FILE='ROOT-NEWTON-
check.DAT')

 open(52,file='w-root-seeking.dat')
 open(62,file='w-root-search1.dat')
 open(72,file='w-root-search2.dat')
 open(82,file='w-s2.dat')

!----** CALCULATION BEGINS HERE *****
!
!-----       << W=WR+j*WI >>
!
    NUM=0
    SRR=CMPLX(0.0,0.0)
        DW=0.0001
!
  WR0=5.404
        WI0=-5.0E-6

        dwr=0.001
        dwi=1.0E-6

  NUMr=41
  NUMi=11
  Ns=0
!** Ns is the number of possible roots. at least
one sign change.

  if(abs(WR0)>=abs(WI0)) then
    N1=NUMr
          N2=NUMi
          N0=1
            do i=1,NUMr
                          WR=WR0+(i-1)*dwr
                          do j=1,NUMi
                            WI=WI0+(j-1)*dwi
                          W=CMPLX(WR,WI)
                          NUM=NUM+1
                    write(*,*) 'W=',W
                  CALL DETR(W,SRR)
                          end do
              write(20,*)
                 end do
        else
          N1=NUMi
          N2=NUMr
          N0=2
            do j=1,NUMi
                 WI=WI0+(j-1)*dwi
                 do i=1,NUMr
                    WR=WR0+(i-1)*dwr
                    W=CMPLX(WR,WI)
                 NUM=NUM+1
                    write(*,*) 'W=',W
                 CALL DETR(W,SRR)
                  end do
               write(20,*)
                  end do
        end if

!--get the first approach to the solution with
original method---13.01.2004--
!************************************
!
    WRITE(*,*) '1--------'
  call FIND(N0,N1,N2,Nt)
WRITE(*,*) '--** finish detr() and find()  **-----'

 !*  Nt=0
          Nx=0
   call wcloser(Nt,Nx)
!************************************
```

```
!------------------------------

    END program new4
!*** END OF MAIN PROGRAM new4 ******
!************************************
!     the following is the subroutine DETR to
calculate the determinant of R.
!
!************************************

          SUBROUTINE DETR(W,SRR)
!--------******** to calculate |R| ******--------
    IMPLICIT NONE
REAL::G,PI,ROUF,ROUS,E,C,H,HI,PU,GAMA
,TM,TI,  &
       FF,EJ,EI,OGB,EM0,C1,                &
WR,WI,XKR,XKI,RSRR,AISRR,DETSRR

INTEGER::I,J,K,II,N

COMPLEX::LAMBDA,AI,W,W2,W3,W4,OME
GA,R(8,8),XK,XK2,XK3,XK4,QI,QI1,QI2,QI3,
QI4,  &

EN,EN0,YN,YN1,YN2,YN3,SS,SRR,SM,SI0

    G=9.8
    PI=4*ATAN(1.0)
    ROUF=1.0E+03
    ROUS=2.4E+03
    E=2.94E+10
    C=1439.0

    H=50.0
    PU=0.80

         HI=PU*H
    AI=CMPLX(0.0,1.0)

!----------HERE H IS H, HI IS h----------
!**     W0=0.1
    GAMA=10.0
    FF=ROUF*H/ROUS/GAMA
    EJ=FF*FF*FF/12
!--- HERE bh^3/12, b=1, unit length weight------
    TM=1.0
    EM0=TM*ROUS*H*FF
!------THIS IS UNIT LENGTH WEIGHT---------
    TI=1.0
    EI=TI*EM0*H*H/1000
!------------------------------

    OGB=SQRT(E*EJ/ROUS/FF)/H/H
    C1=C/OGB/H

!***     NUM=NUM+1

!---------- NUM IS THE NUMBER OF
CALCULATIONS OF FILE 20
! ---------- FOR LATER USE TO FIND
ROOTS.
!
!**     W=CMPLX(WR,WI)
!  here use W in index, not WR,WI ---
!--------------------------------
!
    WR=REAL(W)
         WI=AIMAG(W)
    W2=W*W
         W3=W2*W
         W4=W2*W2
!----
    SI0=W4*EI/ROUS/FF/H/H/H
    SM=W4*EM0/ROUS/FF/H
!------------------------------------------------------
-----
! here change SI0, SM, *=W4, save  calculations.
!------------------------------------------------------
    OMEGA=W2*OGB
!
!    DO 5 I=1,4
!         DO 5 K=1,2
!         R(K,4+I)=CMPLX(0.0,0.0)
!         R(K+2,I)=CMPLX(0.0,0.0)
!   5 CONTINUE

    DO I=1,8
    DO J=1,8
      R(I,J)=CMPLX(0.0,0.0)
           END DO
           END DO

  R(2,1)=AI*W
         R(2,2)=-AI*W
         R(2,3)=W
         R(2,4)=-W

  R(3,5)=-W2-AI*W*SI0
         R(3,6)=-W2+AI*W*SI0
         R(3,7)=W2-W*SI0
         R(3,8)=W2+W*SI0

  R(4,5)=-AI*W3+SM
         R(4,6)=AI*W3+SM
  R(4,7)=W3+SM
         R(4,8)=-W3+SM

  R(5,5)=-EXP(AI*W*(PU-1))
  R(5,6)=-EXP(-AI*W*(PU-1))
  R(5,7)=-EXP(W*(PU-1))
  R(5,8)=-EXP(-W*(PU-1))

  R(6,5)=-AI*W*EXP(AI*W*(PU-1))
```

```
        R(6,6)=AI*W*EXP(-AI*W*(PU-1))
        R(6,7)=-W*EXP(W*(PU-1))
        R(6,8)=W*EXP(-W*(PU-1))

   R(7,5)=W2*EXP(AI*W*(PU-1))
        R(7,6)=W2*EXP(-AI*W*(PU-1))
        R(7,7)=-W2*EXP(W*(PU-1))
        R(7,8)=-W2*EXP(-W*(PU-1))

   R(8,5)=AI*W3*EXP(AI*W*(PU-1))
        R(8,6)=-AI*W3*EXP(-AI*W*(PU-1))
        R(8,7)=-W3*EXP(W*(PU-1))
        R(8,8)=W3*EXP(-W*(PU-1))

! ------------------------------------------------------
!  the above elements is not relative to XK (Kn)
!  LOOK OUT!!! here R(i,j)=-fai(pu),-fai',-fai",-
fai'"
!
!------------------------------------------------------

   R(1,1)=CMPLX(1.0,0.0)
   R(1,2)=CMPLX(1.0,0.0)
   R(1,3)=CMPLX(1.0,0.0)
   R(1,4)=CMPLX(1.0,0.0)

   R(5,1)=EXP(AI*W*PU)
        R(5,2)=EXP(-AI*W*PU)
        R(5,3)=EXP(W*PU)
        R(5,4)=EXP(-W*PU)

   R(6,1)=AI*W*EXP(AI*W*PU)
        R(6,2)=-AI*W*EXP(-AI*W*PU)
        R(6,3)=W*EXP(W*PU)
        R(6,4)=-W*EXP(-W*PU)

   R(7,1)=-W2*EXP(AI*W*PU)
        R(7,2)=-W2*EXP(-AI*W*PU)
        R(7,3)=W2*EXP(W*PU)
        R(7,4)=W2*EXP(-W*PU)

   R(8,1)=-AI*W3*EXP(AI*W*PU)
        R(8,2)=AI*W3*EXP(-AI*W*PU)
        R(8,3)=W3*EXP(W*PU)
        R(8,4)=-W3*EXP(-W*PU)
!------------------------------------------------------
! give some initial values to the above elements
!------------------------------------------------------
    N=20
    REWIND 30
!------------------------------------------------------
 !** here read knr,kni from file 30, by calculation
 !**  from  kncomplex4.f90  subroutine
kncomplex(omeg)

        call kncomplex(OMEGA)

 !*****************
 ! here put N in RR.dat file, N is the number of
 series cos(k*si) 04.05.2004
 !-----------------
 !HERE N IS NUMBER OF XK IN FILE 30.

 !************************************
     REWIND 30
          DO I=1,N
          READ(30,*) XKR,XKI
 ! get lambda first,------- lambda^2=OMG^2/c^2-
 XK^2 ------------

    XK=CMPLX(XKR,XKI)
          XK2=XK*XK
          XK3=XK*XK2
          XK4=XK2*XK2

 LAMBDA=SQRT(OMEGA*OMEGA*H*H/C/
 C-XK2)
 !*****************************----------------
 ! here new update lambda, no sign decision--
 !*****************************----------------

     QI=PU/2.0+SIN(2*XK*PU)/4/XK

 QI1=EXP(AI*(XK+W)*PU)/2/AI/(XK+W)+EX
 P(AI*(W-XK)*PU)/2/AI/(W-XK)   &
       -W/AI/(W2-XK2)
     QI2=EXP(AI*(XK-W)*PU)/2/AI/(XK-W)-
 EXP(-AI*(W+XK)*PU)/2/AI/(W+XK)       &
       -W/AI/(XK2-W2)

 QI3=EXP((AI*XK+W)*PU)/2/(AI*XK+W)+EX
 P((W-AI*XK)*PU)/2/(W-AI*XK)  &
       -W/(W2+XK2)
     QI4=EXP((AI*XK-W)*PU)/2/(AI*XK-W)-
 EXP(-(AI*XK+W)*PU)/2/(AI*XK+W)       &
       +W/(W2+XK2)
 !------------------------------------------------------
 ! QI-->In, QI1, QI2,QI3,QI4 --> In1,In2,In3,In4
 !------------------------------------------------------
 !
     EN=-1/QI/(1+AI*LAMBDA*(XK4-
 W4)/GAMA/W4)
          EN0=-EN*(XK4-W4)

     YN=COS(XK*PU)
          YN1=-XK*SIN(XK*PU)
          YN2=-XK2*YN
          YN3=-XK2*YN1
 !------------------------------------------------------
 !    EN--> En~,  EN0--> En,  YN=Yn(PU),
 YN1=Yn', YN2=Yn", YN3=Yn'"(PU)
 !------------------------------------------------------
```

```
      R(1,1)=R(1,1)+EN*QI1
      R(1,2)=R(1,2)+EN*QI2
      R(1,3)=R(1,3)+EN*QI3
      R(1,4)=R(1,4)+EN*QI4

      R(5,1)=R(5,1)+EN*QI1*YN
      R(5,2)=R(5,2)+EN*QI2*YN
      R(5,3)=R(5,3)+EN*QI3*YN
      R(5,4)=R(5,4)+EN*QI4*YN

      R(6,1)=R(6,1)+EN*QI1*YN1
      R(6,2)=R(6,2)+EN*QI2*YN1
      R(6,3)=R(6,3)+EN*QI3*YN1
      R(6,4)=R(6,4)+EN*QI4*YN1

      R(7,1)=R(7,1)+EN*QI1*YN2
      R(7,2)=R(7,2)+EN*QI2*YN2
      R(7,3)=R(7,3)+EN*QI3*YN2
      R(7,4)=R(7,4)+EN*QI4*YN2

      R(8,1)=R(8,1)+EN*QI1*YN3
      R(8,2)=R(8,2)+EN*QI2*YN3
      R(8,3)=R(8,3)+EN*QI3*YN3
      R(8,4)=R(8,4)+EN*QI4*YN3


    END DO
!**************************************
!------------------------------------------------------
! ----------*******************----------------
!---------- END OF INPUT Rij(8*8), THEN
BEGIN TO CALCULATE |R|----------

!*************|R|=SRR*****************
!
     SRR=CMPLX(1.0,0.0)

   DO K=1,7
      IF(R(K,K) .EQ. CMPLX(0.0,0.0)) THEN
       DO I=K+1,8
        IF(R(I,K) .NE. CMPLX(0.0,0.0)) THEN
         DO II=K,8
!**************************************
!  just here should change all the elements from
K to 9, but
!     this file wrote as K,8, the results not
continuous!!! 2002.12.10
!          ----------------------------
!   !! here is just 8*8 matrix, not 8*9, should be
k,8 again!!
!**************************************
           SS=R(I,II)
           R(I,II)=R(K,II)
           R(K,II)=SS
                          END DO
        SRR=-SRR
           GOTO 149
           END IF
         END DO
        END IF

     SRR=SRR*R(K,K)

  149 DO J=8,K,-1          ! was J=8,K+1,-1
       R(K,J)=R(K,J)/R(K,K)
     END DO

     DO I=K+1,8
       DO J=K+1,8
         R(I,J)=R(I,J)-R(I,K)*R(K,J)
            END DO
          END DO
  END DO

     SRR=SRR*R(8,8)
   ! |R|=R(8,8) XX, other R(K,K)=1, k=1,...,7
 !---- END OF SOLVE EQUATIONS----------
 !**************************************
 !------------------------------------------------------
 !**************************************
 !---- NOW BEGIN TO OUTPUT DATA TO
 'RESULTS.DAT' FOR DRAWING---

     RSRR=REAL(SRR)
     AISRR=AIMAG(SRR)
     DETSRR=RSRR*RSRR+AISRR*AISRR

 WRITE(20,250) WR,WI,RSRR,AISRR
  250 FORMAT(2F14.6,E20.8,E20.8)

 !---- IF |R|-->0, W IS THE RIGHT VALUE.----
 |R|=SRR NOW--------------------

     END subroutine DETR
 !-----------------------------------------------
 !-----------------------------------------------

     SUBROUTINE FIND(N0,N1,N2,Nt)
 !**************************************
 !below is to find the roots from file 20,
 RESULTS.DAT-->ROOT.DAT
 !**************************************
          IMPLICIT NONE

 REAL::WR,WI,RSRR1,AISRR1,RSRR,AISRR,
 WI1,WR1
          INTEGER::N1,N2,m,m2,m3,m4,mr,mi,
 i,j,Ns,Nri,N10,N20,Nt,N0

                    Ns=0
 !** Ns should be added up all, for all possible
 roots. Ns=0 put outside this subroutine
```

```
                !** Ns is the number of Sr or Si
 change sign and written in file 70.

  rewind 20
         do i=1,N1
   read(20,*) WR1,WI1,RSRR1,AISRR1
                    if(RSRR1>0.0) m2=1
                    if(RSRR1<0.0) m2=-1
                    if(AISRR1>0.0) m4=1
                    if(AISRR1<0.0) m4=-1
!* first read one line, get the first sign of sr and si

           do j=1,N2-1
         read(20,*) WR,WI,RSRR,AISRR
                    if(RSRR>0.0) m=1
                    if(RSRR<0.0) m=-1
                    mr=m*m2
                    if(AISRR>0.0) m3=1
                    if(AISRR<0.0) m3=-1

                    mi=m3*m4
                    if(mr<0) then
         write(52,*) '*******SRRr change sign'
         write(52,102) WR,WI,RSRR,AISRR
         write(52,*)
                              Nri=1
   !** use Nri to define Sr or Si change sign
   !** Nri=1, Sr change sign
   !** Nri=2, Si change sign

 write(72,202) Nri,WR,WI,RSRR,AISRR
                              Ns=Ns+1
                    end if
                    if(mi<0) then
    write(52,*) '----------SRRi change sign'
    write(52,102) WR,WI,RSRR,AISRR
    write(52,*)
                              Nri=2
    write(72,202) Nri,WR,WI,RSRR,AISRR
                              Ns=Ns+1
                    end if

 102 FORMAT(2F14.6,E20.8,E20.8)
 202 FORMAT(I2,2F14.6,E20.8,E20.8)

!**                 if(mr<0       .and.       mi<0)
write(35,102) WR,WI,RSRR,AISRR
                    m2=m
                    m4=m3
                    end do
          read(20,*)  !* skip the empty line

          end do

!************************************
!** following is to find possible closer roots.
!************************************

  rewind 72
      !** Nt is the number of possible closer
roots written in file 80.
!** Nx is the number of closer roots, both signs
change.

  if(Ns>=1) then
   read(72,248) N10,WR1,WI1,RSRR1,AISRR1
  write(62,248) N10,WR1,WI1,RSRR1,AISRR1
  end if
      !** need to set if statement to make sure
there is data to be read. 16.02.2005

 248 FORMAT(I2,2F14.6,E20.8,E20.8)

  do i=1,Ns-1
                  !** Ns is the number of Sr or
Si change sign and written in file 70.
    read(72,248) N20,WR,WI,RSRR,AISRR
write(62,248) N20,WR,WI,RSRR,AISRR

!*              write(8,*)       'N1+N2=',N1+N2,'
,N1=',N1,'  ,N2=',N2

  if(N20+N10==3) then
    Nt=Nt+1
           if(N0==1) then
             if(N20==1) then
                    write(82,316) WR,WI1
                  else
                    write(82,316) WR1,WI
                  end if
           end if

           if(N0==2) then
             if(N20==1) then
                    write(82,316) WR1,WI
                  else
                    write(82,316) WR,WI1
                  end if
           end if
316 FORMAT(2F14.6)
         end if

          N10=N20
          WR1=WR
          WI1=WI

 end do
      !** this do loop find out possible closer
roots and write to file 80.
 !-------------------------------------------------------
          write(*,*) '--Nt=',Nt
```

```
!************************************
! the following deal with the hiding roots when
only Nri=1 or Nri=2 appears,
! but Si or Si change signs within these Ns
possible roots. 18.02.2005
!-------------------------------------------------

   if(Nt==0) then
           rewind 72
           if(Ns>=1) then
read(72,248) N10,WR1,WI1,RSRR1,AISRR1
                    if(RSRR1>0.0) m2=1
                    if(RSRR1<0.0) m2=-1
                    if(AISRR1>0.0) m4=1
                    if(AISRR1<0.0) m4=-1
           end if

      !** need to set if statement to make sure
there is data to be read. 16.02.2005

do i=1,Ns-1
                          !** Ns is the number
of Sr or Si change sign and written in file 70.
     read(72,248) N20,WR,WI,RSRR,AISRR
                  if(RSRR>0.0) m=1
                  if(RSRR<0.0) m=-1
                  mr=m*m2
                  if(AISRR>0.0) m3=1
                  if(AISRR<0.0) m3=-1
                  mi=m3*m4

                  if(N20==2 .and. mr<0) then
!** use Nri to define Sr or Si change sign
         !** Nri=1, Sr change sign
         !** Nri=2, Si change sign

                   write(82,316) WR,WI
                          Nt=Nt+1
                  end if
                  if(N20==1 .and. mi<0) then
                   write(82,316) WR,WI
                          Nt=Nt+1
                  end if
                  m2=m
                  m4=m3
          end do
         end if

END subroutine FIND
!------------ END OF subroutine FIND
!************************************
!----------------------------------------

subroutine wcloser(Nt,Nx)
!************************************
!-------------------------------------------------------
 !* this subroutnie is to deal with the duplicate
roots. 04.02.2005
 !-------------------------------------------------------
  implicit none

!** real(8)::sr1,sr2,si1,si2,knr1,knr2,kni1,kni2
 integer::i,Nt,j,Nx  !* N0,Ns,,N1,N2

 real,dimension(:),allocatable::aa1,aa2
 integer,dimension(:),allocatable::N

 allocate(aa1(Nt),aa2(Nt),N(Nt))
!** only use Nt elements for dimension

 rewind 82
 rewind 35
 Nx=0

  do i=1,Nt
    read(82,300) aa1(i),aa2(i)
          N(i)=1
  end do
          !** read all data from file 80
!** use N(i) to decide whether this root is
duplicate.
!** N(i)=1 if unique, N(i)>1 if duplicate

   do i=2,Nt
    do j=1,i-1
                  if(abs(aa1(i)-aa1(j))+abs(aa2(i)-
aa2(j)) <3.0E-5) N(i)=N(i)+1
           end do
          end do

!**     Nx=0  !** move to upper parts, possible
roots can be found there. 14.02.2005

  rewind 82
                          !**  this  is  really
important, re-write the data in file 80.
         do i=1,Nt
          if(N(i)==1) then
            Nx=Nx+1
            write(82,300) aa1(i),aa2(i)
                  write(35,300) aa1(i),aa2(i)
          end if
         end do

300 FORMAT(2F14.6)

                  !** Nx is the number of latest
**different** possible closer roots in file 80
                  write(*,*) '-----Nx=',Nx
         !**      write(9,*) '-----Nx=',Nx

         deallocate(aa1,aa2,N)
```

```
                    !** very important, to free the
 memory used by aa1,aa2
                    !** otherwise, it will take up
 all the heap memory very soon.

 end subroutine wcloser

 !************************************



     SUBROUTINE NEWTON(W,DW,WS)
 !-------------------------------------------------------
 !   subroutine to find roots for |R|=0 using
 Newton's method
 !  W=WR+WI*i, WS is the solution point for
 |R(WS)|=0.
 !-------------------------------------------------------

     IMPLICIT NONE
     REAL::DW,DW0,ADTW
     INTEGER::N

 COMPLEX::W0,W1,WS,SRR0,SRR1,W,DTW,
 DDW

     DW0=DW/10.0
     DDW=CMPLX(DW0,DW0)

     W0=W
          WRITE(45,*) 'W0=',W0

 !    W1=CMPLX(WR1,WI1)

  DO N=1,8
        !***because DDW=DDW/10.0, no need
 too many steps.

     W1=W0-DDW

      SRR0=CMPLX(0.0,0.0)
     CALL DETR(W0,SRR0)
      SRR1=CMPLX(0.0,0.0)
     CALL DETR(W1,SRR1)

  !*     WRITE(10,*) 'N=',N,'    SRR0=',SRR0,'
 SRR1=',SRR1

           if(abs(SRR0)<1.0E-9                .or.
 abs(SRR1)<1.0E-9) then
 !*   SRR0, SRR1 ~ 10E7 or larger
       WS=W0
       ADTW=0.0
          write(45,*)    '~~~~|R|=SRR0=',SRR0,',
 SRR1=',SRR1
       write(71,*)        '~~~~|R|=SRR0=',SRR0,',
 SRR1=',SRR1
                  goto 499
     end if

     IF(ABS(SRR1-SRR0) .LE. 1.0E-9) THEN
       WS=W0
       ADTW=0.0
 write(45,*) '++abs(SRR1-SRR0)<1.0E-9'
  write(71,*) '++abs(SRR1-SRR0)<1.0E-9'
       GOTO 499
     END IF
   WS=(-W0*SRR1+W1*SRR0)/(SRR0-SRR1)
          DTW=WS-W0
     ADTW=ABS(DTW)

          write(71,*) N,'=N,  W=',W,',   W0=',W0
  write(71,*)       'error=ADTW=',ADTW,       ',
 WS=',WS
          WRITE(71,*)

    if(ADTW .LT. 1.0E-9) then
          write(45,*) '...error<1.0E-9'
          write(71,*) '...error<1.0E-9'
          GOTO 499
          end if

    W0=WS
    DDW=DDW/10.0
  END DO

    WRITE(45,*) 'NO SOLUTIONS FOR THIS
 W=',W,'  W0=',W0
 write(45,*)  '~~no   roots~~|R|=SRR0=',SRR0,',
 SRR1=',SRR1
          WRITE(45,*)
          WRITE(71,*) 'NO SOLUTIONS FOR
 THIS W=',W,'  W0=',W0
       write(71,*)                          '~~no
 roots~~|R|=SRR0=',SRR0,',  SRR1=',SRR1
          WRITE(71,*)
    GOTO 497

  499          WRITE(45,*)          '----------
 |ERR|=',ADTW,'   WS=',WS
 write(45,*)  '~~with  roots~~|R|=SRR0=',SRR0,',
 SRR1=',SRR1
          WRITE(45,*)
 WRITE(71,*)       '----------|ERR|=',ADTW,'
 WS=',WS
 write(71,*)  '~~with  roots~~|R|=SRR0=',SRR0,',
 SRR1=',SRR1
          WRITE(71,*)

  497 END subroutine NEWTON
 !------------ END OF subroutine NEWTON
```

Appendix D

Fluid flow equations and fluid representation

D.1 Fluid flow equations

In a Cartesian tensor notation, by following Hirsch (1988) we may express the non-dimensional equations governing a three-dimensional unsteady fluid flow in the form

$$\frac{\partial u_i}{\partial x_i} = 0, \tag{D.1}$$

$$\frac{\partial u_i}{\partial t} + u_j \frac{\partial u_i}{\partial x_j} = -\frac{1}{\rho_f}\frac{\partial p}{\partial x_i} + \nu\left(\frac{\partial^2}{\partial x_1{}^2} + \frac{\partial^2}{\partial x_2{}^2} + \frac{\partial^2}{\partial x_3{}^2}\right)u_i + g_i, \tag{D.2}$$

or

$$\frac{\partial u_i}{\partial t} = \frac{\partial}{\partial x_j}\left(u_i u_j - \tau_{ij}\right), \tag{D.3}$$

where the fluid stress tensor τ_{ij} components due to pressure, viscous stress and turbulence can be written as

$$\tau_{ij} = -p\delta_{ij} + \frac{2}{Re}S_{ij} - \overline{u_i u_j}. \tag{D.4}$$

Here $Re = LU_0 / \nu$ denotes the Reynolds number, ν is the turbulent kinetic viscosity and $\overline{u_i u_j}$ is the Reynolds stress. The strain rate tensor S_{ij} is defined by

$$S_{ij} = \frac{1}{2}\left(\frac{\partial u_i}{\partial x_j} + \frac{\partial u_j}{\partial x_i}\right). \tag{D.5}$$

The coordinates $(x_i) = (x, y, z)$ and velocity components $(u_i) = (u_1, u_2, u_3)$ are non-dimensionalised in terms of a characteristic length L and a characteristic velocity $U_0 = L/T$, the time and pressure p by T and $\rho_f U_0^2$, respectively. The fluid forces and moments acting on the structure are obtained by integration of the normal and tangential stresses over the structure's surface area. The components of fluid forces and moments are determined by carrying out the integration over the solid surface. That is,

$$F_i = \int_\Omega \tau_{ij} n_j d\Omega, \tag{D.6}$$

$$M_i = \varepsilon_{ijk} \int_{\Omega} x_j \sigma_{kl} n_l d\Omega, \tag{D.7}$$

where F_i and M_i represent the components in the *i-th* direction of the fluid force $\mathbf{F}$ and moment $\mathbf{M}$ acting on the structure and n_i denotes the component of the outward normal to the structure's surface.

Equation (6.20) is the Reynolds-averaged form of the Navier-Stokes equation where the instantaneous values of velocity and pressure are replaced by their long-time averaged counterparts (see, for example, Kwak *et al.* (1986)). A result of the averaging process is the appearance of the Reynolds stress terms $\overline{u_i u_j}$. For these terms, various levels of modelling are available, most of which involve a number of assumptions and approximations and require considerable experimental inputs. For illustration and simplicity, the turbulence model adopted in this study is the one-equation model of Baldwin and Barth (1991). The Reynolds stress terms $\overline{u_i u_j}$ in equation (6.21) are replaced by $-2\nu_t S_{ij}$. Here ν_t represents the turbulent eddy viscosity, which appears as part of an effective viscosity $\left(\frac{1}{Re} + \nu_t\right)$ in the diffusion term of the Reynolds-averaged Navier-Stokes equation (see Townsend (1980)).

On the bottom and fixed walls of the towing tank (see Figure 6.1), a no slip boundary condition holds. That is,

$$u_j = 0, \qquad z = 0 \text{ or } y = 0. \tag{D.8}$$

The wave maker is a moving boundary and the water surface is free to the atmosphere. For a wave disturbance $\zeta(x,y,t)$, the profile of the free surface is given by

$$z - \zeta(x,y,t) = 0, \tag{D.9}$$

and because the free surface is a material surface, we have $D(z - \zeta(x,y,t))/Dt = 0$ or

$$u_3 = \frac{\partial \zeta}{\partial t} + u_1 \frac{\partial \zeta}{\partial x} + u_2 \frac{\partial \zeta}{\partial y}. \tag{D.10}$$

The traction force on the free surface is the prescribed atmospheric pressure $\hat{p}_0$ which is assumed to be perpendicular to the free surface if viscosity of the air and surface

tension properties of the fluid are neglected. The dynamic condition on the free surface is therefore expressed as

$$\tau_{ij}\eta_j = -\hat{p}_0\eta_i, \tag{D.11}$$

where η_i is the unit vector along the outer normal of the fluid boundary Γ.

D.2 Fluid representation

Time discretisation.

To derive the governing equations of the body-fitted coordinate system expressed in equation (D.2), the following independent variables are introduced to transform the physical domain into a computational domain. That is,

$$\xi_i = \xi_i(x_i,t), \tag{D.12}$$

$$\bar{t} = t, \tag{D.13}$$

where $\xi_i = \xi,\eta,\zeta$ when $i = 1,2,3$.

Let us suppose that the mesh velocity

$$c_i = \partial x_i / \partial \bar{t}, \tag{D.14}$$

and the Jacobian of the transformation

$$J = \partial(x,y,z)/\partial(\xi,\eta,\zeta), \tag{D.15}$$

is of conservative form in the curvilinear coordinate system. The continuity and momentum equations (D.1) and (D.3) are transformed as follows,

$$-\partial\left(JQ^i\right)/\partial\xi_i = 0, \tag{D.16}$$

$$\partial d/\partial t = -\partial\left(e^i - e_v^i\right)/\partial\xi_i \equiv -r, \tag{D.17}$$

where

$$d = J\begin{bmatrix} u \\ v \\ w \end{bmatrix}, \qquad e^i = J\begin{bmatrix} u_1Q^i + S_1^i\cdot p + S_t^i\cdot u_1 \\ u_2Q^i + S_2^i\cdot p + S_t^i\cdot u_2 \\ u_3Q^i + S_3^i\cdot p + S_t^i\cdot u_3 \end{bmatrix},$$

$$S_m^i = \partial\xi_i/\partial x_m, \qquad Q^i = S_m^i\cdot u_m, \qquad S_t^i = \partial\xi_i/\partial t = c_m S_m^i,$$

$$e_v^i = J\begin{bmatrix} \left(\frac{1}{Re}+\nu_t\right)S_m^i S_m^k \frac{\partial u_1}{\partial \xi_k} + \nu_t S_m^i S_1^k \frac{\partial u_m}{\partial \xi_k} \\ \left(\frac{1}{Re}+\nu_t\right)S_m^i S_m^k \frac{\partial u_2}{\partial \xi_k} + \nu_t S_m^i S_2^k \frac{\partial u_m}{\partial \xi_k} \\ \left(\frac{1}{Re}+\nu_t\right)S_m^i S_m^k \frac{\partial u_3}{\partial \xi_k} + \nu_t S_m^i S_3^k \frac{\partial u_m}{\partial \xi_k} \end{bmatrix}.$$

In these relations, Q^i denotes the contravariant component of velocity, $S_t^i u_j$ denotes the contribution of the mesh motions to the convective terms e^i in the Navier-Stokes equations. If the flow is laminar, ν_t vanishes from the viscous fluxes e_v^i.

The time derivative in the momentum difference equation is represented by the second-order, three-point, backward-difference implicit formula

$$\frac{1.5d^{n+1} - 2d^n + 0.5d^{n-1}}{\Delta t} \equiv -r^{n+1}, \tag{D.18}$$

where r denotes the residual vector. The superscript n indicates the nth physical time level.

To construct an iterative scheme to solve equations (D.16) and (D.17), an artificial compressibility relation is introduced by adding a pseudo-time derivative of pressure to the continuity equation in the form

$$\frac{\partial \phi}{\partial \tau} = -\frac{\beta}{J}\frac{\partial\left(JQ^i\right)}{\partial \xi_i}, \tag{D.19}$$

where $\phi = p + \frac{z}{Fn^2}$ with Froude number $Fn = U_0 / \sqrt{Lg}$, τ indicates the pseudo-time variable and β is the artificial compressibility constant.

The pseudo-time derivative in equation (D.19) is replaced by an implicit Euler back-forward difference formula and equation (D.18) is rewritten as

$$\frac{\hat{p}^{n+1,m+1} - \hat{p}^{n+1,m}}{\partial \tau} = -\beta\left(\frac{\partial\left(JQ^i\right)}{\partial \xi_i}\right)^{n+1,m+1}, \tag{D.20}$$

$$\frac{1.5d^{n+1,m+1} - 1.5d^{n+1,m}}{\Delta t} = -r^{n+1,m+1} - \frac{1.5d^{n+1,m} - 2d^n + 0.5d^{n-1}}{\Delta t}, \tag{D.21}$$

where $\hat{p} = p / J$ and the second superscript m denotes the level of the sub-iteration used to converge the equations to the solutions of equations (D.16) and (D.17) for each time step.

Combining equations (D.20) and (D.21), we find that the discretised incremental equation is obtained by linearising the right-hand side residual term R at the $(n+1)$-*th* pseudo-time level. That is,

$$\left[\frac{I_{tr}}{J^{n+1}} + \left(\frac{\partial R}{\partial D}\right)^{n+1,m}\right]\left(D^{n+1,m+1} - D^{n+1,m}\right)$$

$$= -R^{n+1,m} - \frac{I_m}{\Delta t}\left(1.5\tilde{D}^{n+1,m} - 2\tilde{D}^{n} + 0.5\tilde{D}^{n-1}\right), \qquad \text{(D.22)}$$

where

$$\tilde{D} = J\begin{bmatrix} p \\ u \\ v \\ w \end{bmatrix} = JD,$$

$$R = \partial\left(E^i - E^i_v\right) / \partial\xi_i,$$

$$E^i = \begin{bmatrix} J\beta Q^i \\ e^i \end{bmatrix}, \quad E^i_v = \begin{bmatrix} 0 \\ e^i_v \end{bmatrix}.$$

Here I_{tr} represents a diagonal matrix and I_m is a modified unit matrix defined as

$$I_{tr} = diag\left[\frac{1}{\Delta\tau}, \frac{1.5}{\Delta t}, \frac{1.5}{\Delta t}, \frac{1.5}{\Delta t}\right],$$

$$I_m = diag[0,1,1,1].$$

Spatial discretisation.

The incremental solution of equation (D.22) is derived using the implicit scheme described by Rogers *et al.* (1991), Anderson and Bonhaus (1994), Shen *et al.* (1996), Koomullil and Soni (1999), Frink (1996), Xing *et al.* (2002). The viscous fluxes are approximated using a second-order central difference scheme. The derivatives of the convective fluxes in vector R and $\partial R / \partial D$ are discretised using second and first-order

upwind difference schemes based on the flux-difference splitting method. The derivative of the convective flux in the *j-th* direction is approximated by

$$\frac{\partial E^i}{\partial \xi_j} \approx \frac{\tilde{E}^i_j - \tilde{E}^i_{j-1}}{\Delta \xi_j}, \tag{D.23}$$

where the numerical flux $\tilde{E}^i_j$ is calculated using the approximate Riemann solver developed by Roe (1981) in the form

$$\tilde{E}^i_j = \frac{1}{2}\left[E^j(D_{i+1}) + E^j(D_i) - \left|\overline{A}\left(\frac{1}{2}(D_{i+1} + D_i)\right)\right| \times (D_{i+1} - D_i) \right] - \Phi_j, \tag{D.24}$$

where A is the Jacobian of the convective flux vector E^i and $\left|\overline{A}\right| = T|\Lambda|T^{-1}$. Here T is the matrix whose columns are the right eigenvectors of A, T^{-1} is the matrix whose rows is the left eigenvectors of A, and $|\Lambda|$ is a diagonal matrix whose diagonal elements are the absolute values of the eigenvalues of A. The matrix $\overline{A}$ is evaluated by using Roe-average variables, and Φ_j denotes a dissipation term. A second-order central difference scheme is obtained by setting $\Phi_j = 0$.

Overset grids.

The multi-zone overlap grid technique provides a conceptually simple method for domain decomposition. For instance, the background grid is constructed to cover the main body element and overset grids are imposed on the background grid to improve geometric flexibility and so effectively captures the interesting features of the flow field as described by Kao *et al.* (1994), Xing *et al.* (2002). The overset grid may be assembled using several grid blocks and, if required, each grid block can be treated exactly the same as the background grid blocks, but, if required, different solution methods may be employed for different sub-domains.

In addition to the boundaries of the computational domain, sub-grids have intergrid boundaries with neighbouring donor sub-grids but may also contain holes. Proper boundary conditions, therefore, are needed on the intergrid boundaries and the hole points are blanked or excluded from the flow solution of Navier-Stokes equations. Details

describing the overset grid technique are given by Baysal *et al.* (1991), and Kao *et al.* (1994).

Information transfer between the overlapping grids is of primary importance to develop an efficient overset grid technique. In the present study, a trilinear interpolation function (which has been proved to be more effective than a Taylor series expansion), is used to obtain the boundary values of the flow field variables for the overset grid from the background grid. That is,

$$\phi = a_1 + a_2\alpha + a_3\beta + a_4\gamma + a_5\beta\gamma + a_6\alpha\gamma + a_7\beta\gamma + a_8\alpha\beta\gamma , \qquad \text{(D.25)}$$

where, $0 \le \alpha,\beta,\gamma \le 1$ are interpolation weights and the coefficients a_i for $i = 1,\cdots,8$ are determined from known values at the eight base vertices of the hexahedron surrounding the target point. Since the trilinear interpolation can only be used on cubes and the hexahedron formed around a target point is generally warped due to the curvilinearity of a body-fitted grid, it is therefore necessary to map a warped hexahedron to a unit cube by means of an isoparametric mapping. The relations between the coordinates (x_1,x_2,x_3) of the target point and the coefficients (α,β,γ) can be expressed as

$$x_i = a_1^i + a_2^i\alpha + a_3^i\beta + a_4^i\gamma + a_5^i\beta\gamma + a_6^i\alpha\gamma + a_7^i\beta\gamma + a_8^i\alpha\beta\gamma , \qquad \text{(D.26)}$$

where the coefficient a_j^i is determined by the coordinates of the eight vertices of the hexahedron similar to calculating the coefficient a_i of equation (D.25). A Newton iteration method can be used to obtain the coefficients (α,β,γ).